19TH SYMPOSIUM
TECTONICS, STRUCTURAL GEOLOGY AND GEOLOGY OF CRYSTALLINE ROCKS

C.-H. FRIEDEL, B. LEISS, M. STIPP, D. TANNER (EDS.)

VOLUME II: EXCURSION GUIDE

TSK *Halle (Saale)* **19**
09.-11.03.2022
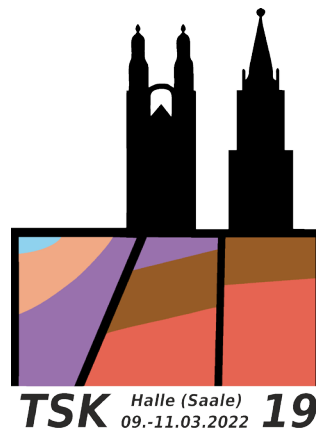
HALLE (SAALE) 2022

HALLESCHES JAHRBUCH FÜR GEOWISSENSCHAFTEN

BEIHEFT 51

19th Symposium on Tectonics, Structural geology and Crystalline Geology

TSK *Halle (Saale) 09.-11.03.2022* **19**
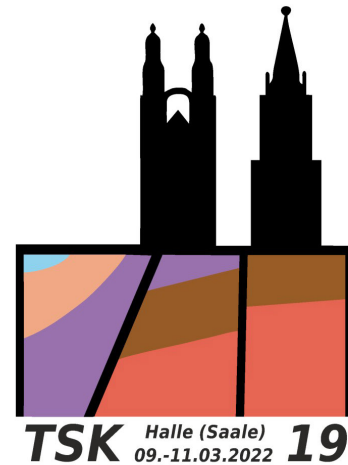
Excursion guide

"Geotectonic development of the Harz Mountains"

11.-13.03.2022
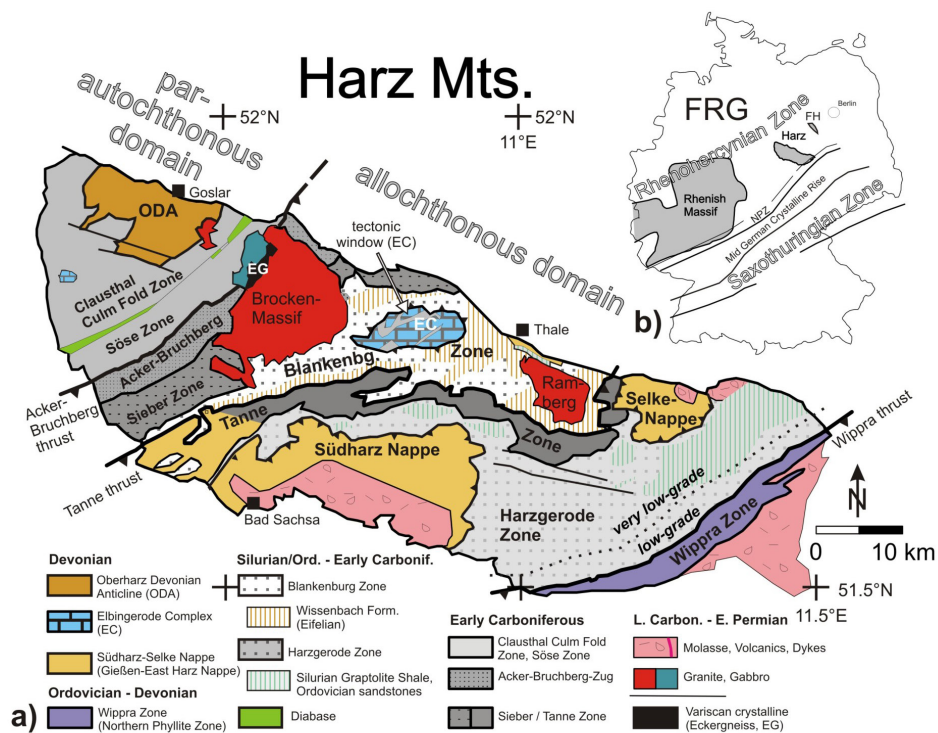
a) Tectono-sedimentary units of the Harz Mountains and their general subdivision in parautochthonous and allochthonous domains. b) The Harz Mts. within the German part of the Rhenohercynian Zone (Friedel et al. 2019; reprinted with permission from Springer Nature).

Location of the stops 1-11

CFZ: Clausthal Culm Fold Zone
ODA: Oberharz Devonian Anticline
TZ: Tanne Zone
BZ: Blankenburg Zone
HgZ: Harzgerode Zone
ShN: Südharz nappe } Parts of the Gießen-
SeN: Selke nappe   } (Ost)Harz nappe
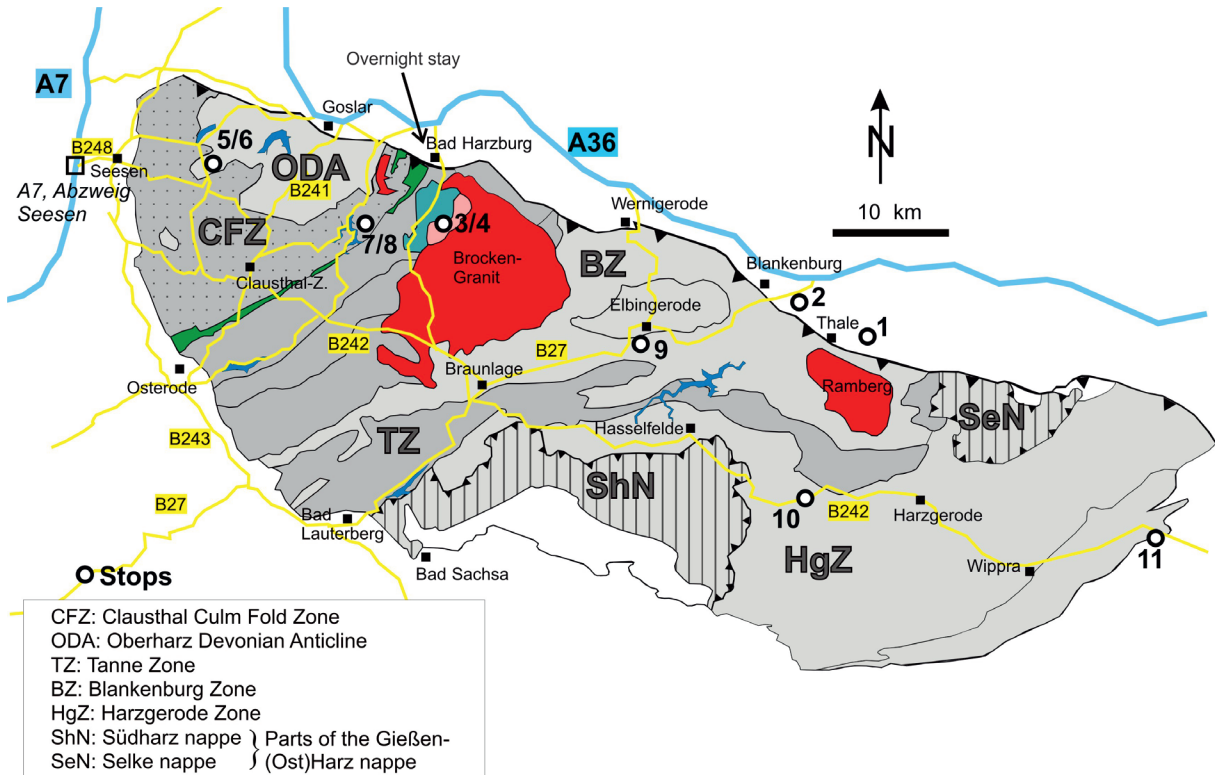
TSK19-Field Guide "Geotectonic development of the Harz mountains"

Organisers Dr. Carl-Heinz Friedel (Leipzig), Dr. Bernd Leiss (Univ. Göttingen), Dr. David C. Tanner (LIAG Hannover), Prof. Dr. Michael Stipp (Univ. Halle)

Program

Friday, March 11, 2022

Stop 1: Devil's wall, south of Weddersleben near Neinstedt (D.C. Tanner)

Stop 2: Devil's Wall, "Hamburger Wappen", Timmenrode (D.C. Tanner, Chr. Brandes)

Overnight stay: Bad Harzburg

Saturday, March 12, 2022

Stop 3: Harzburgite and Harzburg gabbro, Kolebornskehre, Radautal (M. Stipp)

Stop 4: Metamorphic and structural data from the Ecker Gneiss Complex; outcrops at Käsewieter bridge, Ecker valley (M. Stipp, C.-H. Friedel, S. Kurtenbach)

Stop 5: Folded Lower Carboniferous cherts, Innerste valley, Lautenthal (B. Leiss, D.C. Tanner)

Stop 6: Internal structure and kinematic of a Variscan thrust fault– the Sparenberg Breccia at Lautenthal (C.-H. Friedel, M. Schmidt, B. Leiss)

Stop 7: Triangle Zone in Lower Carboniferous siliclastics (D.C. Tanner, B. Leiss)

Stop 8: Kellwasser Horizon in Devonian carbonates (D.C. Tanner, B. Leiss)

Overnight stay: Bad Harzburg

Sunday, March 13, 2022

Stop 9: Sedimentary vs tectonic origin - mélange and broken formation in the classic outcrop of the "Hüttenrode Olistostrome" near Königshütte (C.-H. Friedel, J. Kreitz, N. Brouwer-Miosca, B. Leiss)

Stop 10: Blocks of imbricate stacks of Devonian limestones as indicator for a tectonic origin of chaotic rock units in the Harz Mountains - the Herzynkalk block of Güntersberge as an example. (C.-H. Friedel, J. Kreitz, B. Leiss)

Stop 11: Common tectonic features of the epizonal Wippra zone – the Klippmühle Quartzite Formation in the Wipper valley (C.-H. Friedel, M. Stipp)

Stop 1: Devil's Wall, south of Weddersleben near Neinstedt

David C. Tanner

Leibniz Institute for Applied Geophysics, Stilleweg 2, D-30655 Hannover, Germany

davidcolin.tanner@liag-leibniz.de

Locality: Famous tourist and hiking natural monument (Königstein hill).

UTM co-ordinates: East 643843.473, North 5736096.676 (Zone 32N, WGS84)

Geographic co-ordinates: N 51°45'26.168" E 11°5'2.954"

This locality offers a good view of the Harz Mountains to the south and the Subhercynian Cretaceous basin (SHB) to the north. The Devil's wall is actually an outcrop of vertically-standing Upper Cretaceous (Coniacian and Santonian) sandstone beds. (Fig. 1.1) The Königstein is the most striking outcrop of the Devil's wall (Königstein); sandstones of the Heidelberg Formation (Upper Santonian) are exposed here. The beds are strongly cemented by quartz, which accounts for their prominence over the surrounding area.

Figure 1.1: Devil's wall exposes nearly vertically-standing Cretaceous sandstones.

In map view, the Harz Mountains form an approximately lozenge-shaped, NW–SE striking, ca. 95 km long and 35 km wide positive topographic anomaly. In cross-section (Fig. 1.2), the topographic shape is distinctly asymmetric, skewed to the north.

The cause of the rotation of the Upper Cretaceous beds in the SHB from horizontal to vertical was the uplift and thrusting of the Harz Mountains in the Upper Cretaceous on the northern Harz boundary fault (HNBF). According sedimentary records and unconformities in the SHB, thrusting took place during Santonian to Campanian, i.e. 85.8 to 71.3 Ma (Voigt et al. 2004).

The Schöth 2/65 borehole met the HNBF at ca. 1 km depth, giving the dip of the fault to be 55° (Fig. 1.3, Franzke et al. 2004). Franzke et al. (2004) estimated the throw (vertical displacement) to be at least 6 km. Note how all the beds of the SHB, including the Cretaceous beds, are folded and over-turned at the fault. This is the reason for the present-day vertical attitude of the Devil's wall beds. The reason for the strong cementation is that, as the Harz Mountains were thrust upwards, fluids were circulated in front of the thrust and probably could quickly ascend the vertical bedding.
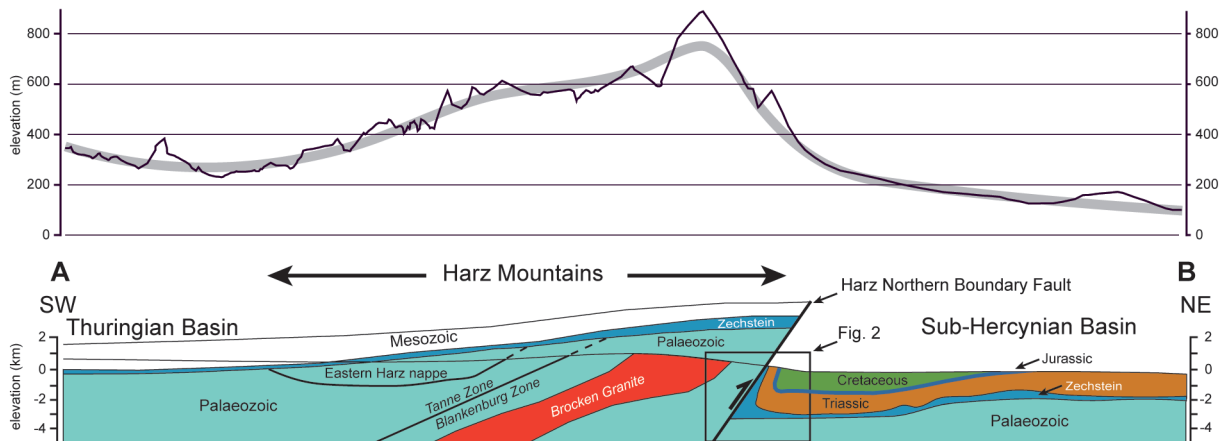
Figure 1.2: Above: topographic elevation taken from Google Earth, grey line—moving average (window 500 m). Below: simplified cross section of the Harz Mountains, after Kley et al. (2008), showing the position of the Harz northern boundary fault (Tanner & Krawczyk 2017; reprinted with permission from Springer Nature).
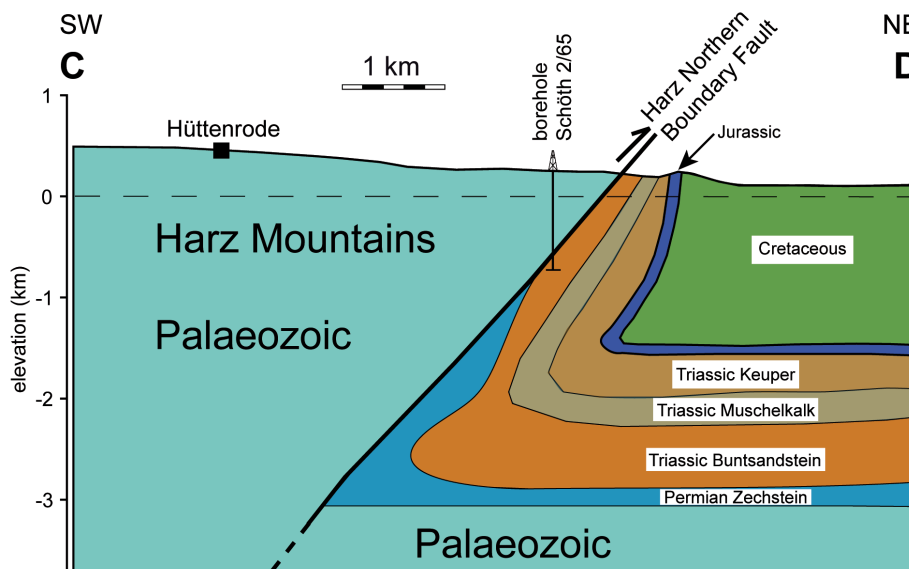
Figure 1.3: Simplified cross-section of the northern boundary of the Harz Mountains near Hüttenrode. Diagram modified after Franzke et al. (2004), (Tanner & Krawczyk 2017; reprinted with permission from Springer Nature).

Estimations of the geometry of the fault at depth (or detachment depth) are difficult, due to the lack of good geophysical information. By using kinematic modelling, Tanner and Krawczyk (2017) predicted, using the "inclined shear" algorithm, that, given the upper geometry of the HNBF and the shape of the Base Permian over the Harz Mountains (Figs. 1.2 and 1.3), the fault could meet a detachment between ca. 25 km and the Moho at 30 km (Fig. 1.4). The authors argue that the former depth is more probable. Either way, this suggests that the Cretaceous event in Germany and Northern Europe was thick-thinned, involving most of the crust, with a lower crustal detachment.

The thick-skinned nature of the Cretaceous deformation is even more apparent when the 30° inclined-shear Harz model is placed together with the DEKORP BASIN 9601 (DEKORP-Basin Research Group 1999; Krawczyk et al. 1999; Fig. 1.4).

The detachment depth for the HNBF of ca. 25 km fits extremely well with the interpreted detachment depths of the Haldensleben and Gardelegen Faults in the interpreted DEKORP profile (Fig. 1.5; Krawczyk et al. 1999). Together, they form a foreland-propagating splay of emergent thrusts with a detachment level that rises, from south to north, from a depth of 25–16 km. One consequence of the listric shape of the major faults is that to achieve the geometry of previous fabrics before the Cretaceous, they have to be back-rotated by ca. 11°. This means that any pre-Cretaceous fabrics have been steepened by the same amount.

Kley & Voigt (2008) correlated the Late Cretaceous inversion phase in middle Europe with the convergence of Africa–Iberia–Europe, and not the Alpine collision. This caused, for instance, the Pyrenean Orogeny, dated at ca. 85 Ma (Capote et al. 2002), and it was coeval with pulses of tectonic inversion or accelerated subsidence in many basins throughout Europe (Reicherter and Pletsch 2000, Kockel 2003).
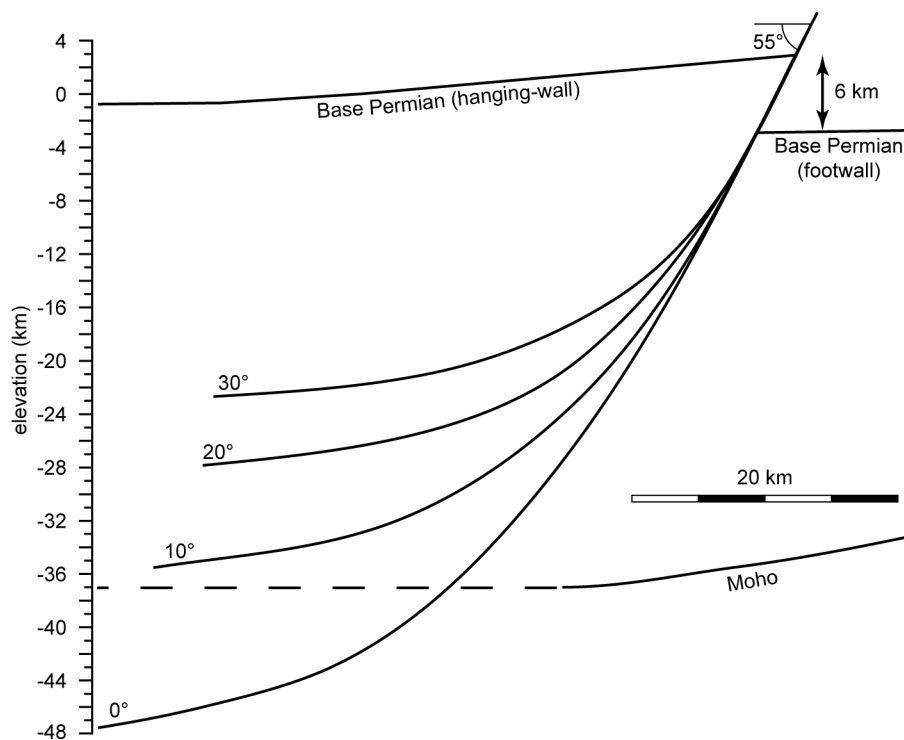
Figure 1.4: Possible fault traces and depth to detachment predicted by the shape of the hanging-wall, using inclined shear with antithetic shear angles at 0°, 10°, 20°, and 30° (Tanner & Krawczyk 2017; reprinted with permission from Springer Nature).
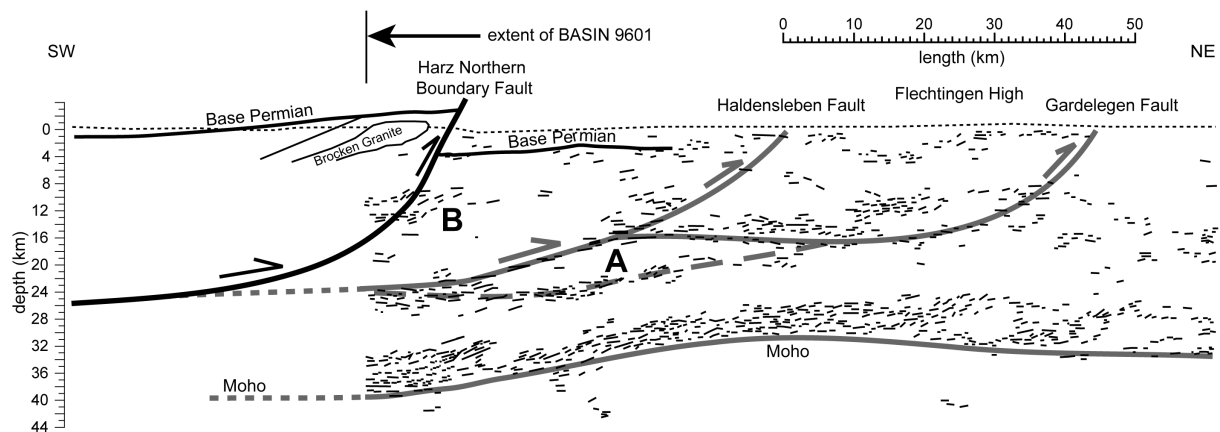
Figure 1.5: The Harz model presented together with the line drawing of the DEKORP BASIN 9601 seismic section. The Harz structure fits well with the detachment depths of the Gardelegen and Haldensleben Faults, as interpreted in the seismic (DEKORP-Basin Research Group 1999; Krawczyk et al. 1999), (Tanner & Krawczyk 2017; reprinted with permission from Springer Nature).

References

Capote, R., Muñoz, J.A., Simón, J.L., Liesa, C.-L. & Arlegui, L.E. (2002): Alpine tectonics, I: the Alpine system north of the Betic Cordillera. In: Gibbons, W. & Moreno, T. (eds): The geology of Spain. The Geological Society of London, 367-400, London. doi: 10.1144/GOSPP.15.

DEKORP-Basin Research Group (1999): Deep crustal structure of the northeast German Basin: new DEKORP BASIN 96 deep-profiling results. Geology, 27, 55-58. doi: 10.1130/0091-7613(1999)027<0055:DCSOTN>2.3.CO;2.

Franzke, H.-J., Voigt, T., von Eynatten, H., Brix, M.R. & Burmester, G. (2004): Geometrie und Kinematik der Harznordrandstörung, erläutert an Profilen aus dem Gebiet von Blankenburg. Geowiss. Mitt. Thüringen, 11, 39-62.

Kley, J. & Voigt, T. (2008): Late Cretaceous intraplate thrusting in central Europe: effect of Africa-Iberia-Europe convergence, not Alpine collision. Geology, 36 (11), 839–842. doi:10.1130/G24930A.1.

Kockel, F. (2003): Inversion structures in central Europe–expressions and reasons, an open discussion. Geol. Mijnb., 82, 367-382. doi: 10.1017/S0016774600020187.

Krawczyk, C.M., Stiller, M. and DEKORP-Basin Research Group (1999): Reflection seismic constraints on Paleozoic crustal structure and Moho beneath the NE German Basin. Tectonophysics, 314, 241-253. doi: 10.1016/S0040-1951(99)00246-2.

Reicherter, K.R. & Pletsch, T.K. (2000): Evidence for a synchronous circum-Iberian subsidence event and its relation to the African-Iberian plate convergence in the Late Cretaceous. Terra Nova, 12, 141-147. doi: 10.1046/j.1365-3121.2000.00276.x.

Tanner, D.C. & Krawczyk, C.M. (2017): Restoration of the Cretaceous uplift of the Harz Mountains, North Germany: Evidence for the geometry of a thick-skinned thrust. International Journal of Earth Sciences, 106/8, 2963-2972. doi: 10.1007/s00531-017-1475-8.

Stop 2: Devil's Wall, "Hamburger Wappen", Timmenrode

David C. Tanner[1], Christian Brandes [2]
1) Leibniz Institute for Applied Geophysics, Stilleweg 2, D-30655 Hannover, Germany
davidcolin.tanner@liag-leibniz.de
2) Institut für Geologie, Leibniz Universität Hannover, Callinstr. 30, 30167 Hannover, Germany
brandes@geowi.uni-hannover.de

Locality: Devil's Wall near Timmenrode, known as the "Hamburger Wappen".
UTM co-ordinates: East 638089.729, North 5738117.397 (Zone 32N, WGS84)
Geographic co-ordinates: N 51°46'36.75" E 11°0'5.93"

We visit another outcrop of the Devil's Wall, which also consists of Heidelberg sandstones of the Upper Santonian. Again, the sandstones are very hard due to quartz cementation, similar to Stop 1. However, in addition, the beds are display so-called "deformation band" structures (Fig. 2.1).
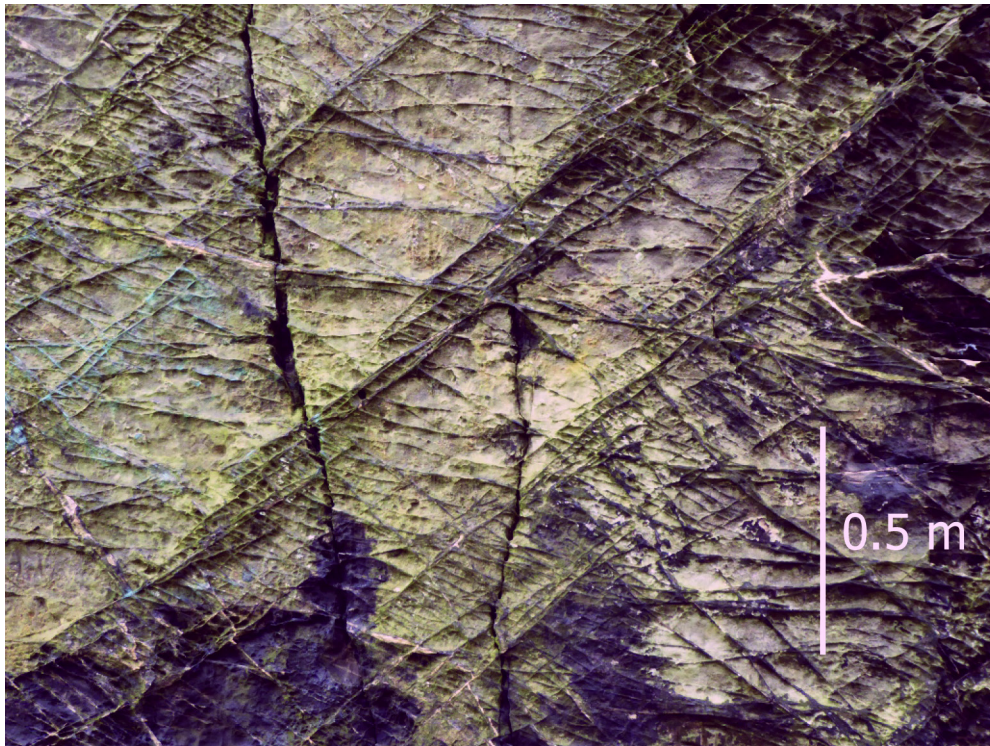
Fig. 2.1: Tabular, conjugate deformation bands at the Devil's wall.

Deformation bands are planar structural elements that develop in porous sands and sandstones in the upper crust (Aydin 1978, Fossen et al. 2007). They are the equivalent to fractures and faults in other lithologies. They can be further subdivided by the processes involved into cataclastic and non-cataclastic bands; the latter are also known as disaggregation bands and preferentially form at the near-surface in unconsolidated (Brandes et al. 2018) or weakly-consolidated sandy sediments by grain rolling and sliding processes, i.e., particulate or granular flow (Fossen et al. 2007; Fossen 2010). The former occur at deeper depths of the crust.

Typically, deformation bands are tabular bodies, around one or more centimetre(s) thick (Brandes & Tanner 2020). They can also anastomose and form ladders and conjugate pairs, as is the case in this outcrop. In cataclastic deformation bands, grain-size reduction and thus porosity reduction can

occur (Shipton et al. 2005). For instance, Klimczak & Schultz (2013) calculated that the Heidelberg Sandstone has host rock porosities of ~15–20 %, which are reduced to as low as 10–1 %, depending on the micro-mechanism causing the decrease in porosity in the deformation band. As such, they negatively influence the passage of fluids through the crust. For instance, they can partition reservoirs.

Deformation bands usually form in the process zone or damage zone of major faults (Brandes & Tanner 2020; Brandes et al. accepted). As the former, they can thus indicate hidden blind faults at depth and are an indicator for neotectonic movement on the blind faults (Brandes et al. 2022). The deformation bands exposed here are thought to be in the damage zone of a branch fault of the Harz northern boundary fault (Klimczak & Schultz 2013). From the conjugate orientation of the deformation bands, it is proposed that they were formed in the stress field as the beds rotated into the vertical during the Upper Cretaceous (Klimczak & Schultz 2013).

References

Aydin, A. (1978): Small faults formed as deformation bands in sandstone. Pure Appl. Geophys., 116, 913-930. doi: 10.1007/BF00876546.

Brandes, C. & Tanner, D. (2020): Fault mechanics and earthquakes. In: D. Tanner, D. & Brandes, C. (eds.): Understanding Faults, 11-80, Elsevier.

Brandes, C., Igel, J., Loewer, M., Tanner, D.C., Lang, J., Müller, K. & Winsemann, J. (2018): Visualisation and analysis of shear-deformation bands in unconsolidated Pleistocene sand using ground-penetrating radar: Implications for paleoseismological studies. Sedimentary Geology, 367, 135-145. doi: 10.1016/j.sedgeo.2018.02.005.

Brandes, C., Tanner, D.C., Fossen, H., Halisch, M. & Müller, K. (accepted): Disaggregation bands as an indicator for slow creep activity on blind faults. Communications, Earth & Environment, 18.02.2022.

Fossen, H., Schultz, R.A., Shipton, Z.K. & Mair, K. (2007): Deformation bands in sandstone: a review. J. Geol. Soc. London, 164, 755-769. doi: 10.1144/0016-76492006-036.

Fossen, H. (2010): Deformation bands formed during soft-sediment deformation: Observations from SE Utah. Mar. Petrol. Geol., 27, 215-222. doi:10.1016/j.marpetgeo.2009.06.005.

Klimczak, C. & Schultz, R. (2013): Fault damage zone origin of the Teufelsmauer, Subhercynian Cretaceous basin, northern Germany. International Journal of Earth Sciences, 102, 121-138. doi: 10.1007/s00531-012-0794-z.

Shipton, Z.K., Evans, J.P. & Thompson, L.B. (2005): The geometry and thickness of deformation band fault core and its influence on sealing characteristics of deformation-band fault zones. In: Faults, fluid flow, and petroleum traps (eds. Sorkhabi, R. & Tsuji, Y.). AAPG Memoir, 85, 181-195. doi: 10.1306/M851033.

Stop 3: Harzburgite and Harzburg gabbro, Kolebornskehre, Radautal

Michael Stipp

Martin-Luther-Universität Halle-Wittenberg, Institut für Geowissenschaften und Geographie, Von-Seckendorff-Platz 3, 06120 Halle, michael.stipp@geo.uni-halle.de

Locality: Kolebornskehre, Radautal south of Bad Harzburg
UTM co-ordinates: East 607008.942, North 5744425.144 (Zone 32N, WGS84)
Geographic co-ordinates: N 51° 50' 25.35", E 10° 33' 11.79"

Harzburgite is an ultramafic igneous rock type from the upper mantle. It belongs to the peridotite group and consists mainly of olivine and orthopyroxene. Hence, it is enriched in orthopyroxene and depleted in clinopyroxene in contrast to the predominant lherzolite peridotite composition. Garnet lherzolite is the most frequent rock of the upper mantle down to 300 km depth. In the mantle lithosphere garnet, the dominant aluminous phase, is replaced by spinel towards shallow level at < 80-90 km and by plagioclase at < 20-30 km depth. Due to the decompressive ascent of the original lherzolite in rift and mid-ocean ridge (MOR) systems, clinopyroxene and plagioclase are largely affected by partial melting. The resulting tholeiitic basalt melts generate the MOR magmatism. With a loss of up to 20 vol.-% the restite is converted from a lherzolite into a harzburgite composition. Apart from such a residual layer harzburgite can also be formed by fractionation and plumbing resulting in a cumulate layer at the base of basaltic/gabbroic magma chambers. Accordingly, it frequently occurs at the base of an ophiolite sequence.

The harzburgite was first described by Rosenbusch (1887) and termed after its type locality 'Kolebornskehre' in the Radau valley close to Bad Harzburg. There, harzburgite is composed of approx. 43 vol.-% olivine, 56 vol.-% orthopyroxene, 1 vol.-% plagioclase as well as accessory ore minerals and apatite. It is associated with the large intrusive body of the Harzburg gabbro, a suite of ultramafic to mafic magmas largely composed of gabbros, olivine gabbros, gabbronorites and diorites (Fig. 3.1). Harzburgite and dunite occur as inclusions/ultramafic enclaves in the gabbros or as cumulate layer at their base. Two fractionation sequences have been described for these gabbros by Sano et al. (2002), one as ultramafic cumulate and the other one as mafic non-cumulate series. The most primitive olivine composition of Fo89.5 with 0.4 wt.-% NiO may point to equilibrium conditions with primitive mantle melts. Pb, Sr, Nd isotopic data and geochemical variations similar to those of an island-arc(?) tholeiite (Fig. 3.1) as well as the differentiation up to quartz diorite compositions imply that even the most primitive mantle magma assimilated crustal material during its ascend (Sano et al. 2002). The contamination of the ultramafic to mafic magmas by crustal melts was especially strong during late-stage crystallization. Therefore, the Harzburg gabbro shows such an unusually wide lithological spectrum ranging from dunite to quartz diorite.

Mafic intrusions are also associated with the Brocken granite, the largest pluton of the Harz mountains. Whereas the Brocken granite and related intrusions are located north, east and south of the Ecker Gneiss Complex, the Harzburg gabbro is westerly adjacent to the latter (Fig. 3.2). To the north and the east of the Brocken granite the northern and eastern margin diorite zones are exposed, which have been correlated due to their compositional similarity (Erdmannsdörfer 1908, Lotze 1933).

According to the mineralogy as well as chemical main and trace element analytics, Heilmann et al. (2016) show that the quartz gabbronorite from the Harzburg gabbro and the gabbroic and quartz diorites from the northern margin diorite zone belong to one magmatic suite that is systematically different to Brocken granite and other granites that occur in the vicinity of the margin diorite zone. Harker diagrams indicate a well-developed fractionation curve for Al_2O_3 (Fig. 3.3a). There is also a systematic increase in TiO_2 and FeO resulting in the crystallization of ilmenite (Fig. 3.3b). Further geochemical similarities to the Harzburg gabbros (cf. Heilmann et al. 2016) and the fact that the

Table 6: Estimated primary melt composition for Harz intrusion and some terrestrial basalt compositions

	Harz Mountain primary magma[1]	Continental flood basalts				IAT	IACA	N-MORB
		Karoo	Snake River	Deccan	Average			
SiO$_2$	51·50	51·50	46·18	50·56	50·01	49·20	49·40	50·45
TiO$_2$	0·45	0·95	2·06	2·57	1·00	0·52	0·70	1·62
Al$_2$O$_3$	16·02	15·69	14·47	13·83	17·08	15·30	13·29	15·26
Fe$_2$O$_3$*		10·96	13·52	13·79				
FeO*	7·09					10·01	9·00	10·15	10·43
MnO	0·15	0·16	0·19	0·17	0·14	0·18	0·20	
MgO	10·15	7·01	9·99	5·12	7·84	10·10	10·44	7·58
CaO	10·16	10·69	9·68	9·62	11·01	13·00	12·22	11·30
Na$_2$O	1·25	2·17	2·63	2·65	2·44	1·51	2·16	2·68
K$_2$O	0·80	0·70	0·61	0·93	0·27	0·17	1·06	0·11
P$_2$O$_5$	0·07	0·16	0·44	0·22	0·19	0·06	0·20	
H$_2$O	2·10							
Total	99·73	99·99	99·77	99·46	99·99	99·04	99·82	99·41

[1]Composition is introduced by cubic equation fitting for whole-rock analyses at *mg*-number = 71. The *mg*-number is estimated from the most forsterite-rich olivine (Fo$_{89}$) in cumulate using K_D = 0·3 for melt and olivine.
Data for Karoo basalt from Cox (1983); Snake River and Deccan basalts from Thompson *et al.* (1983); average continental flood basalts from Basaltic Volcanism Study Project (1981); island-arc tholeiite (IAT) and island-arc calc-alkaline basalt (IACA) from Perfit *et al.* (1980); N-MORB from Hofmann (1988).
*Fe reported as Fe$_2$O$_3$ or as FeO.

Figure 3.1: Primary melt composition from the Harzburg gabbro in comparison to some other basalts (Sano et al., 2002; reprinted with permission from Oxford University Press).
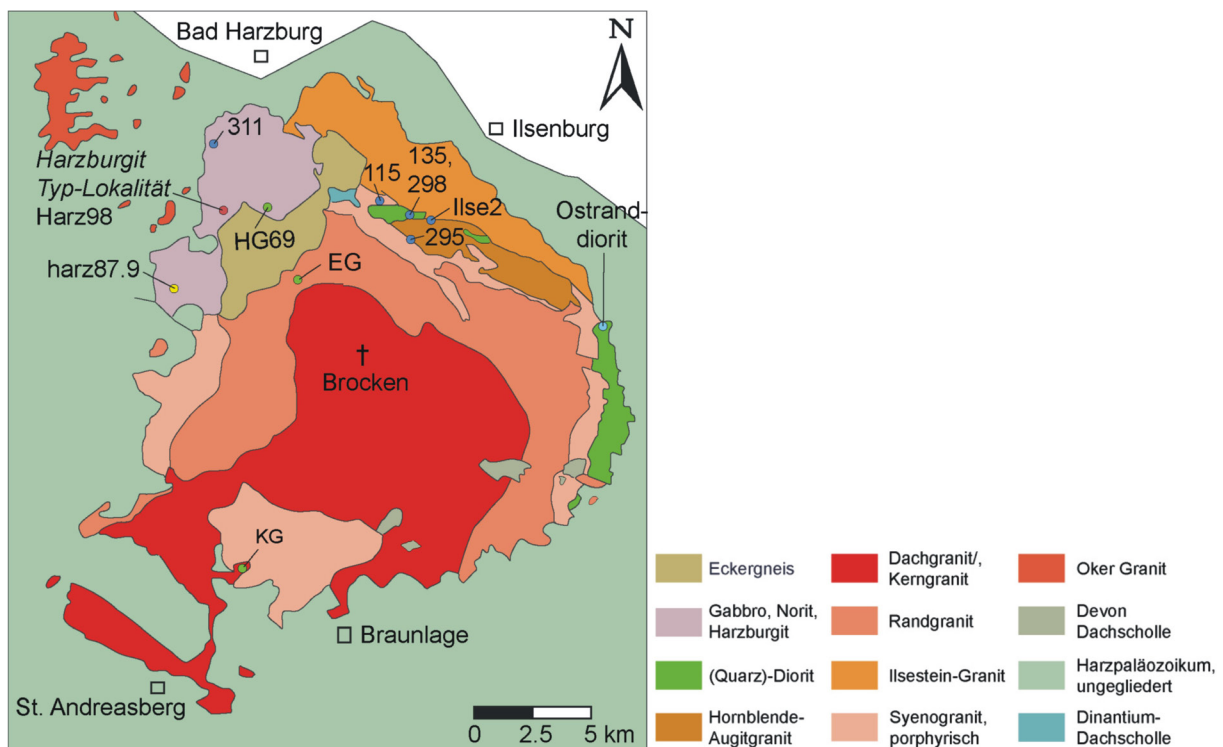
Figure 3.2: Map view distribution of Ecker gneiss Complex, as well as post-Variscan Harzburg and Brocken intrusions surrounded by the Paleozoic sedimentary units that have been deformed by the Variscan orogeny (reprinted from Heilmann et al. 2016).
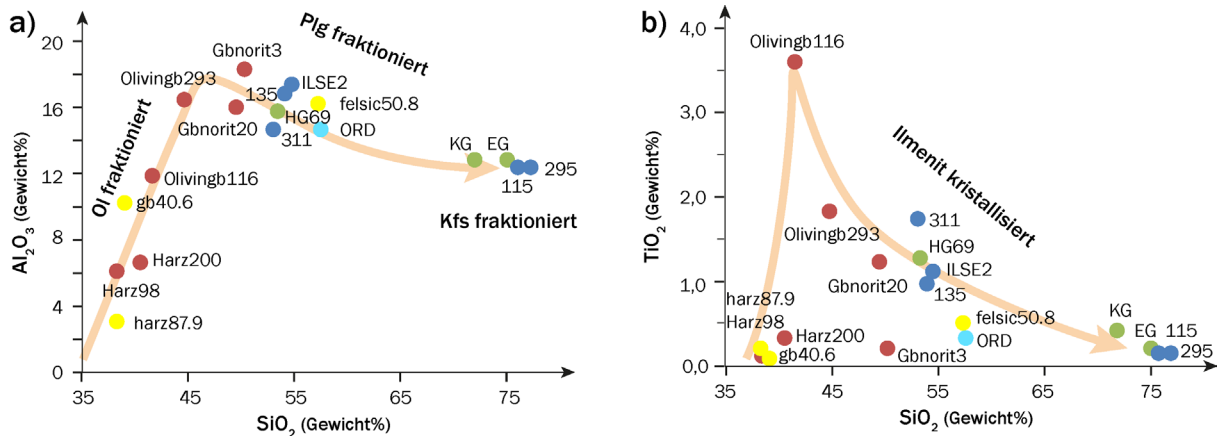
Figure 3.3: Harker diagrams of Harzburg gabbro (reprinted from Heilmann et al. 2016).

diorites are cut by the differing and later granite intrusions indicate that the margin diorite zone was formed by further differentiation of the mafic non-cumulate series. Thus, the diorites probably intruded together with the Harzburg gabbros that have been dated at 295-293 Ma using zircon U/Pb geochronology (Baumann et al. 1991). The Brocken pluton displays a wider range in zircon U/Pb-ages of 293-283 Ma that are consistent with a younger emplacement (Baumann et al. 1991, Zech et al. 2010). Harzburg gabbro and northern margin diorite much likely belong to one common intrusive complex that is connected below the Ecker gneiss unit and later dissected by the Brocken granite.

The Brocken pluton intruded as lakkolith in (sub)horizontal sheets indicated by an AMS hyper-solidus flow foliation with NNE–SSW- and ESE–WNW-oriented fabric trends (Fig. 3.4). This corresponds to a post-Variscan emplacement parallel to deep fault structures within an E-W extensive system. These fabrics are contradictory for an upwards drag and hence for the exhumation of the Ecker Gneiss Complex by the emplacement of Harzburg gabbro or Brocken granite pluton (Zundel et al. 2019).
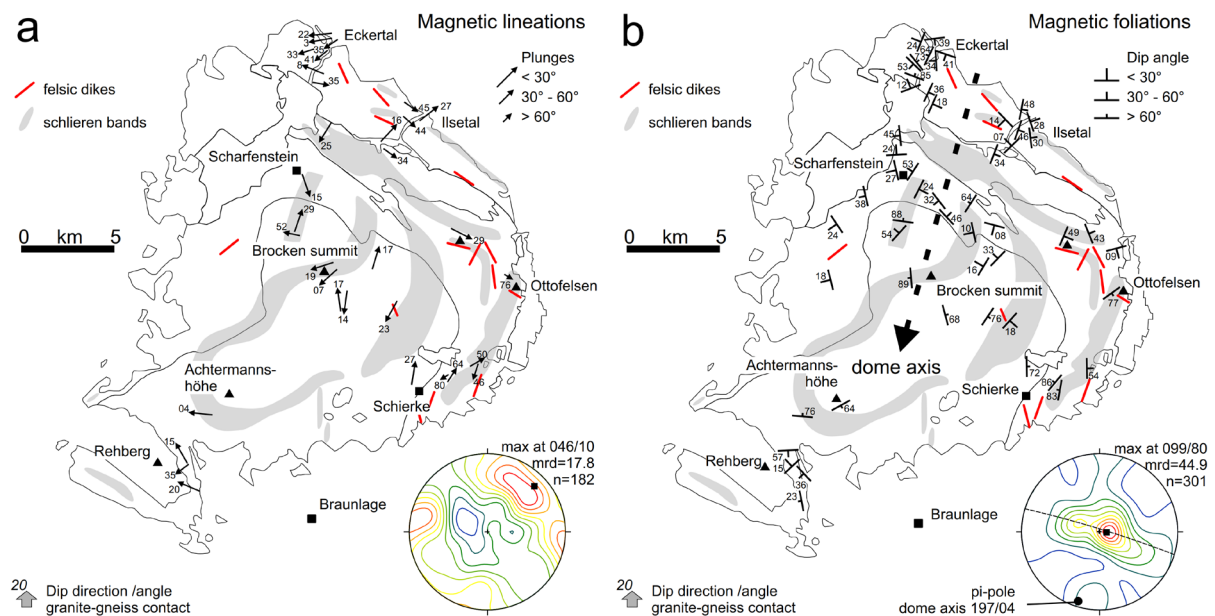
Figure 3.4: Magnetic foliation and lineation within the Brocken pluton (Zundel et al., 2019; reprinted with permission from Springer Nature).

References

Baumann, A., Grauert, B., Mecklenburg, S. & Vinx, R. (1991): Isotopic age determinations of crystalline rocks of the Upper Harz Mountains, Germany. Geol. Rundschau, 80, 669-690.

Erdmannsdörffer, O.H. (1908): Über Bau und Bildungsweise des Brockenmassivs. Jb. Königlich-Preuss. Geol. Landesanstalt, Bergakademie Berlin, 26(1905), 379-405.

Heilmann, C., Bousquet, R. & Düsterhöft, E. (2016): Einordnung der Nordranddioritzone in den magmatischen Kontext des Brockenmassivs. Göttingen Contributions to Geosciences, 78, 19-23.

Lotze, F. (1933): Das tektonische Bild des Brockenmassivs. Cent. für Mineral. Geol. und Paläontologie, Abteilung B, 633-647.

Rosenbusch, H. (1887): Mikroskopische Physiographie der Mineralien und Gesteine. Vol. II. Massige Gesteine. Schweizerbart, Stuttgart. Zweite Auflage, 877 S.

Sano, S., Oberhänsli, R., Romer, R. L. & Vinx, R. (2002): Petrological, Geochemical and Constraints at the Origin of the Harzburg Intrusion, Germany. Journal of Petrology, 43(8), 1529-1549. doi:10.1093/petrology/43.8.1529.

Zech, J., Jeffries, T., Faust, D., Ullrich, B. & Linnemann, U. (2010): U/Pb-dating and geochemical characterization of the Brocken and the Ramberg Pluton, Harz Mountains, Germany. Geol. Sax., 56, 9-24.

Zundel, M., Friedel, C.H. & Grimmer, J.C. (2019): Magnetic fabric constraints for syn-magmatic doming of the laccolithic Brocken granite pluton (Harz Mountains, northern Germany). Int. J. Earth Sci., 108, 799-816. doi:10.1007/s0053 1-019-01679 -w.

Stop 4: Metamorphic and structural data from the Ecker Gneiss Complex; outcrops at Käsewieter bridge, Ecker valley

Michael Stipp [1], Carl-Heinz Friedel [2], Stefan Kurtenbach [1]

1) Martin-Luther-Universität Halle-Wittenberg, Institut für Geowissenschaften und Geographie, Von-Seckendorff-Platz 3, 06120 Halle, michael.stipp@geo.uni-halle.de
2) Karl-Marx-Str. 56, 04158 Leipzig, chfriedel@gmx.de

Locality: Ecker valley c. 1.5 km north of the Ecker dam, two outcrops close to the Käsewieter bridge.
UTM co-ordinates (Käsewieter bridge): East 609978, North 5746003 (Zone 32N, WGS84)
Geographic co-ordinates: N 51°51'14.34" E 10°35'48.66"

The post-Variscan plutons of the Harzburg Gabbro and Brocken Granite surround the Ecker Gneiss Complex (EC) and this entire setting is as well surrounded by the parautochthonous to allochthonous Devonian to early Carboniferous sedimentary rock sequence. The EC itself represents a Variscan high-grade tectonometamorphic series of metasediments mainly consisting of metapelites, metapsammites, metaquartzites as well as amphibolites. The protoliths of the EC largely represent early Devonian clastic sediments of Baltic provenance (Geisler et al. 2005). Hence, the EC does not belong to the Avalonian basement, but represents a large allochthonous gneiss block. Peak metamorphism reached upper amphibolite to granulite facies grade at approximately 328-313 Ma as revealed by U-Th-total Pb dating of monazite (Appel et al. 2019; Figs. 4.1 and 4.2).
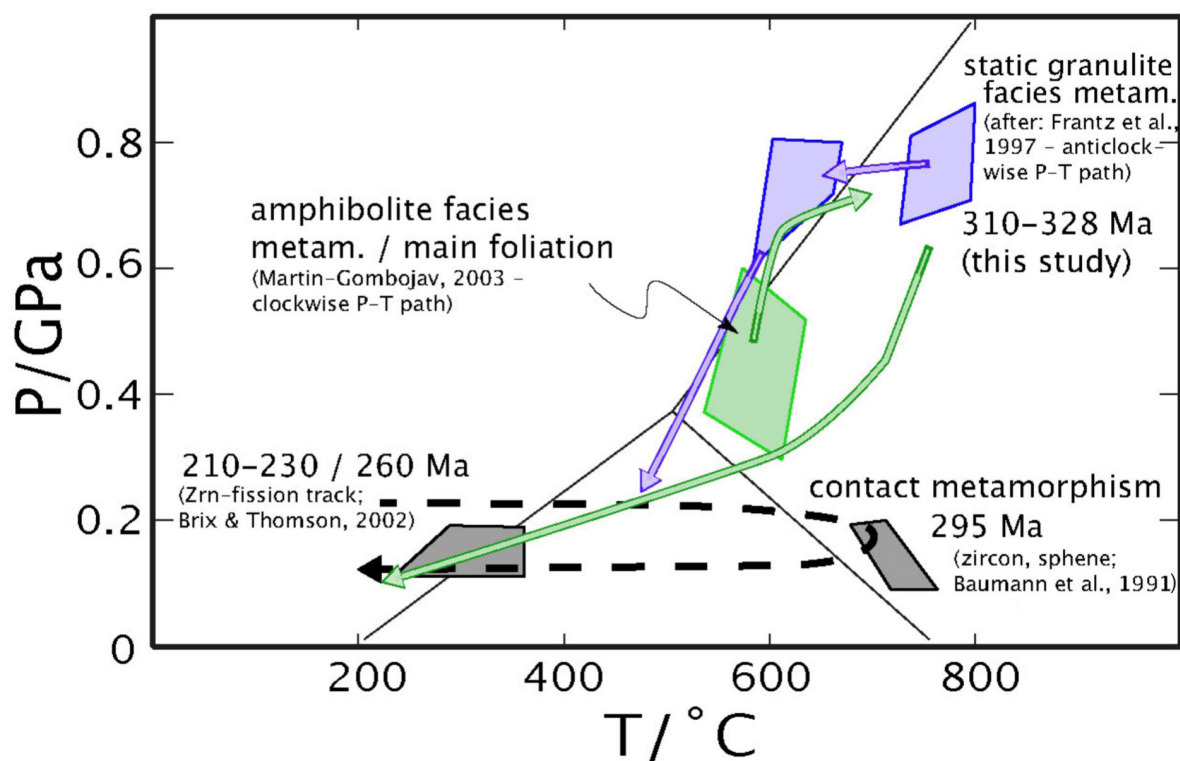
Figure 4.1: Suggested clockwise and anti-clockwise p/T-paths of the Ecker gneiss Complex with geochronological constraints. The age of approx. 328-313 Ma of the granulite facies metamorphism is based on U-Th-total Pb dating of monazite (Appel et al. 2019; reprinted with permission from Springer Nature).
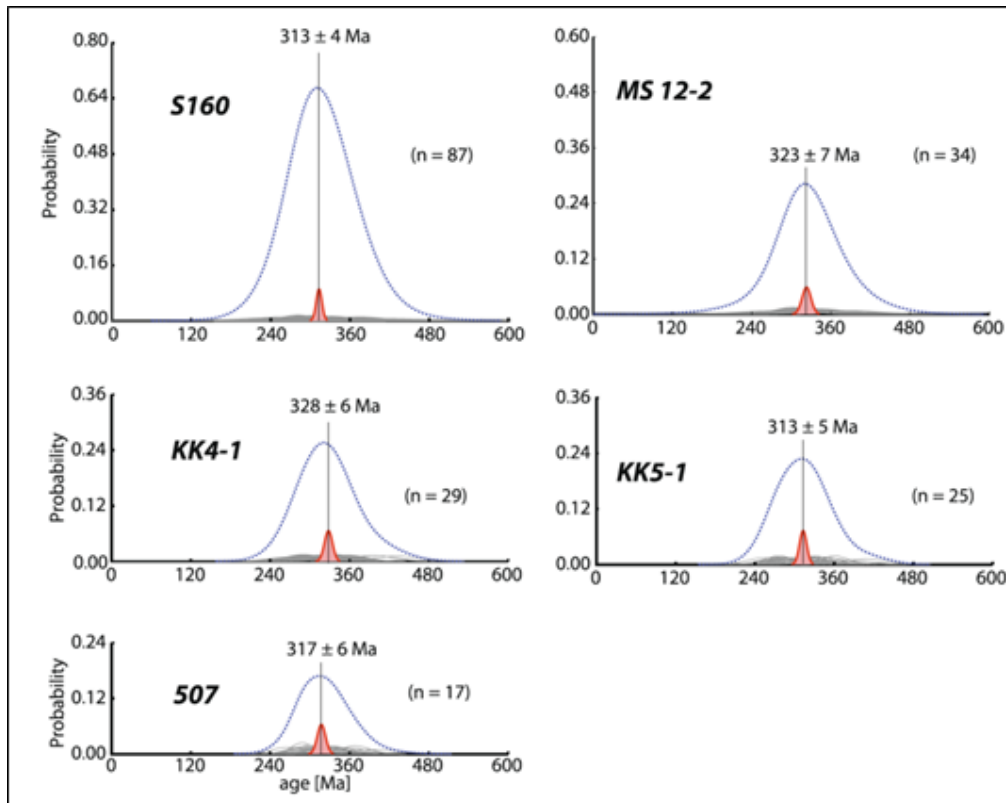
Figure 4.2: U-Th-total Pb dating results of monazite (Appel et al. 2019; reprinted with permission from Springer Nature).
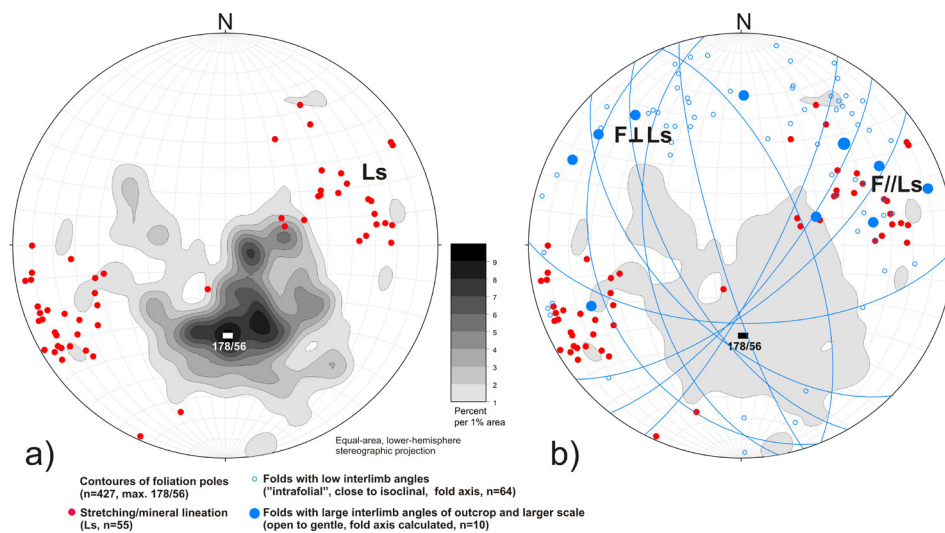
Figure 4.3: Structural data from the Ecker gneiss complex, equal-area, lower hemisphere projection (compiled from Fischer 2009, Kraus 2014, Fischbach 2020 and own data). a) Main foliation of the gneiss (contour lines) and associated stretching lineation (Ls, red dots). b) Axes of close to isoclinal folds and gentle to open folds (blue open circles and large blue dots); blue great circles represent foliation planes that form large-scale folds. Light-grey area of contouring and stretching lineations of a are shown for comparison. See text for further explanation.
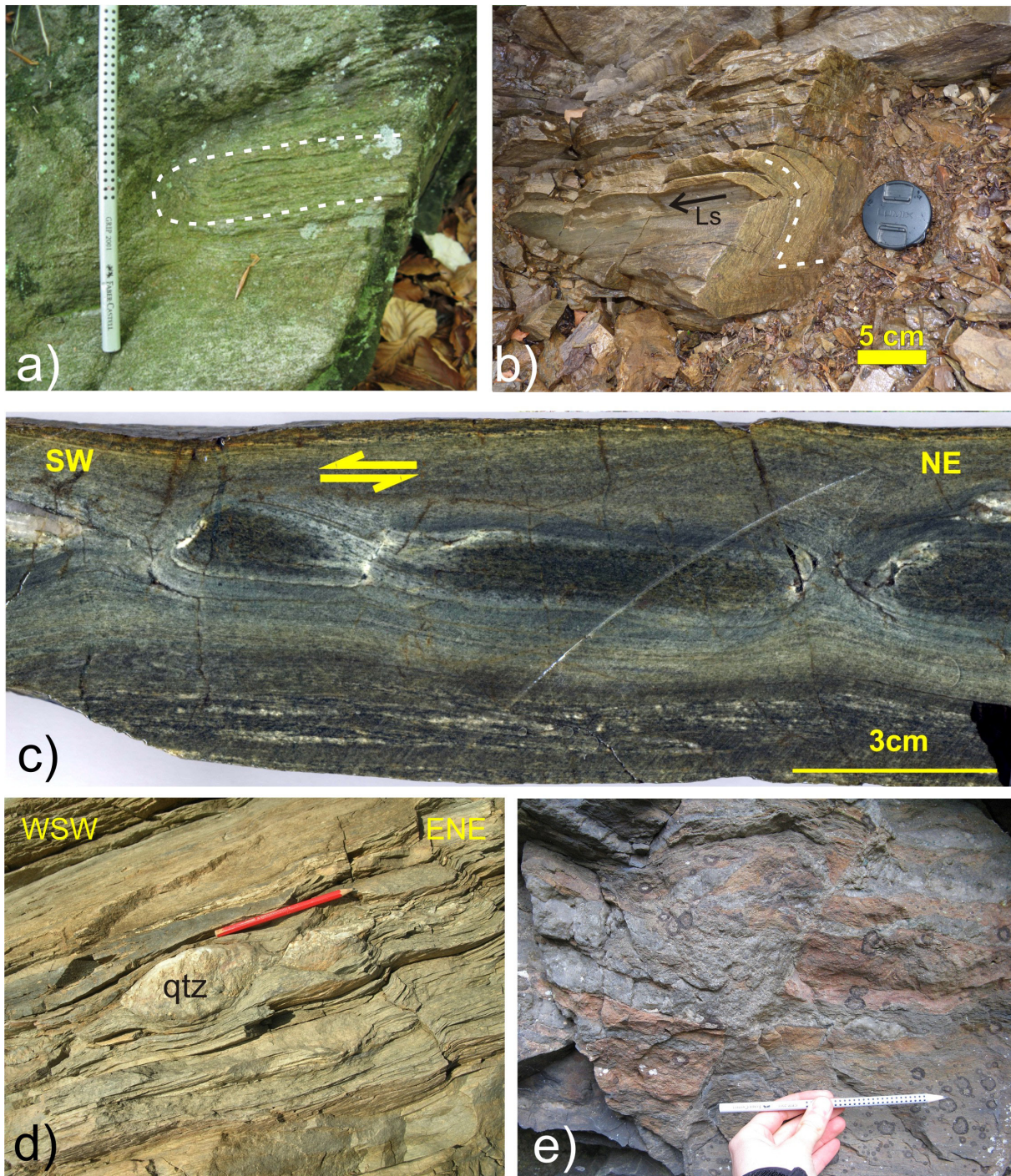
Figure 4.4: Ecker gneiss field structures. a) Isoclinal and b) close to tight intrafolial folds. The fold axis in b is parallel to the main stretching lineation (Ls, gently dipping to WSW); c) Sheared boudinage, top to the SW sense of shear; d) Sheared boudinaged layer of quartz segregation in mica schists and gneisses (these rocks also contain andalusite grains). On the right side some NE dipping kink bands occur pointing to a top to SW faulting; e) Post-Variscan normal faulting. Locations: a, c, e: northern Ecker valley, southern slope; b, d: northeastern shore of the Ecker reservoir.
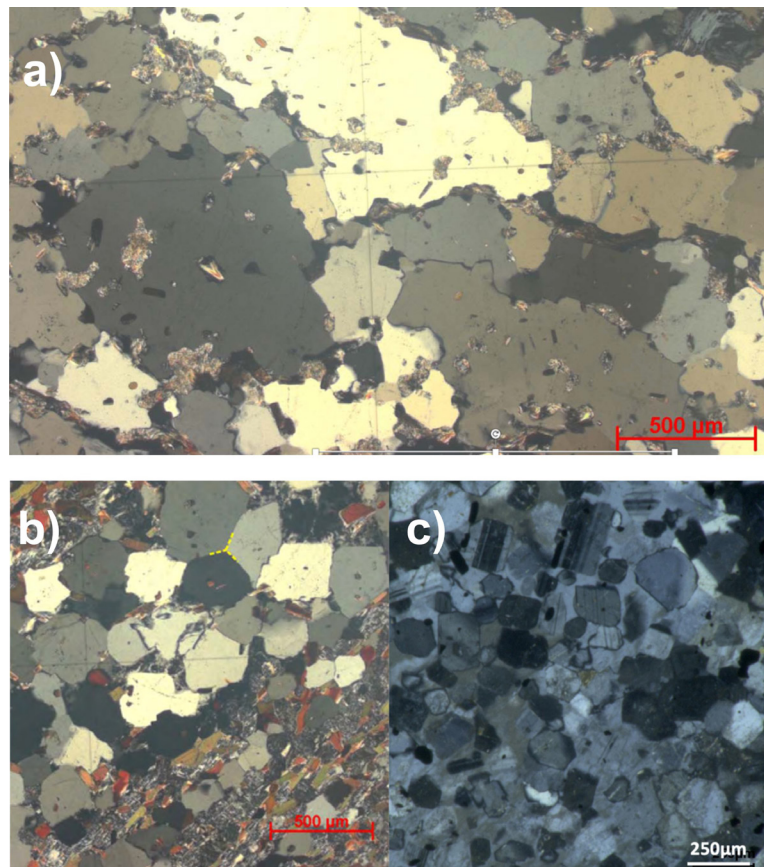
Figure 4.5: a) Dynamic recrystallization microstructure of quartz with large irregular quartz grains, lobate grain boundaries and dissection microstructures indicative of grain boundary migration recrystallization, sample 21, Eckertal; b) Static recrystallization microstructure of quartz with equilibrated grains, straight grain boundaries and 120° triple junctions, sample F6, Großes Gierstal; c) Partially molten microstructure with feldspar and quartz clasts swimming in a matrix of a eutectic melt composition, sample KK 43.1, northern Ecker valley.

The predominantly N to NNW-ward dipping main foliation of the EC is associated with a preferentially WSW-ENE striking stretching lineation (Fig. 4.3a). There are at least two fold generations, older tight to isoclinal folds (mostly intrafolial, Fig. 4.4a, b) and younger gentle to open folds (folds with high interlimb angles). The axes of small-scale folds with low interlimb angles spread along a great circle distribution that dips gently to the N. There are local maxima of this great circle that are aligned parallel to the ENE-WSW striking stretching lineation and also at a high angle to the stretching lineation. The gentle to open folds show a similar tendency in orientation (Fig 4.3b). Overall, the gneiss structure (e.g., Fig. 4.4c) contrasts with the commonly SE dipping foliation and NW directed tectonic transport in the surrounding very low-grade sedimentary rocks.

The main foliation of the EC that is characterized by grain boundary migration recrystallization microstructures is overprinted by partial melting and static recrystallization of the dynamic fabric as well as by a few localized migmatitic shear zones (Fig. 4.5a-c). During exhumation and tectonic emplacement from the granulite facies metamorphic condition to the ambient very low-grade metamorphism of the Rhenohercynian domain the EC was further deformed by large scale open folding, localized shear zones, kink bands and faults (Fig. 4.4d, e). After the Variscan orogeny and exhumation, the post-tectonic intrusions caused a marginal contact-metamorphism of the EC.

Exact p/T-conditions as well as the sequence of deformation and metamorphism remain unclear. Stretched and broken andalusite grains on the foliation plane and parallel to the stretching lineation suggest quite low-pressure conditions for the main deformation similar to the so-called regional
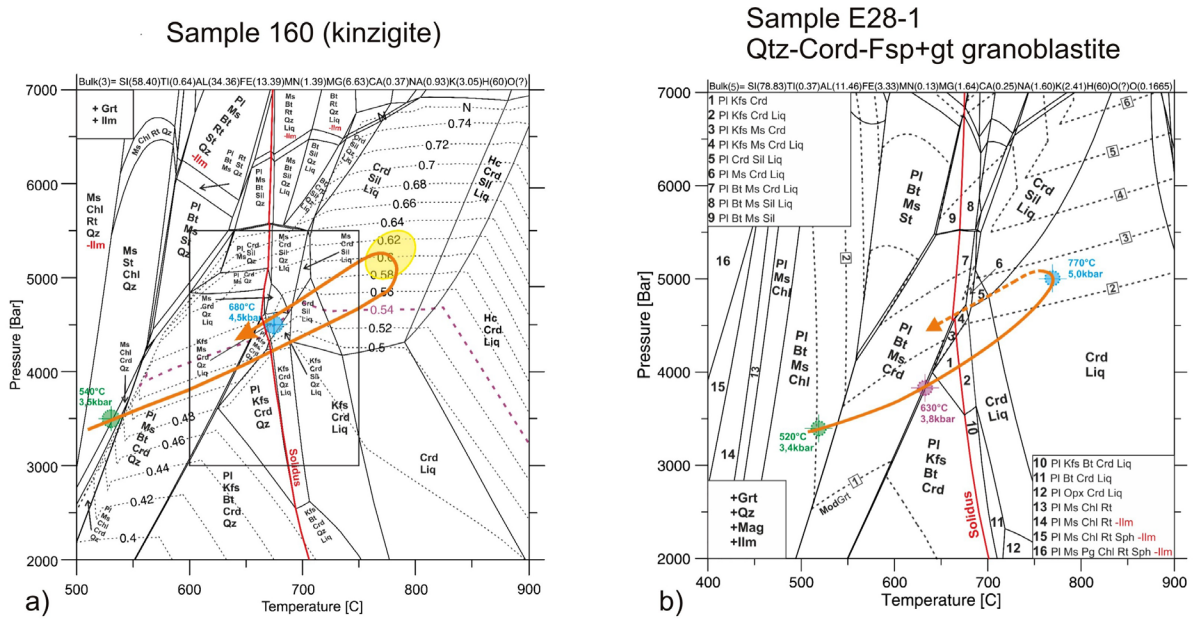
Figure 4.6: Equilibrium phase diagram of the a) kinzigite (sample 160A) and b) quartz-corderite-feldspar-garnet granoblastite (sample E28-1) (Kurtenbach 2020).

contact metamorphism in Variscan rock units of the Pyrenees (e.g., Mezger and Regnier 2016).

To better constrain the p/T-conditions, pseudosection calculations were carried out on one sillimanite-biotite-garnet-cordierite gneiss (kinzigite) and one quartz-cordierite(pinite)-feldspar-garnet granoblastite sample using Theriak-Domino. The pseudosections of the two samples indicate a prograde metamorphism at approximately 750-800°C and 500-550 MPa that is overprinted by a second static metamorphism at approximately 670-720°C and 450 MPa on an anticlockwise p/T-path (Fig. 4.6).

This is in accordance with the presence of sillimanite and inclusions of spinell as well as micro-
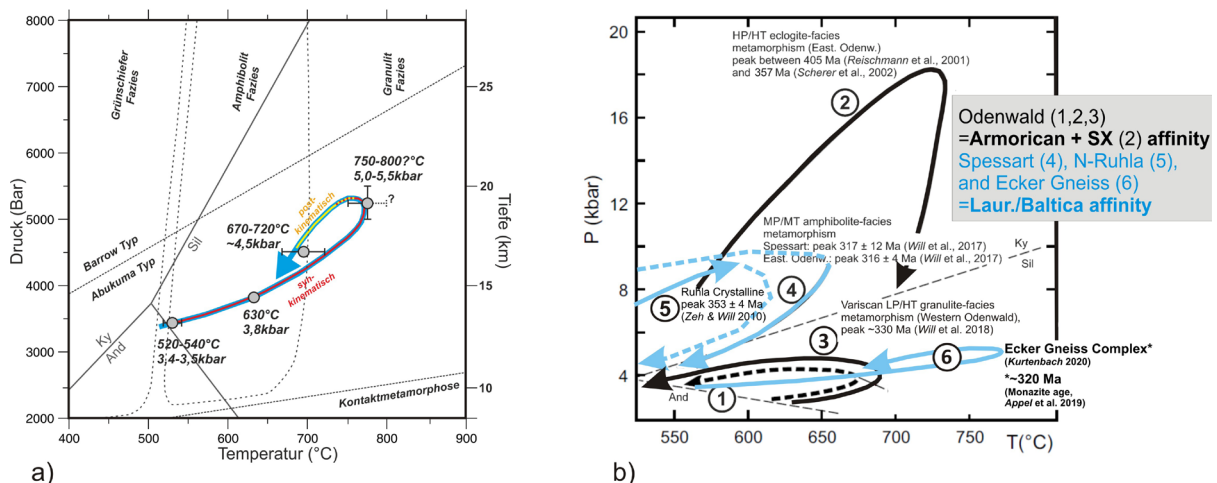
Figure 4.7: a) Conclusive pT-path for the Ecker Gneiss Complex (EC) of the study of Kurtenbach (2020); b) Provenance and pT-path diagrams of different units of the Mid-German Crystalline High (Will et al. 2017, 2018; Zeh & Will 2010, Dörr et al. 2017) in comparison to the provenance (Geisler et al. 2005) and pT-path of the EC (6, Kurtenbach 2020). (Figure modified after Will et al. 2017; reprinted with permission from Springer Nature). SX=Saxothuringian area (northern Böllstein Odenwald, Dörr et al. 2017). The ~320 Ma age of the Ecker Gneiss granulite-facies metamorphism is based on monazite dating (Appel et al. 2019, comp. Fig. 4.2).

structures of partial melting indicating previous higher temperatures and thus lower granulite facies metamorphic conditions at least for some parts of the EC. We interpret that the main foliation and stretching lineation were already formed under prograde metamorphic conditions (Fig. 4.7a). Then, after peak temperature and pressure, at least the investigated kinzigite sample was quite penetratively overprinted under amphibolite facies conditions. The relatively low pressure and high temperature metamorphic conditions together with the range of monazite age data indicate a very high thermal gradient for the Variscan lithosphere of the EC that lasted for at least 10-15 Ma. This Variscan high-grade metamorphism of the EC very likely developed within the Mid-German Crystalline Zone. Recent investigations show that the individual units of this zone are of different provenance and show a divergent pressure-temperature-time evolution regardless of their provenance, with the Eckergneiss representing a very intense HT metamorphism (Fig. 4.7b). Final exhumation and cooling of the EC to very low metamorphic grade at upper crustal conditions need to have taken place quickly along localized detachment faults, for example the Acker-Bruchberg Thrust Zone, until the end of the Variscan orogeny. Further post-Variscan tectonic overprinting is widespread across the EC, but preferentially in localized zones (e.g., Fig. 4.4e).

Outcrop description

In general, the outcrop conditions of the EC are rather poor. The two outcrops we are looking at are located near the Käsewieter bridge. In the first outcrop (A8) at the northern slope of the Ecker valley and ca. 60 m west of the bridge, some W-dipping shear zones and W-vergent folds with NW to NNW plunging axes are exposed (Fig. 4.8). The position of the fold axes within the shear zone plane may indicate a common formation of the two structures, for example, shearing parallel to fold axial planes (Fig. 4.8c, d).

The second outcrop ca. 200 m west of the bridge on the southern slope of the Ecker valley also shows fold structures. In this outcrop, a NW-SE striking open fold and a NE-SW striking tight fold are exposed immediately adjacent to each other (Fig. 4.9). Here, the hinge of the open fold has
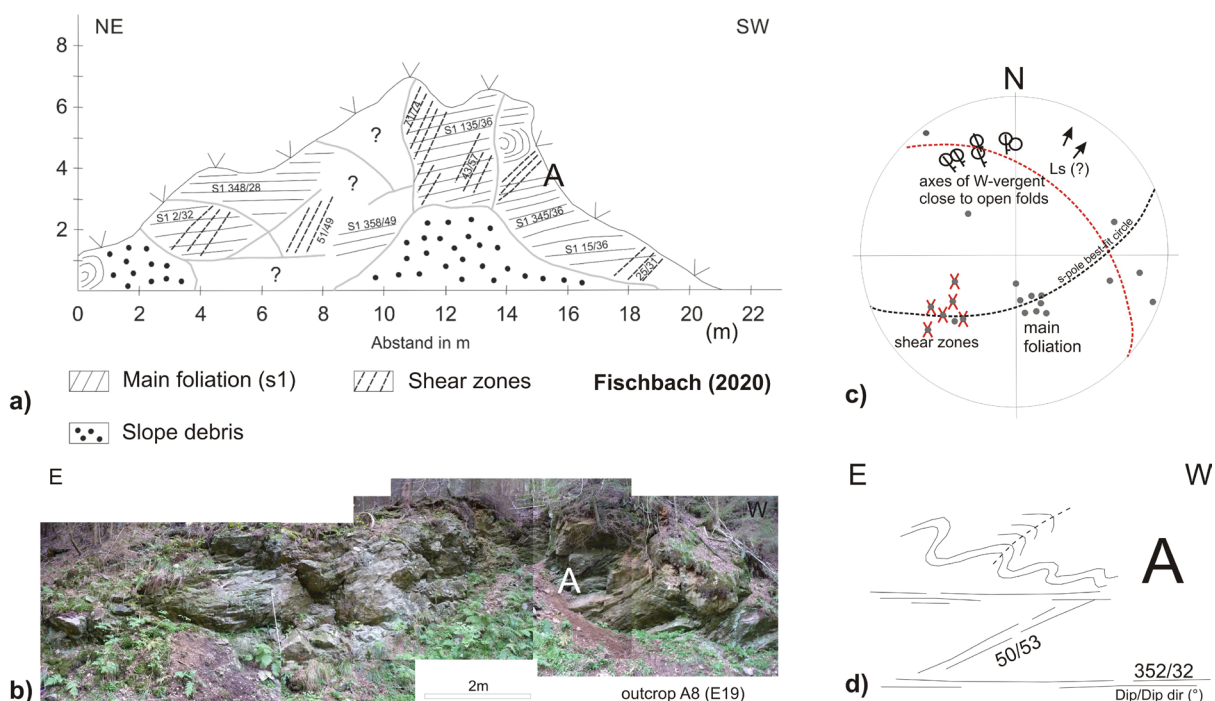
Figure 4.8: a) Drawing (Fischbach 2020) and b) photo of outcrop A8 ca. 60 m west of the Käsewieter bridge at the northern slope of the Ecker valley. Exposed are some shear zones and W-vergent close to open folds (area A); c) equal-area, lower hemispheric, stereographic projections of the main fabric, Ls = stretching lineation, red stippled great circle represents mean orientation of shear zone plane; d) sketch of the NW-SE striking folds and shear zones of area A. See text for further explanation.

a)

Outcrop A41/E18East), Ecker valley
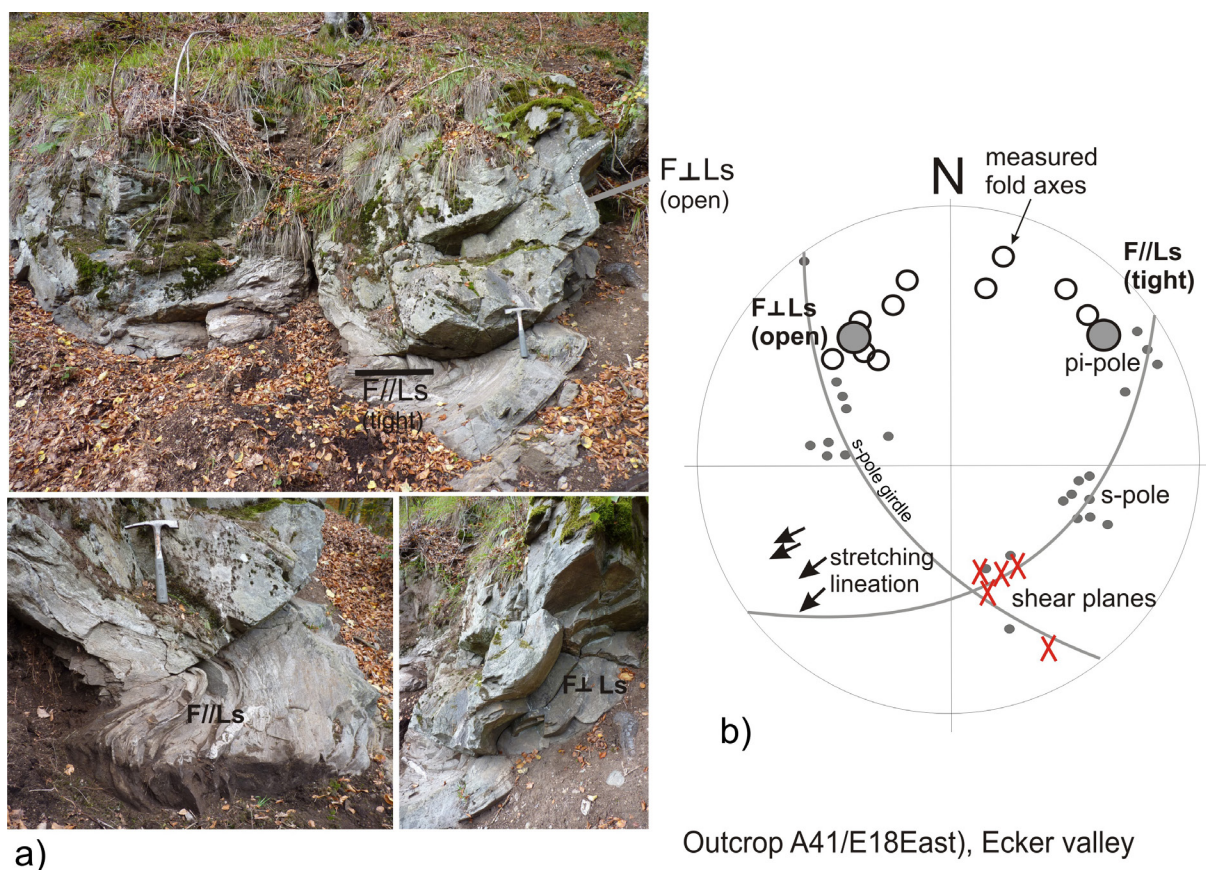
Figure 4.9: a) Photographs of outcrop A41 located ca. 200 m west of the Käsewieter bridge at the southern slope of the valley; b) equal-area, lower hemispheric, stereographic projections of the foliation poles and fold axes; rotation of the former NW-SE striking axes of the open folds towards the NE-SW trending stretching lineation, associated with interlimb tightening is suggested.

apparently been rotated and tightened subparallel to the NE-SW striking stretching lineation.

Regarding the differing orientations especially of folds with small interlimb angles (Fig. 4.3b), our field observations suggest that this scatter is due to the rotation of hinge lines of earlier folds by progressive deformation during continuous stretching and also with respect to deformation in obliquely oriented local shear zones (Figs. 4.8, 4.9).

References

Appel, P., Stipp, M.· Friedel, C.-H., Fiedrich, A., Kraus, K. & Berger, S. (2019): U–Th-total Pb ages of monazite from the Eckergneiss (Harz Mountains, Germany): evidence for Namurian to Westfalian granulite facies metamorphism at the margin of Laurussia. International Journal of Earth Sciences, 108, 1741-1753.

Dörr, W., Zulauf, G., Gerdes, A. & Loeckle, F. (2017): Provenance of Upper Devonian clastic (meta)sediments of the Böllstein Odenwald (Mid-German-Crystalline-Zone, Variscides). International Journal of Earth Sciences, 106, 2927-2943.

Fischbach, M. (2020): Strukturgeologische und Mikrogefüge-Untersuchungen im Eckergneis, Harz. Master thesis, Martin-Luther University Halle-Wittenberg.

Fischer, K. (2009): Petrographie und Deformationsgefüge im Eckergneis, Harz. Bachelor thesis, Martin-Luther University Halle-Wittenberg.

Geisler, T., Vinx, R., Martin-Gombojav, N. & Pidgeon, R.T. (2005): Ion microprobe (SHRIMP) dating of detrital zircon grains from quartzites of the Eckergneiss Complex, Harz Mountains (Germany): implications for the provenance and the geological history. International Journal of Earth Sciences, 94(3), 369-384.

Kraus, K. (2014): Strukturgeologische Untersuchungen im Eckergneis zwischen Bad Harzburg und dem Eckertal (Harz). Bachelor thesis, Christian-Albrechts-University Kiel.

Kurtenbach, St. (2020): Petrologische Untersuchungen im Eckergneis, Harz. Master thesis, Martin-Luther-University Halle-Wittenberg.

Mezger, J.E. & Regnier, L.-R. (2016): Stable staurolite–cordierite assemblages in K-poor metapelitic schists in Aston and Hospitalet gneiss domes of the central Pyrenees (France, Andorra). J. metamorphic Geol., 34, 167-190.

Will, T.M., Schmädicke, E., Ling, X.-X., Li, X.-H. & Li, Q.-L. (2018): New evidence for an old idea: Geochronological constraints for a paired metamorphic belt in the central European Variscides. Lithos, 302, 278-297.

Will, T.M., Schulz, B. & Schmädicke, E. (2017): The timing of metamorphism in the Odenwald–Spessart basement, Mid-German Crystalline Zone. International Journal of Earth Sciences, 106, 1631-1649.

Zeh, A. & Will, T.M. (2010): The Mid-German Crystalline Zone. In: Linnemann, U., Kroner, U. & Romer, R.L. (eds): From the Cadomian Active Margin to the Variscan Orogen: The pre-Mesozoic Geology of Saxo-Thuringia (NE Bohemian Massif). 195-220, E. Schweizerbart Science Publishers, Stuttgart.

Stop 5: Folded Lower Carboniferous cherts, Innerste valley, Lautenthal

Bernd Leiss [1], David C. Tanner [2]

1) Geowissenschaftliches Zentrum der Universität Göttingen, Goldschmidtstr. 3, D-37077 Göttingen

 bleiss1@gwdg.de

2) Leibniz Institute for Applied Geophysics, Stilleweg 2, D-30655 Hannover

davidcolin.tanner@liag-leibniz.de

Locality: small abandoned quarry of folded Culm cherts (two sections altogether 80m wide, ca. 4 to 10 m high) behind the primary school of Langelsheim-Lautenthal and southeast of the river Innerste as part of the geological trail "Lautenthal/Harz" (stop 1 in Stoppel 2002).
UTM co-ordinates: East 588923.095, North 5747831.324 (Zone 32N, WGS84)
Geographic co-ordinates: N 51° 52' 26.9976 E 10° 17' 30.1488 (WGS84)

The excellently exposed folds of this outcrop allow to study the geometries and fold mechanisms of rheologically-contrasting rock layers of Lower Carboniferous age. These folds at outcrop scale are representative of the autochthonous western Harz Mountains and allow to postulate the large-scale fold style (Friedel et al. 2019). Rheologically stiff layers, such as the bedded cherts composed of quartz-rich radiolarites (lydites) in the lower part, meta-tuffs (adinoles) in the upper part and a few greywackes with thicknesses up to 0.7 m dominate the intercalations with the subordinate, rheologically weak layers of slate with thicknesses up to a maximum of only a few centimetres Stratigraphically they are of Upper Tournaisian to Upper Visean age forming part of the Culm facies of the Lower Carboniferous/Mississippian (Zellmer 1996).
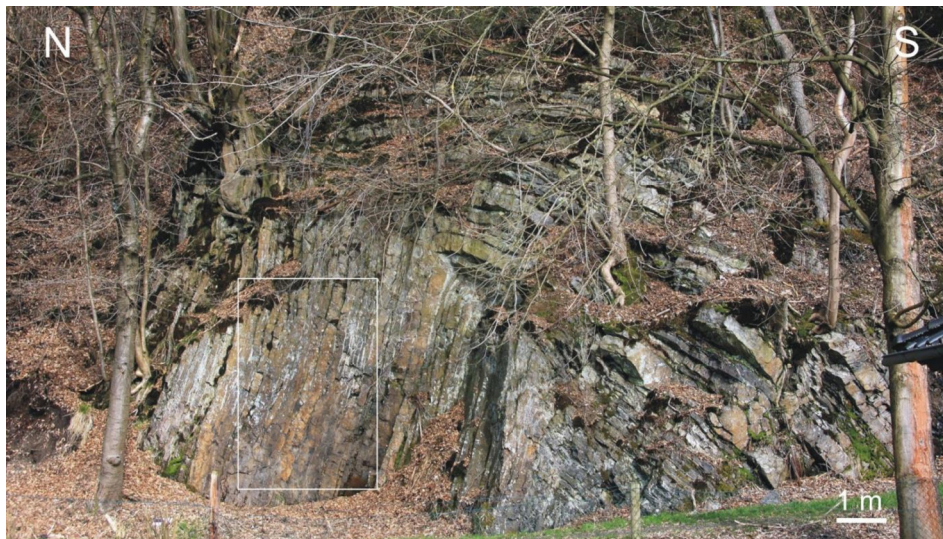
Figure 5.1: The middle part of the Lautenthal exposure with an antiform of the folded metasedimentary successions of lydite, meta-tuffs, greywackes and slates (from Wagner et al. 2016). White rectangle see Fig. 5.2a.

The disharmonic, NW-vergent antiforms with steeply NW-dipping or nearly vertical and moderate to sub-horizontal SE-dipping limbs show wavelengths between 1.5 m to 20 m with opening angles between 66° and 138° (Gössmann 2010) and nearly subparallel fold axes (Fig. 5.1). While the dominating stiff layers mechanically form mainly parallel folds, the weak layers of the slates form similar folds. Mechanically-related fold hinge thickening, however, does not work only by the displacement of the slate material, but also by brecciation and hinge filling of the stiff material as well
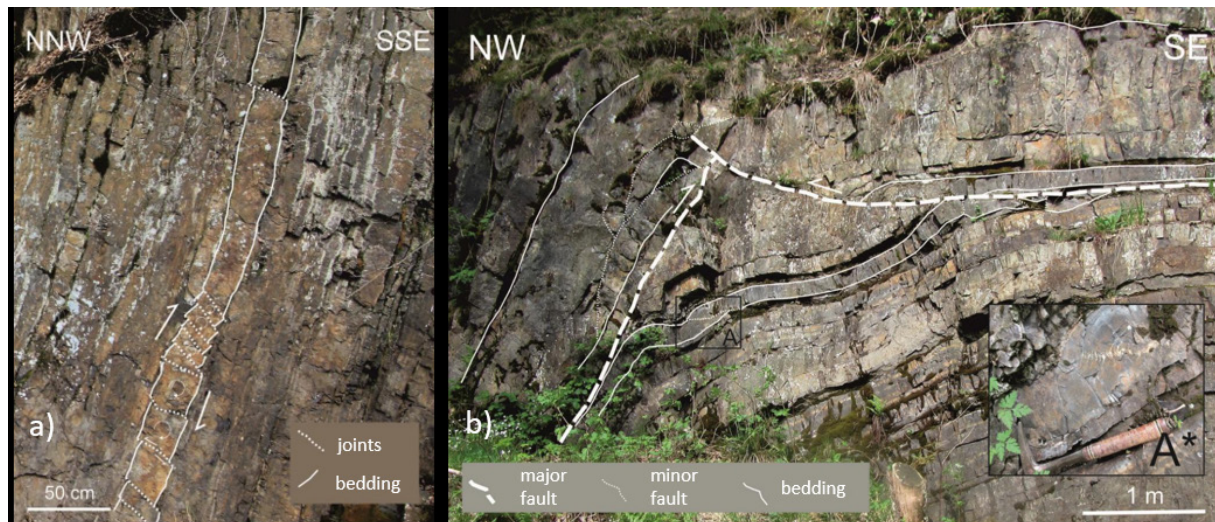
Figure 5.2: a) Close up of the books shelf structure in the steep limb of Fig 5.1 (see white rectangle) for the discussion of material mobilisation by Peacock & Leiss 2022, b) Triangle structure in the southern part of the exposure. The A*-marked close-up shows quartz-filled, en echelon tension gashes. Veins are well-represented in the exposure in manifold appearances.

as by mineralisation and small-scale thrusting. The cleavage of the slates dips to SE with 75° to 90° and the stiff layers show an intensive jointing normal to the bedding. Due to the flexural-slip fold mechanism, well-developed slickensides can be found on the bedding planes. In the NW part of the outcrop, nicely-developed bookshelf structures can be observed in a steeply-dipping fold limb (Fig. 5.2a).

Material displacement of the weak clay or slate material, which allowed blocks of the stiff layer to rotate, provokes the discussion on the condition of the clay/slate during this deformation (Peacock & Leiss 2022). In the SW-part of the exposure, a well-developed triangle zone is exposed (Fig. 5.2b). In contrast to the triangle zone of Stop 7 of this excursion (see also Tanner et al. 2010), the internal structure is not visible due to a joint surface coating.

For the exploration and exploitation of the deep geothermal potential of the Variscan fold and thrust belt beneath Göttingen, the western Harz mountains are utilised as an analogue study area (Leiss et al. 2022). This exposure plays a key role in view of the question on the scale invariance between outcrop and reservoir (km-)scale (Figs. 5.1 to 5.4). Previous and ongoing work focuses on the quantification of the fold structures. Gössmann (2010) carried out cross-section balancing, Stöpler (2017) and Zahnow (2017) acquired 3D-surveys by means of photogrammetry and laserscanning, and Walther (2021) has just finished the modelling of sections at a larger scale in this region for a basis of a local structural 3D-model (Fig. 5.3). This will be the interlink to a reservoir scale 3D-structural model of the western Harz Mountains (Abdelkhalek et al. 2022, Leiss et al. 2022). For further details of this exposure, see Stoppel (2002) and Wagner et al. (2016).
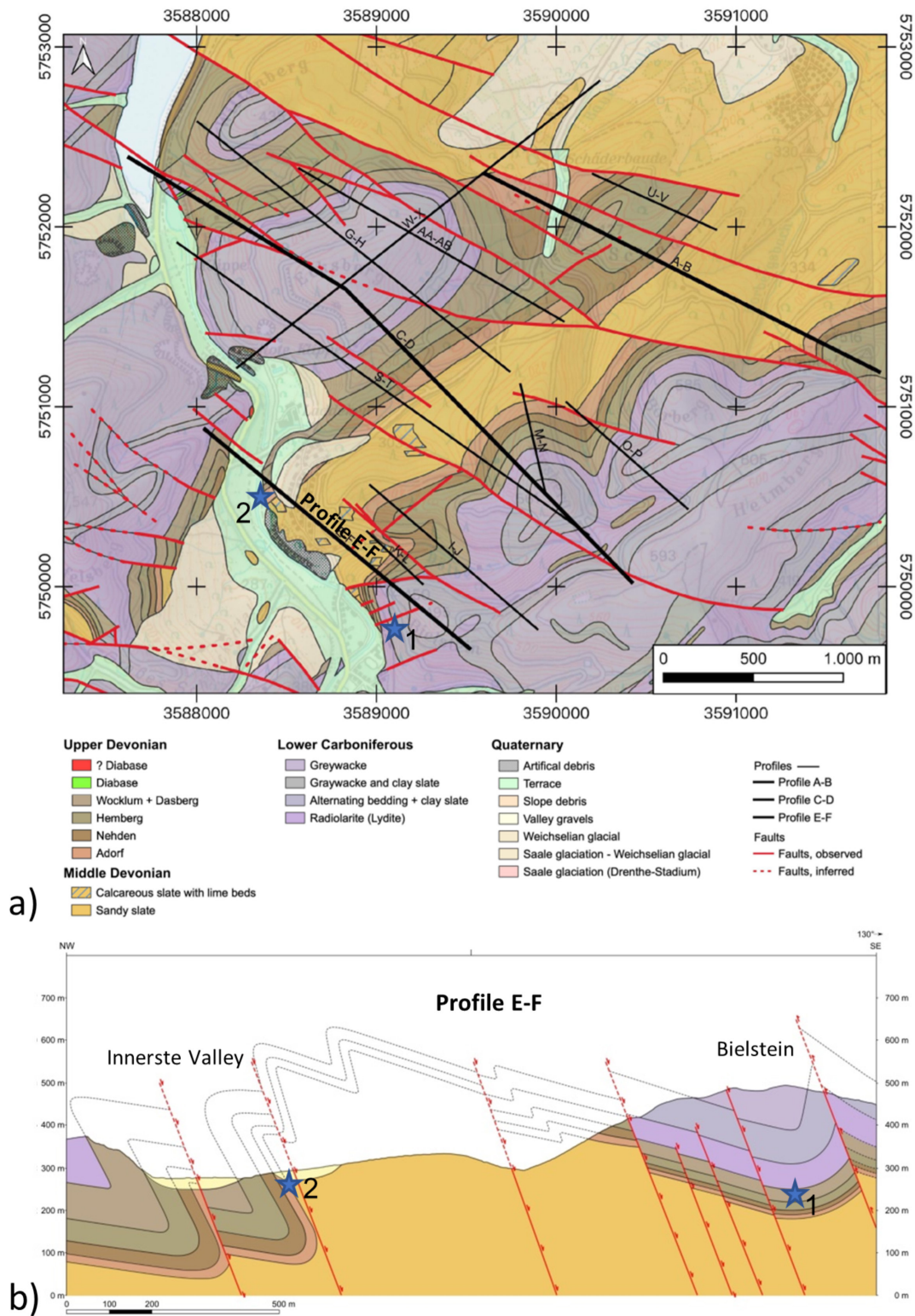
Figure 5.3: a) Geological map (originally 1:15,000 scale) showing the geological units and faults in the terrain around Lautenthal in the western Harz Mountains. The geological map is modified from Eickhoff (1962) and Hinze (1976). The coordinate system is DHDN/3-degree Gauss-Kruger zone 3 (EPSG: 31467). Star1 = Location of this stop 5; Star2 = Location of stop 6. b) The NW-SE cross-section E-F represents the local NW-verging Variscan folds for the Innerste Valley and Bielstein area. The folds are offset by syn- to post-Variscan faults and strike-slip faults (from Walther 2021).
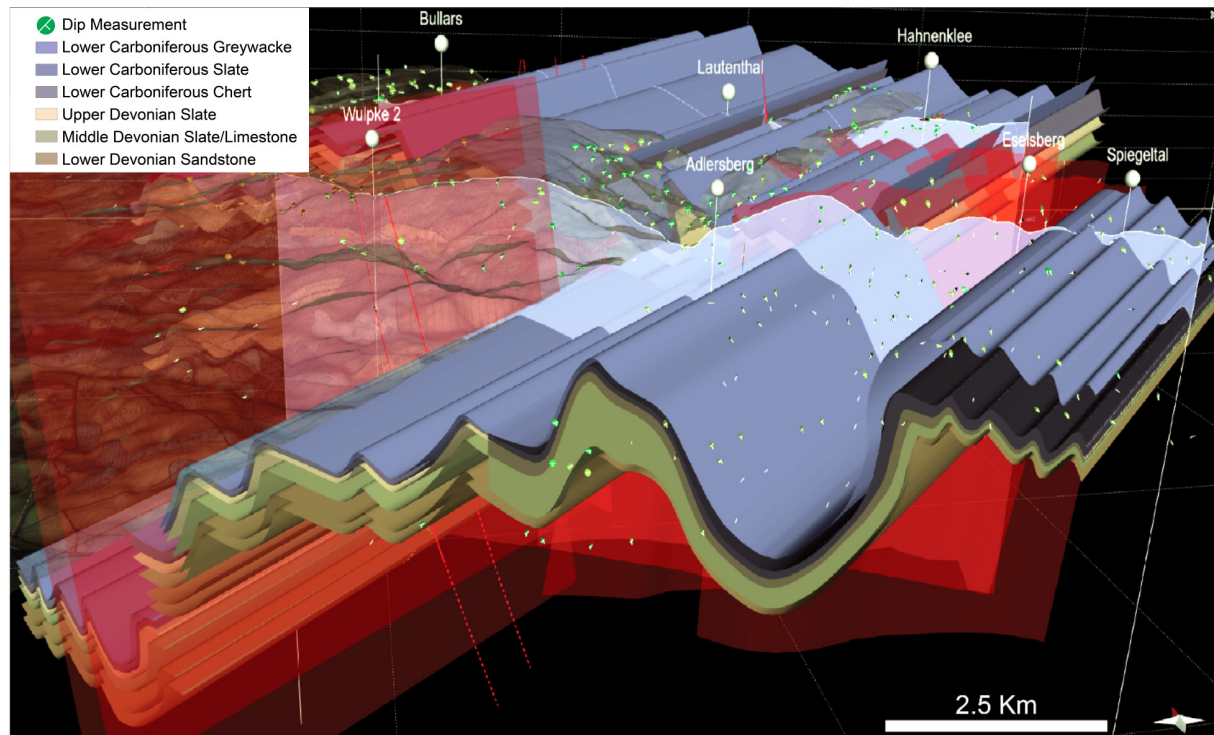
Figure 5.4: 3D structural model of the analogue area in the western Harz Mountains, northern Germany. This model was constructed using a database of field measurements and borehole data (Brinckmann and Brüning, 1986). It shows the Carboniferous and Devonian strata folded and faulted during the Variscan Orogeny at deep geothermal reservoir scale. Fault planes are shown in semi-transparent red. These faults may control either compartmentalisation of the reservoir or the fluid flow and pressure distribution in the target zones (from Abdelkhalek et al. 2022, see also Leiss et al. 2022).

References

Abdelkhalek, A., Leiss, B., Peacock, D.C.P. & Wagner, B., (2022): 3D structural modelling of Variscan metasedimentary rocks in the western Harz Mountains, Germany: implications for geothermal exploration. TSK19-Abstract-Volume, p. 80.

Eickhoff, H.G. (1962): Zur Stratigraphie Und Tektonik Des Oberdevons Nördlich Lautenthal/Harz (Mtb. Seesen 4127). Unpublished Diploma thesis, Georg-August-Universität, Göttingen.

Friedel, C.-H., Huckriede, H., Leiss, B. & Zweig, M. (2019): Large-scale Variscan shearing at the south-eastern margin of the eastern Rhenohercynian belt: a reinterpretation of chaotic rock fabrics in the Harz Mountains, Germany. Int. J. Earth Sci. (Geol. Rundsch.), 108, 2295-2323 (2019). doi.org/10.1007/s00531-019-01763-1.

Hinze, C. (1976): Geologische Karte von Niedersachsen 1:25000. Erläuterungen zu Blatt Seesen Nr. 4127, Erl., 4127. Niedersächsisches Landesamt für Bodenforschung, Hannover, 152 S.

Leiss, B., Peacock, D.C.P., Wagner, B., Abdelkhalek, A., Luijendijk, E., Ford, K., Sosa, G., Klee, J., Chabani, A., Trullenque G., Vanbrabant, Y., Wynants, M.-A., Cabidoche, M., Leclercq, V., Hebert, R., Ledésert, B., Turan, A., Bossenec, C. & Bär, K. (2021): Field-based characterisation of the four reservoir types completed, MEET report, Deliverable D5.9, August 2022, 207 pp., https://www.meet-h2020.com/project-results/deliverables/.

Gössmann, N. (2010): Strukturanalyse karbonzeitlicher Kieselschiefer im Oberharz. Unpublished BSc thesis, Course of studies Geosciences of the Leibniz Universität Hannover, Germany, 42 S.

Peacock, D.C.P. & Leiss, B (2022): Models for the origins of chaotic meta-sedimentary rocks in the Harz Mountains, Germany. TSK19-Abstract-Volume, p. 80.

Tanner, D.C., Brandes, C. & Leiss, B. (2010): Structure and kinematics of an outcrop-scale, fold-cored triangle zone. Bulletin of the American Association of Petroleum Geologists, 94/12, 1799–1809. doi: 10.1306/06301009188.

Stöpler, R. (2017): Digitale 3D-Geländeaufnahme und strukturelle Analyse gefalteter Kieselschiefer im Nordwestharz/3D-Surveying and structural analysis of folded cherts in the Northwest of the Harz-mountains. Unpublished MSc thesis, University of Göttingen, Germany.

Stoppel, D. (2002): Der Geologische Lehrpfad. In: Bergwerks- und Geschichtsverein Bergstadt Lautenthal von 1976 e.V. (eds.): Lautenthal - Bergstadt im Oberharz, Bergbau und Hüttengeschichte, p. 293-301 (last access: 30.03.2022).

Wagner, B., Leiss, B. & Tanner, D.C. (2016): Gefalteter unterkarbonischer Kieselschiefer am Bielstein nördlich Lautenthal (Innerstetal). In: Friedel, C.-H. & Leiss, B. (eds.): Harzgeologie 2016. 5. Workshop Harzgeologie – Kurzfassungen und Exkursionsführer. Göttingen Contributions to Geosciences, 78, 69-78. doi.org/10.17875/gup2016-1000.

Walther, C. (2021). 3D structural modeling of Variscan fold-and-thrust belts in the Devonian-Lower Carboniferous sequences of the Upper Harz Mountains, Germany. Unpublished MSc thesis, University of Göttingen, Germany.

Zahnow, F. (2017): Strukturanalyse unterkarbonischer Kieselschiefer im Nordwestharz mit Hilfe von terrestrischem Laserscanning und 3D-Modellierung/Structural analysis of Lower Carboniferous cherts in the Northwest of the Harz-mountains based on Terrestrial Laser Scanning and 3D-modelling. Unpublished MSc thesis, University of Göttingen, Germany.

Zellmer, H. (1996): Stratigraphie und Petrographie der Kieselschiefer-Fazies im Harz (Mitteldevon - Unterkarbon). Braunschweiger geowiss. Arb., 19, 72 S., Braunschweig.

Stop 6: Internal structure and kinematic of a Variscan thrust fault - the Sparenberg Breccia at Lautenthal

Friedel, C.-H. [1], Schmidt, M. [2], Leiss, B. [3]

1) Karl-Marx-Str. 56, 04158 Leipzig, chfriedel@gmx.de

2) Fachdienst Umwelt Stadt Göttingen, Neues Rathaus Hiroshimaplatz 1-4, 37083 Göttingen, m.schmidt2@goettingen.de

3) Geowissenschaftliches Zentrum der Universität Göttingen, Strukturgeologie und Geodynamik
Goldschmidtstr. 3, 37077 Göttingen, bleiss1@gwdg.de

Locality: Innerste valley, NW of Lautenthal, at the foot of the western slope of the Sparenberg hill
UTM Co-ordinates: East: 588319.053 North 5748585.031 (Zone 32N)
Geographic co-ordinates: N 51° 52'51.733", E 10°16'59.264"

In the Innerste Valley near Lautenthal there is a classic geological cross-section that exposed beds of Middle Devonian to Lower Carboniferous beds of the Oberharz Devonian Anticline. The outcrops belong to a geological educational trail that runs along the north-eastern side of the Innerste River (Stoppel 2002, see also Stop 5). The site itself is described as stop 6 in Stoppel (2002).

On the western flank of the Sparenberg, in overturned position, from south to north, there are exposures of Wissenbacher Shale (Eifelian, old slate quarry), cleaved mudstone with calcareous nodules (Givetian) and lumpy limestone (Stringocephalus limestone) of the upper Givetian. Further to the north follow clayey and banded marly slates ("Adorf" beds, with Kellwasser carbonates), followed by green and red slates and slates with calcareous nodules of the Upper Devonian (Stoppel & Zscheked 1973, Stoppel 1977b, 2002). The entire sequence is penetratively cleaved, and forms the overturned limb of a large-scale NW-verging fold (Müller & Franzke 2014).

At the actual outcrop the boundary of the Middle/Upper Devonian is exposed (Givetian/Frasnian boundary). The outcrop, starts at the valley level and extends for ca. 10 m upslope. On the slope, below the overturned Givetian slates, an several meters thick block-in-matrix structure is exposed, consisting of blocks of broken Stringocephalus limestone embedded in a clayey-marly matrix (Figs. 6.1, 6.2). The commonly well bedded Stringocephalus limestone is broken into separate blocks and these blocks are mostly displaced and rotated (Figs. 6.2, 6.3). The fragmented blocks reach a size of ca. 1 m. The matrix also contains many small, angular, partially lenticular clasts of limestone (Figs. 6.4b, c). Apart from limestone blocks, some clasts are composed of dark shales/slates. Reworked older limestones have not been observed (Stoppel 1977b).

This exposure was interpreted by Stoppel & Zscheked (1963) to be a sedimentary breccia (by sedifluction), whereby the chaotic orientation of the blocks was used as an argument for the sedimentary origin of the textures (Stoppel 1977a, b). The authors attributed the brecciation to early diagenic sliding (subaqueous sedimentary gliding) and described the outcrop to represent an occurrence of submarine block or mud-slides (Stoppel & Zscheked 1963, Stoppel 1977b). For this reason, this outcrop was the key to the hypothesis that submarine sliding and redeposition took place in the Middle and Upper Devonian in the western Harz (e.g. Stoppel & Zscheked 1963, Stoppel 1977a, b, Buchholz et al. 1989, 1990).

Friedel & Zweig (2013) and Schmidt (2013) reinterpreted this outcrop as a tectonic breccia. The basis for this view is the spatial arrangement of the limestone blocks. Texture measurement show that the blocks are not chaotically arranged. The poles of the bedding planes of the clasts in the breccia form a great-circle distribution with the pole plunging shallowly NE/ENE. This is the orientation of the regional Variscan fold axes (Fig. 6.5). This orientation also applies to the small-scale fold axes in the breccia and along the interface with the Givetian slates above (drag folds; Figs. 6.3, 6.5b). In
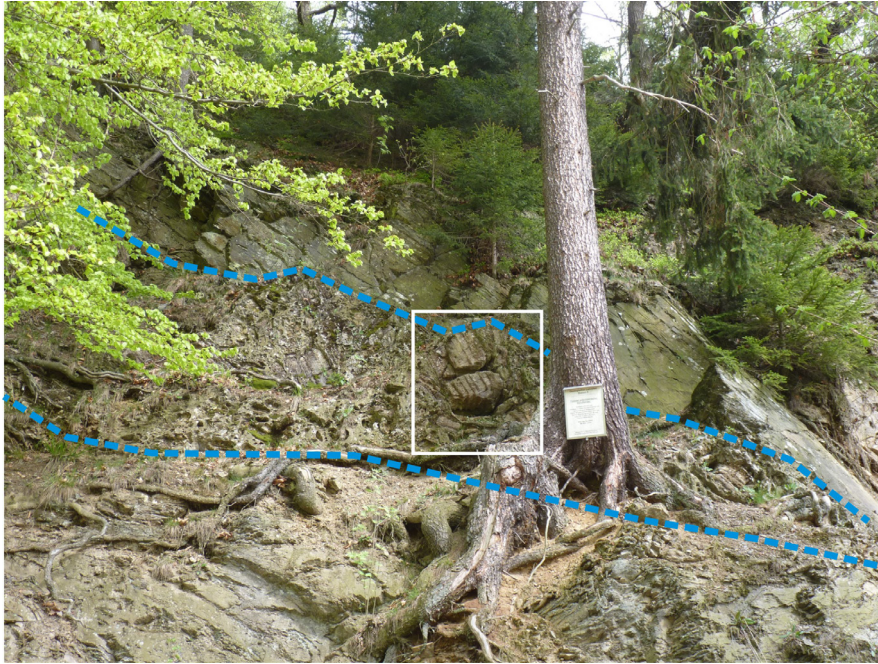
Figure 6.1: Outcrop at the western flank of the Sparenberg hill (Station 6 of the geological trail, Stoppel 2002). Photo from May 2013 (Friedel & Leiss 2015). The blue line marks the area with block-in-matrix fabrics (breccia) below the calcareous nodule-bearing slates (cf. Fig. 6.2a). The rectangle marks the area of Fig. 6.3a.

addition, the cleavage of the limestone clasts is also rotated with the bedding and fits to the great-circle arrangement of the rotated bedding planes (Fig. 6.5b). In limestone, the cleavage is formed by narrow to anastomosing planes that have a steep angle to the bedding (Fig. 6.4). Thin-section and cathode-luminescence microscopy prove that the steep, flaser-like appearance of the cleavage was caused by pressure-solution; a crystallographic preferred orientation in the limestone is not developed (Schmidt 2013).

The block-bearing clayey matrix is also somewhat cleaved. The cleavage of the matrix is evident in the preferred orientation of smaller limestone blocks (Fig. 6.4b). Occasionally, shear fabrics occur on the edges of limestone blocks so that the blocks are torn apart and filled with the clayey matrix (Fig. 6.4b, c).

A spectacular occurrence of displaced limestone blocks shows Figure 6.3b. Immediately at the edge of the slate, some blocks are even vertically erected. Only one metre further up, the limestone is again in its original position, parallel to the dip of the slate (cf. Fig. 6.2b). Due to the steep position of the limestone blocks, the area below was obviously also folded or broken (white arrow in Fig. 6.3b). It is also noticeable that the flat shear planes between the misaligned limestone clasts are often tied to protrusions and folds in the clayey slate along the interface with the intact slate above (Fig. 6.2b). The shallowly-branching shear planes thus indicate this interface is itself a thrust fault. Thrusting is also indicated by the bending of the slates below the major shear plane (right side of Fig. 6.6). The complex normal- and reverse-faulting in the adjacent stratigraphically younger area could also have developed as a reaction to the deformation of the limestone strata by this thrust zone (Fig. 6.6).

Conclusions

The great-circle distribution of the bedding and cleavage fabrics of the blocks and its correspondence with fold axes of regional fold structures are clear evidence that the structure of this breccia is not sedimentary, but Variscan in origin, and developed due to tectonic shearing. Subsequent foliation of previously atectonically steeply reoriented or inclined limestone blocks by cleavage refraction offers no explanation for this Variscan type great-circle distribution of the block structure.
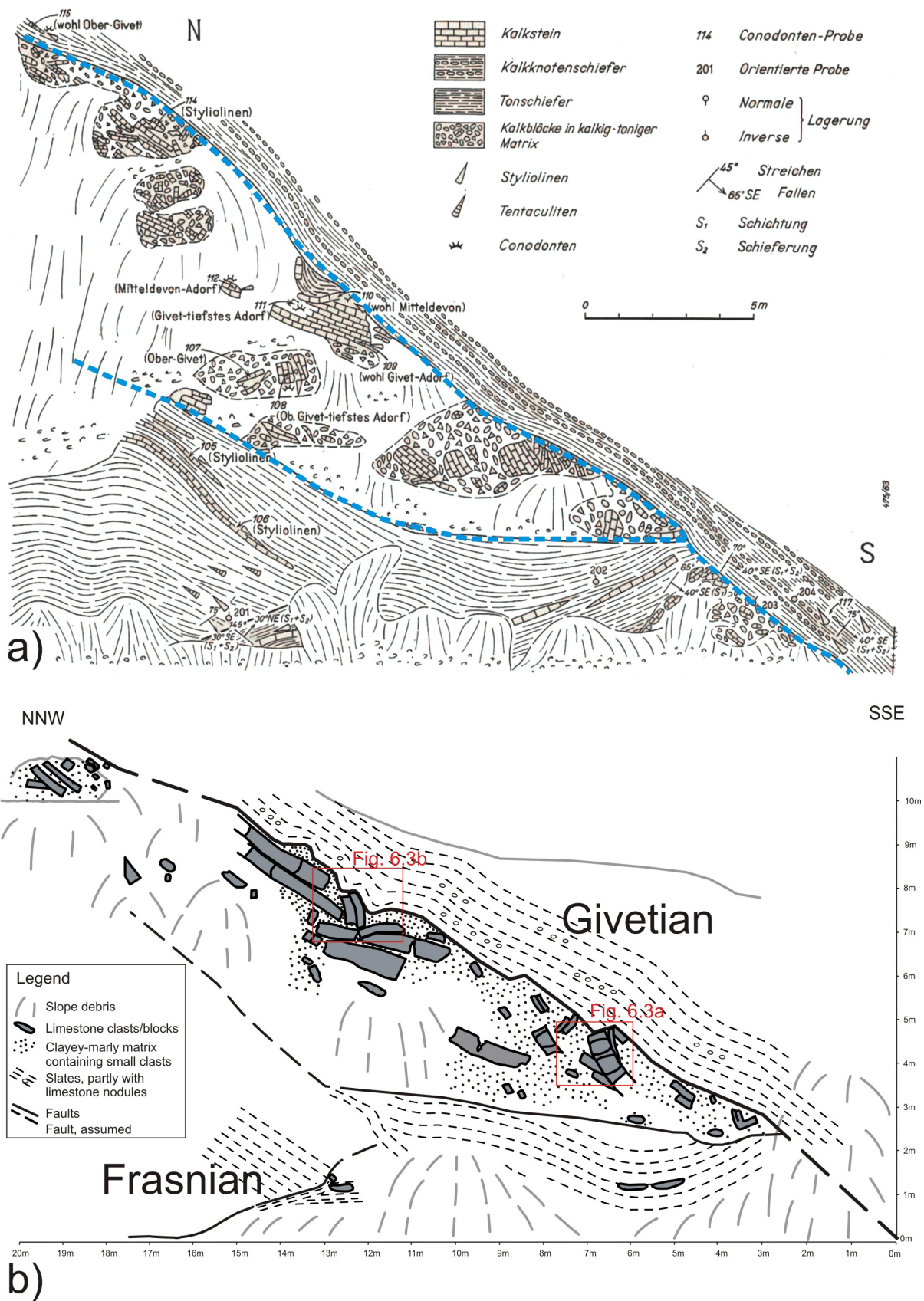
Figure 6.2: a) Geological sketch of the breccia ("Sedifluction horizon") of Stoppel & Zscheked (1963, Fig. 6.1). b) Sketch from the same outcrop 50 years later (Schmidt 2013; from Friedel & Leiss 2015).
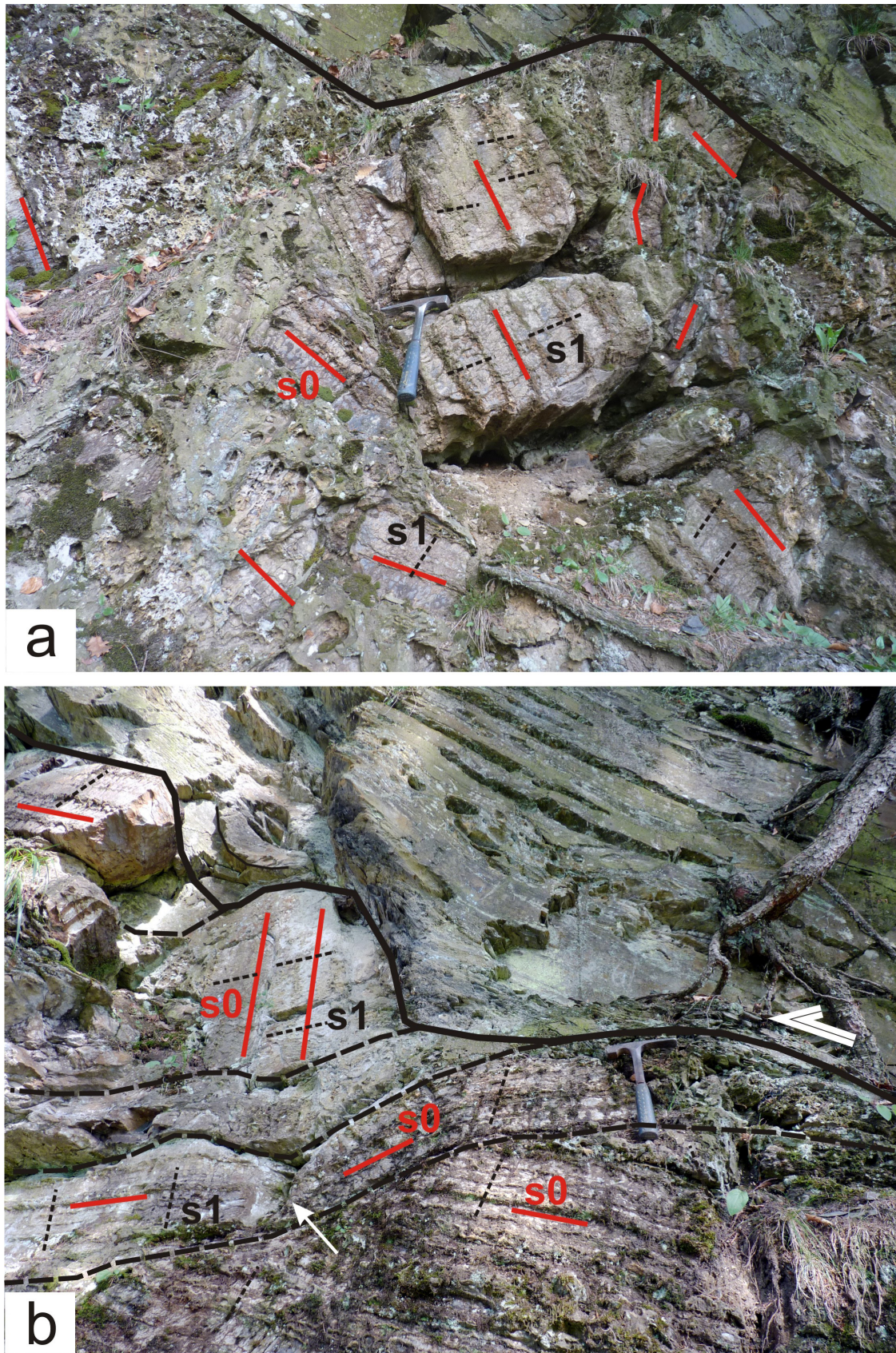
Figure 6.3: a), b) Rotated limestone blocks of the breccia (location of photos see Figure 6.2b, s0: bedding, s1: cleavage, from Friedel & Leiss 2015). With rotation of the limestone blocks, their pressure solution cleavage was also rotated. Note the flat-dipping faults branching from the main shear plane on the right side (b, comp. Fig. 6.6).
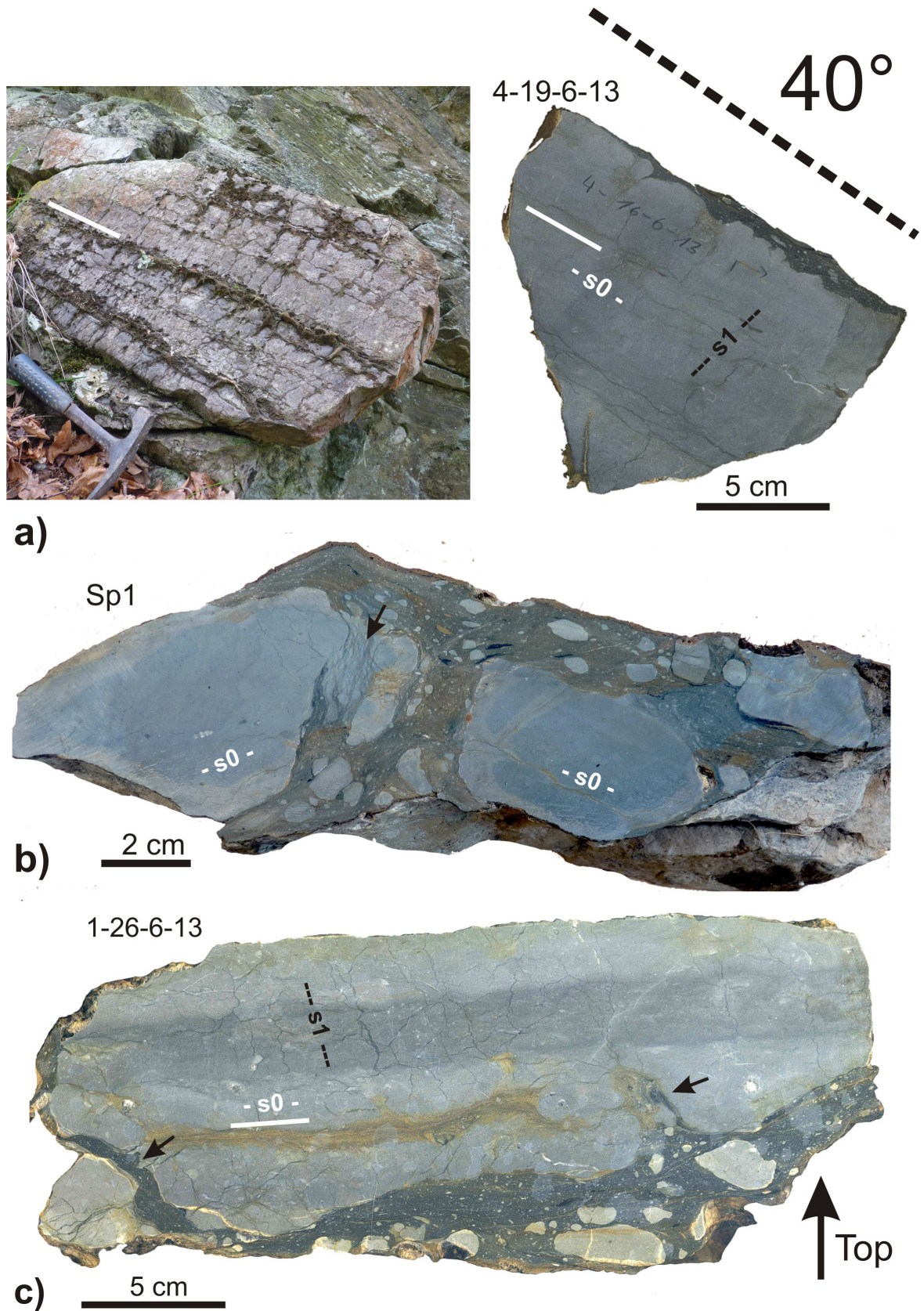
Figure 6.4: a) Well-developed pressure solution cleavage in Stringocephalus limestone (right: polished section). b) Two oppositely-rotated clasts. The matrix is foliated. Note the strong deformed shear fracture on the left clast (arrow). c) Limestone clast with some fractures parallel to the cleavage (arrows). s0: stratification, s1: foliation. All clasts are arranged in their position to the main shear plane (40°, dotted line) (Friedel & Leiss 2015).

a) Slate in the further vicinity

Bedding (n=23)   π-pole
Cleavage (n=15)

062/12
best-fit circle
of bedding poles

b) Brecciated area

Bedding of blocks/clasts (n=46)   π-pole
Cleavage of blocks/clasts (n=18)
Small scale folds
Main shear plane

075/17
best-fit circle
of bedding poles
of blocks
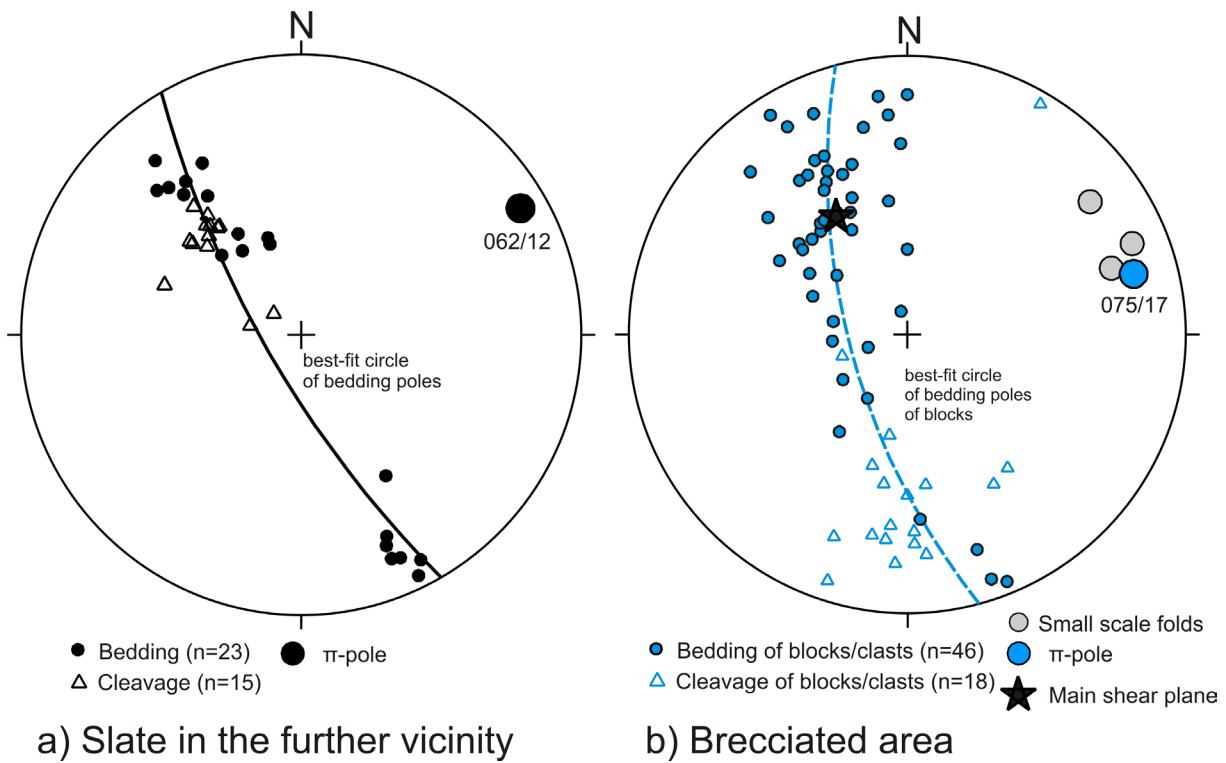
Figure 6.5: a) Equal-area, lower hemispheric, stereographic projections of the Variscan structure elements from the Middle and Upper Devonian rocks outcropping along the Innerste river on the SW foot of the Sparenberg hill. b) Spatial arrangement of bedding and cleavage planes of limestone blocks in the breccia. The cleavage of rotated blocks is also rotated and fits to the Variscan great-circle distribution of their bedding planes of blocks (see text). The interface to the slates on top is the main shear plane of the tectonic breccia (cf. Fig. 6.6; Friedel & Leiss 2015).
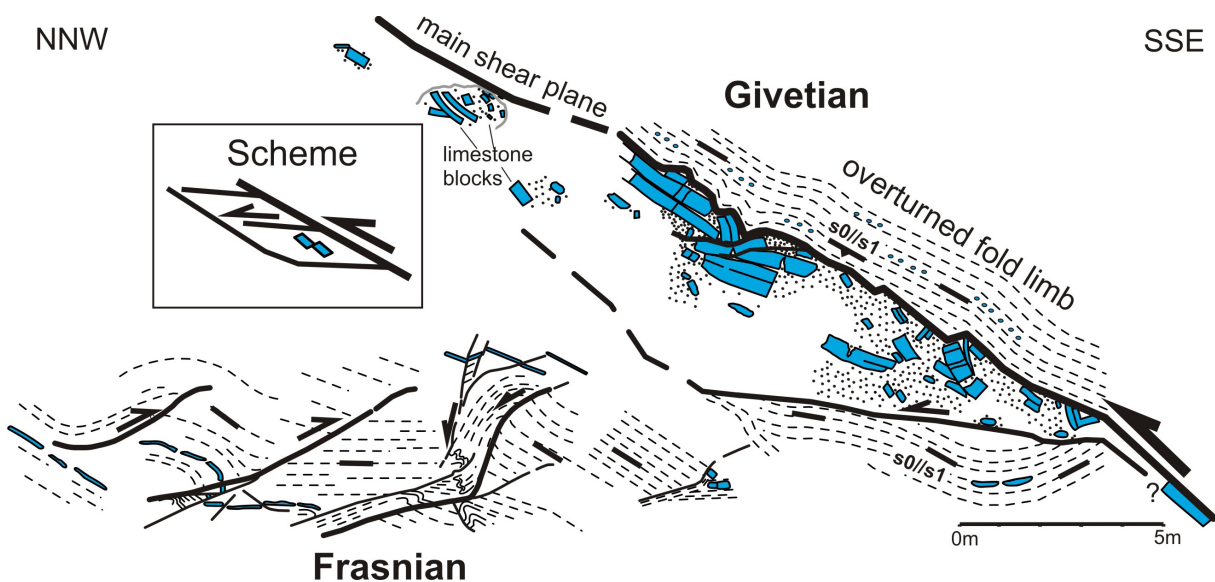
Figure 6.6: Sketch of the breccia area and the slate in the NW (stratigraphically the hanging wall). Faults branching off from the main thrust (right) led to the brecciation and created the space for this tectonic breccia (see scheme). The complex reverse- and normal-faulting in the NW probably have originated in response to the thrust movement of the main shear plane (Friedel et al. 2019; reprinted with permission from Springer Nature).

The spatial position and formation of the blocks indicate the effectiveness of brittle-ductile over-thrust tectonics in a late phase of folding and cleavage development. The main shear plane was the interface with the overturned intact calcareous nodule-bearing clayey Givetian slates on the top. Pull-apart-like extensional structures associated with the thrust tectonics probably created the necessary space to accommodate the brecciated limestone blocks and their matrix (Fig. 6.6). Tectonic shearing and fragmentation was apparently accompanied by increased fluid pore pressure, resulting in a cataclastic breccia structure.

Instead of a mudflow deposit, we interpret this outcrop as a tectonic breccia. This calls into question this outcrop as a frequently-cited example of Devonian mass-sliding. This observation applies not only here, but also to other outcrops in the Harz Mountains that were formerly interpreted as submarine mudflows or large mass-flow deposits (Friedel & Leiss 2015, Friedel et al. 2019).

References

Buchholz, P., Wachendorf, H. & Zweig, M. (1989): Synsedimentäre versus tektonische Deformation: Rutschung, Schlammstrom, Olisthostrom und Mélange. Dt. geol. Ges., 141. Hauptvers., Exkursionsführer, Exkursion E4, 139-170, Braunschweig.

Buchholz, P., Wachendorf, H. & Zweig, M. (1990): Resedimente der Präflysch- und der Flysch-Phase – Merkmale für Beginn und Ablauf orogener Sedimentation im Harz. N. Jb. Geol. Paläont., 179, 1-40, Stuttgart.

Friedel, C.-H. & Zweig, M. (2013): Bimrockexkursion Harz. Exkursionspunkt 3: Tektonische Brekzie statt Schlammstromsediment am Sparenberg. Hall. Jb. Geow. Beiheft, 31, 21-25, Halle/S.

Friedel, C-H. & Leiss, B. (2015): Variszische Tektonik im Harz (östliches Rhenoherzynikum). In: Röhling, H.-G. (ed.): GeoBerlin 2015. DYNAMISCHE ERDE – von Alfred Wegener bis heute und in die Zukunft. Exkursionsführer. Exkursionsführer und Veröffentlichungen der Deutschen Gesellschaft für Geowissenschaften, 255,44-86.

Friedel, C.-H., Huckriede, H., Leiss, B. & Zweig, M. (2019): Large-scale Variscan shearing at the southeastern margin of the eastern Rhenohercynian belt: a reinterpretation of chaotic rock fabrics in the Harz Mountains, Germany. Int. J. Earth Sci. (Geol. Rundsch.), 108, 2295–2323 (2019). doi.org/10.1007/s00531-019-01763-1.

Müller, H., & Franzke, H.J. (2014): Oberharz. Tiefe Gruben und hohe Rücken. Streifzüge durch die Erdgeschichte, 1-144, Quelle & Meyer, Wiebelsheim.

SCHMIDT, M. (2013): Gefügecharakterisierung devonischer „Block-in-Matrix-Gesteine" vom Sparenberg, Lautenthal im Harz. Bachelorarbeit, 51 S., Geowiss. Zentrum Göttingen, Georg-August-Universität, Göttingen.

STOPPEL, D. (1977a): Schlammstrom-Sedimente im Oberdevon des Südwestharzes und des südlichen Kellerwaldgebirges. Z. dt. geol. Ges., 128, 81-97, Hannover.

STOPPEL, D. (1977b): Aufschluß 1: Innerste-Ufer am Sparenberg. Exkursionsführer Geotagung 1977, Exkursion H, 179-181,Göttingen.

STOPPEL, D. (2002): Der geologische Lehrpfad. In: Bergwerks- und Geschichtsverein Lautenthal (eds): Lautenthal, Bergstadt im Oberharz, Bergbau und Hüttengeschichte, 293-301, Lautenthal.

STOPPEL, D. & ZSCHEKED, J.G. (1963): Frühdiagenetische Sedifluktionen im Mittel- und Oberdevon des Westharzes. Ber. Naturhist. Ges., 107, 5-18, Hannover.

Stop 7: Triangle Zone in Lower Carboniferous siliclastics

David C. Tanner [1], Bernd Leiss [2]

1) Leibniz Institute for Applied Geophysics, Stilleweg 2, D-30655 Hannover

davidcolin.tanner@liag-leibniz.de

2) Geowissenschaftliches Zentrum der Universität Göttingen, Strukturgeologie und Geodynamik Goldschmidtstr. 3, 37077 Göttingen, bleiss1@gwdg.de

Locality: small outcrop (6m wide, ca. 4m high), set off the road (ca. 10m), on the embankment road, south of the hill Schadleben on the east side of the Okertal reservoir

UTM co-ordinates: East 600286.378, North 5744550.657 (Zone 32N, WGS84)

Geographic co-ordinates: N 51°50'33.904" E 10°27'20.758"

At this locality an alternating succession of dark-grey argillaceous slates and fine grey-beige silt-stone beds is exposed (Culm alternating succession of Upper Visean age, Mississippian). The 6-metre wide outcrop displays a complex structural enclave, bounded by an upper north-west dipping detachment and a lower south-east dipping detachment (Fig. 7.1). The detachments converge and tip-out to the north-west to give the triangular shape, known as a triangle zone.
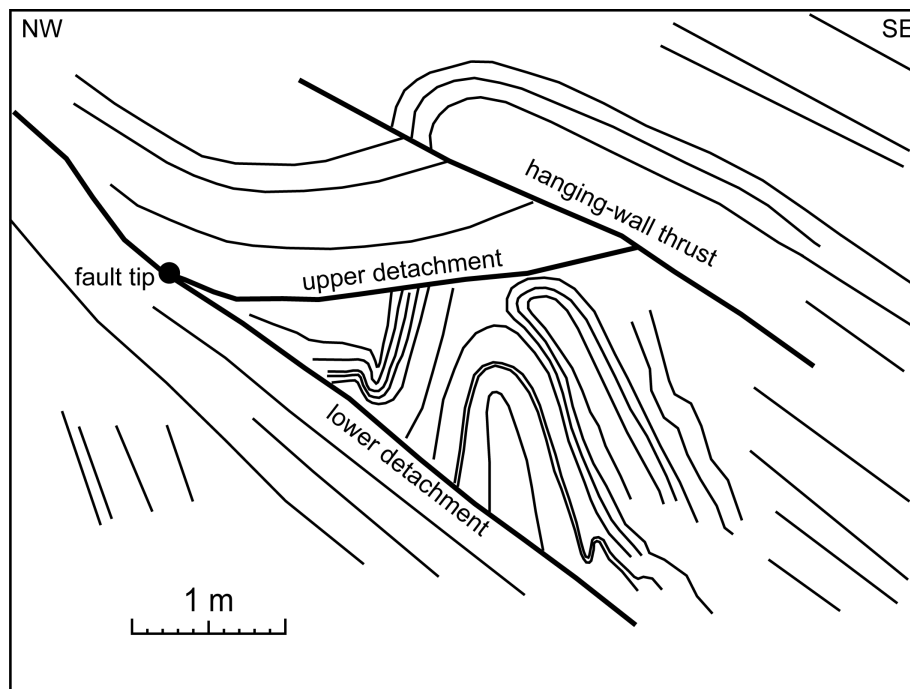
Figure 7.1: Sketch of the triangle zone, showing the major elements (Tanner et al. 2010).

The strata outside of the triangle zone are weakly deformed, as opposed to the strongly-deformed beds within. In the footwall of the lower detachment, the bedding dips 40-50° southeast. The upper detachment is curved, convex-up; beds form a synform above it. Above the upper detachment, there is a hanging-wall thrust, above which is a tight hanging-wall anticline. In terms of the kinematics of the Harz deformation, the lower detachment and the hanging-wall thrust are foreland-propagating, north-west verging thrusts and the upper detachment is a back thrust.

Internally, the triangle zone consists of a three folds (Fig. 7.1), from back (southeast) to front (north-west) they are: an isoclinal antiform (2 m height), a tight to isoclinal antiform (1.5 m height), and a tight to open synform (1 m height). Continuation of beds from one fold to another is unclear, but very unlikely, i.e. these are all rootless folds.
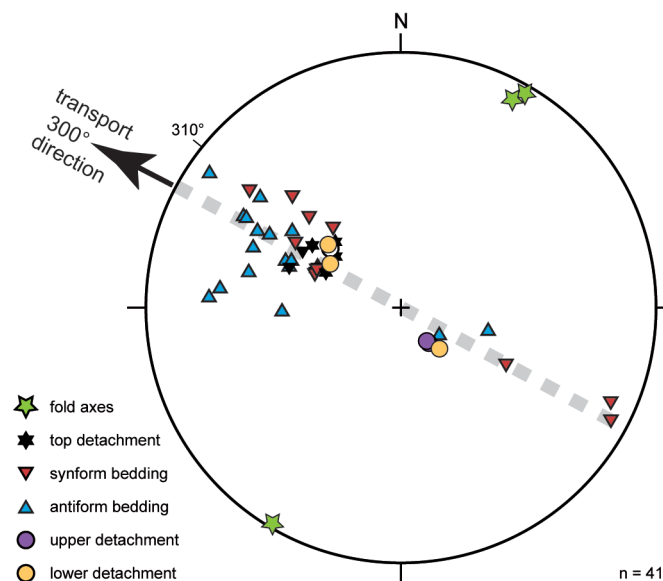
Figure 7.2: Lower hemisphere, equal-area stereographic projection of the poles to elements of the triangle zone. Note the clear cylindricity of the folding and thrusting, and vergence to the northwest (Tanner et al. 2010).

We envisage that below the outcrop there is a ramp on the lower detachment. As beds passed over the ramp, they were passively folded as fault-bend folds. The fold-bend folds then entered the flat above the lower detachment. The folded material congested at the tip of the lower detachment. The folds were further tighten and flattened by new material coming from behind. Finally, the hang-wall thrust bypassed the triangle zone.

For the triangle zone examined here, we propose that the mechanical stratigraphy was the main controlling factor. Modelling has shown that the friction along the upper and lower detachment controls the distribution of deformation within the triangle zone (Jamison 1996). Strong detachments cause a high internal strain and vice versa (Couzens-Schultz & Wiltschko, 1996, Couzens-Schultz et al. 2003), which leads us to suggest the detachments in this case were very strong.

This location and development of this triangle zone is anomalous in two ways:

1. A triangle zone usually develops at the front of an orogenc zone. This is not the case here, but can be explained by being the front of the orogenic zone, or structural zone, at some point in time during the deformation.

2. Typically triangle zones are envisaged to be brittle structures, if not otherwise known, filled by more brittle structures, such as small duplex structures (Stockmal et al. 2001). This is often the case in seismic interpretation, where the outer triangle zone can be recognised, but not the infill (Thomas et al. 2006). This outcrop demonstrates that it is possible to fill the triangle zone with tightly folded material. This different interpretation has consequences for e.g., oil and gas exploration (Slotboom et al. 1996).

References

Couzens-Schultz, B. A. & Wiltschko, D.V. (1996): The control of mechanical stratigraphy on the formation of triangle zones. Bulletin of Canadian Petroleum Geology, 44, 165-179.

Couzens-Schultz, B.A., Vendeville, B.C. & Wiltschko, D.V. (2003): Duplex style triangle zone formation: Insights from physical modeling. Journal of Structural Geology, 25, 1623-1644. doi: 10.1016/S0191-8141(03)00004-X.

Jamison, W.R. (1996): Mechanical models of triangle zone evolution. Bulletin of Canadian Petroleum Geology, 44, 180-194.

Slotboom, R.T., Lawton, D.C. & Spratt, D.A. (1996): Seismic interpretation of the triangle zone at Jumping Pound, Alberta. Bulletin of Canadian Petroleum Geology, 44, 233-243.

Stockmal, G.S., Lebel, D., McMechan, M.E. & MacKay, P.A. (2001): Structural style and evolution of the triangle zone and external Foothills, southwestern Alberta: Implications for thin-skinned thrust-and-fold belt mechanics. Bulletin of Canadian Petroleum Geology, 49(4), 472-496. doi:10.2113/49.4.472.

Tanner, D.C., Brandes, C. & Leiss, B. (2010): Structure and kinematics of an outcrop-scale, fold-cored triangle zone. Bulletin of the American Association of Petroleum Geologists, 94/12, 1799-1809. doi: 10.1306/06301009188.

Thomas, R., Schwerd, K., Bram, K. & Fertig, J. (2006): Shallow high-resolution seismics and reprocessing of industry profiles in southern Bavaria: The Molasse and the northern Alpine front. Tectonophysics, 414, 87-522. doi:10.1016/j.tecto.2005.10.025.

Stop 8: Kellwasser Horizon in Devonian carbonates

David C. Tanner [1], Bernd Leiss [2]

1) Leibniz Institute for Applied Geophysics, Stilleweg 2, D-30655 Hannover,
 DavidColin.Tanner@liag-leibniz.de

2) Geowissenschaftliches Zentrum der Universität Göttingen, Strukturgeologie und Geodynamik Goldschmidtstr. 3, 37077 Göttingen, bleiss1@gwdg.de

Locality: artificially extended outcrop on the side of the road, on the east side of the Oker lake, opposite small bridge/dam.

UTM co-ordinates: East 599831.281, North 5742151.709 (Zone 32N, WGS84)

Geographic co-ordinates: N 51°49'16.572", E 10°26'54.492"

At this outcrop, the exposed section ranges from the upper Frasnian Limestones to the Lower Carboniferous Kulm-Kieselschiefer (Gereke et al. 2014). The outcrop is famous for a number of things. F.A. Roemer first described from here unusually grey/black, carbon-rich, marly carbonates within lighter limestone in 1850. It has become the world-famous ,type locality' of the two dark organic shale beds that outcrop at this valley representing the Kellwasser Event that occurs at the Devonian Frasnian/Famennian boundary (372.2 ± 1.6 Ma).

There are two organic-rich shale beds that are known as the upper and lower Kellwasser horizons (Fig. 8.1, Gereke et al. 2014). The Kellwasser Event is one of the "big five" mass extinction events that have occurred on Earth. It mainly affected marine organisms; land-based animals and plants were less affected. 19% of all families and 50% of all genera became extinct. The taxa that were most affected were the trilobites, acritarchs, the tabulate und rugosa corals, graptolites, stromatoporoidea, brachiopods and placoderms (armoured fish). There is good evidence of widespread anoxia at the bottom of the oceans, and the global rate of carbon burial rose rapidly (Algeo & Scheckler 1998). It has also become clear that sea levels rose to an all-time high at this time (Bond & Wignalla 2008). Nevertheless, the cause of the mass extinction is still under debate. The following events have been hypothesised:

1. Extra-terrestrial events have been invoked, but the few impact craters that can be attributed to the Devonian, cannot be dated with enough precision (McGhee 1996).

2. Recently, even a nearby supernova has been suggested as a cause of extinction in the Devonian (Fields et al. 2020). The supernova would be far enough away not to wipe out Earth completely, but close enough for cosmic rays that can deliver ionizing radiation to strip away the Earth's ozone layer.

3. Increased volcanic activity would able to darken the sky and kill life in the oceans. Possible candidates are the extremely widespread plume-related trap magmatism and rifting on the Russian and Siberian platforms (Kravchinsky 2012).

4. Alternatively, the land plants, which first made their way on to the land in the Devonian, could have increased the process of weathering, and so released silicates and carbonates that subsequently sequestered carbon from the atmosphere, thus causing global cooling (Algeo and Scheckler 1998).

Structurally, bodies of Devonian carbonates are thrust into the Lower Carboniferous Culm siliclastics at various points along the Oker valley sections. They are usually a few metres to tens of metres thick. This outcrop shows similar characteristics, in that a number of thrusts ramps and horses (units completely bounded by faults) are visible, which verge to the east and west. In addition, the whole outcrop is openly upright folded, so it can be referred to as an antiformal stack. In this tectonic milieu, it is probable that a ramp thrust underlies the antiform. At the top of the outcrop, Lower Carboniferous shales (Alaun Schiefer) are present, but above a detachment.
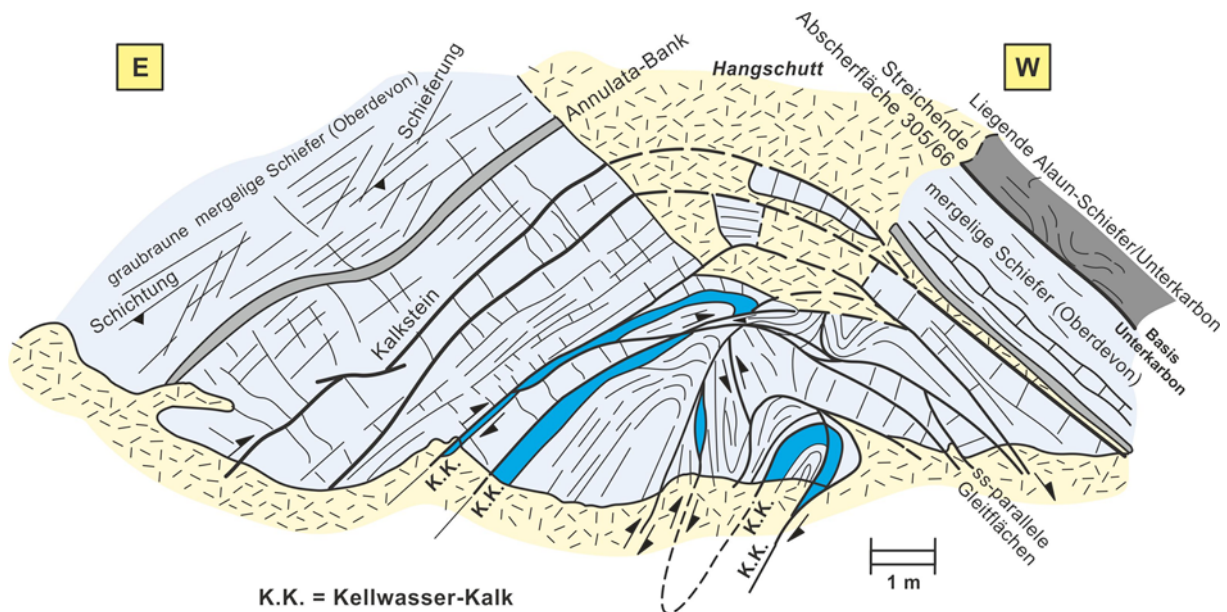
Figure 8.1: A sketch of the Kellwasser outcrop (Franzke & Müller 2012). Thick lines are thrust faults, and detachments, blue-shaded areas are Kellwasser beds. The repetition of the Kellwasser beds shows the kinematics of the thrusts in the centre of the fold.

Although an outcrop at this location was described by Roemer in 1850, it was lost due to soil movement and vegetation by 1875. In 2009 and 2010, a team of volunteers cleared the outcrop and widen it. It is now a protected geotope (Geopunkt 7, Landmarke 2).

References

Algeo, T.J. & Scheckler, S.E. (1998): Terrestrial-marine teleconnections in the Devonian: links between the evolution of land plants, weathering processes, and marine anoxic events. Philosophical Transactions of the Royal Society B: Biological Sciences, 353 (1365), 113-130. doi:10.1098/rstb.1998.0195.

Bond, D.P.G. & Wignalla, P.B. (2008): The role of sea-level change and marine anoxia in the Frasnian-Famennian (Late Devonian) mass extinction. Palaeogeography, Palaeoclimatology, Palaeoecology, 263 (3-4), 107-118. doi:10.1016/j.palaeo.2008.02.015.

Franzke, H.J. & Müller, R. (2012): 2.4 Aufschluss im Kellwasser-Kalk an der Oker-Vorsperre (S-Seite des Kellwassertals). In: Stipp, M. & Friedel, C.-H. (eds.): Exkursionsführer. 14. Symposium, Tektonik, Strukturgeologie und Kristallingeologie (TSK 14), Kiel, 26.3. - 1.4.2012.

Gereke, M., Luppold, F. W., Piecha, M., Schindler, E. & Stoppel, D. (2014): Die Typlokalität der Kellwasser-Horizonte im Oberharz, Deutschland. Z. Dt. Ges. Geowiss. (German J. Geosci.), 165 (2), 145-162.

Kravchinsky, V.A. (2012): Paleozoic large igneous provinces of Northern Eurasia: Correlation with mass extinction events. Global and Planetary Change, 86–87, 31-36. doi:10.1016/j.gloplacha.2012.01.007.

McGhee, G. R. Jr, (1996): The Late Devonian Mass Extinction: the Frasnian/Famennian Crisis (Columbia University Press). ISBN 0-231-07504-9.

Roemer, F.A. (1850): Beiträge zur geologischen Kenntnis des nordwestlichen Harzgebirges. Palaeontographica, 3(1), 1-67.

Stop 9: Sedimentary vs tectonic origin - mélange and broken formation in the classic outcrop of the "Hüttenrode Olistostrome" near Königshütte

Friedel, C.-H.[1], Kreitz, J.[2], Brouwer-Miosca, N.[3], Leiss, B.[4], Zweig, M.[5]

1) Karl-Marx-Str. 56, 04158 Leipzig, chfriedel@gmx.de

2) Smart Asphalt Solutions GmbH, Goethestraße 2, 37120 Bovenden, j.kreitz@smart-asphalt-so-lutions.de

3) APS Antriebs-, Prüf- und Steuertechnik GmbH, Götzenbreite 12, D-37124 Rosdorf, nbrouwer-miosca@wille-geotechnik.com

4) Geowissenschaftliches Zentrum der Universität Göttingen, Strukturgeologie und Geodynamik Goldschmidtstr. 3, 37077 Göttingen, bleiss1@gwdg.de

5) Sächsisches Landesamt für Umwelt, Landwirtschaft und Geologie, Referat 105, Halsbrücker Str. 31, 09599 Freiberg, Maren.Zweig@smul.sachsen.de

Locality: Forest road (now Bodetal road), north of the Bode river retention basin, approx. 500 m east of Königshütte. Geological map 1:25.000, Sheet No. 4230, Elbingerode,
UTM co-ordinates (0 m point, road gully): East 622565.454, North 5733810.345 (Zone 32N, WGS84)
Geographic co-ordinates: N 51°44'30.42" E 10°46' 30.81"

East of Königshütte, one of the few relatively well-preserved rock sequences of mélange and broken formation of the Harz Mts. is exposed in the Blankenburg zone at the southern margin of the Elbingerode window (Elbingerode complex). Along the now Bodetal road, north of the Bode river retention basin, the exposed strata have been regarded as one of the typical outcrops of submarine mass-flow deposits called the "Hüttenrode Olistostrome" (Lutzens 1969, 1972). The term "Hüttenrode Olistostrome" is used to describe the largest part of the rock strata in the Blankenburg zone that surround the Elbingerode complex (Lutzens & Schwab 1972, Lutzens 1978). These include, in particular, lithologically-varied sequences, formerly designated as Hüttenröder Schichten (e.g. Zimmermann 1968), and the area of mainly quartzitic rocks ("Hauptquarzit") on the geological map sheets (Fig. 9.1). Coherent units within the chaotic rocks have been interpreted as sliding nappes associated with submarine mass-flow processes (e.g. Schwab 1976, Lutzens 1991, Schwab & Ehling 2008). The relatively good outcrops along the then new forest road proved a lithological diversity of clasts or olistostolihs (e.g. quartzite, limestone, chert, Figs. 9.2, 9.3a), which was considered as important evidence for the olistostrome model.

The cross section along the road originally extended from west to east to the valley where the Papenbach stream joins the reservoir (Lutzens 1969, Schwab 1976). The eastern part is meanwhile heavily covered and the outcrop shown in Fig. 9.2 is hardly recognisable today. The presented area is therefore limited to the western part (0-110 m, Fig. 9.3).

Lithology and deformation features

The predominant lithologies are clayey to silty slates, cherts and quartzites. The rocks are cleaved and intersected by numerous faults, dipping moderately steeply to flat to the SE (Figs. 9.3, 9.4a). Especially the area between 40 and 70 m is strongly tectonically overprinted. Besides folding and NW-directed thrust tectonics (D1/2), dextral strike-slip faulting (D3) is very pronounced here (Fig. 9.4a). Cleavage and bedding are at an acute angle to almost parallel to each other, and dip moderately (50-70°) to the SE. According to the cleavage-bedding relationship, the normal limb (backlimb) of an asymmetric NW vergent fold structure with a northeast-plunging fold axis is exposed (Fig. 9.4a).

The profile starts in the west with a massive mica-rich calcareous greywacke block (Kalkgrauwacke). The Kalkgrauwacke is followed to the east by dark and light slates, in which calcareous greywacke
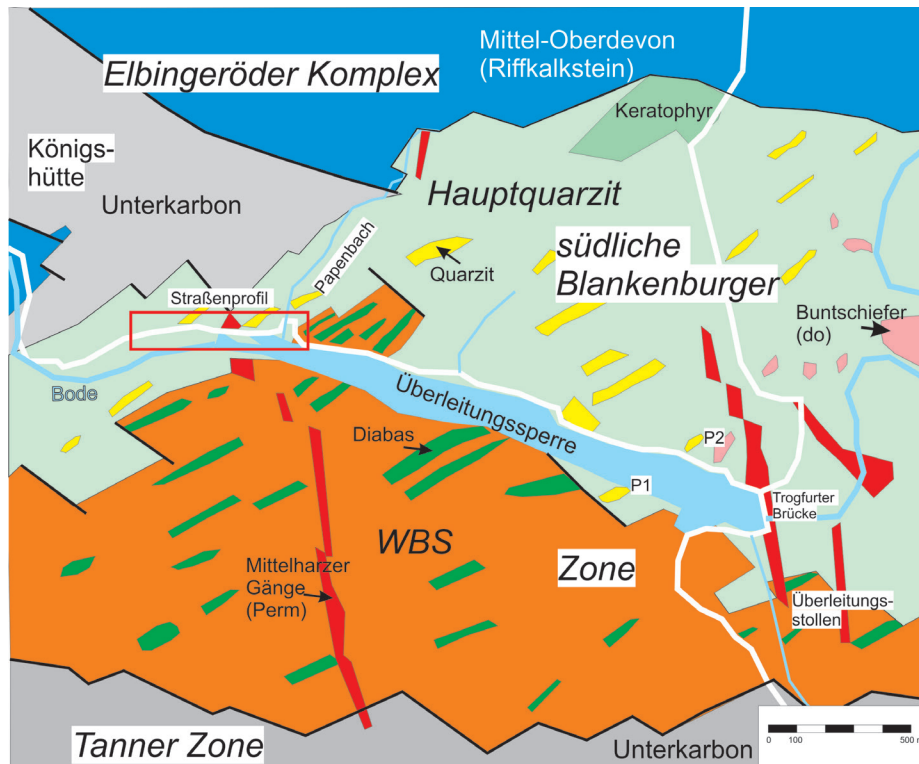
Figure 9.1: Location of the road profile (red rectangle) in the southern Blankenburg zone (after Friedel & Leiss 2015). Wissenbach Formation: slates with diabase (Eifelian), Buntschiefer: Upper Devonian variegated slate, P1 and P2: outcrops dated as Upper Devonian in the "Hauptquarzit" unit (quartzite-slate sequence, Reichstein 1961, see text).
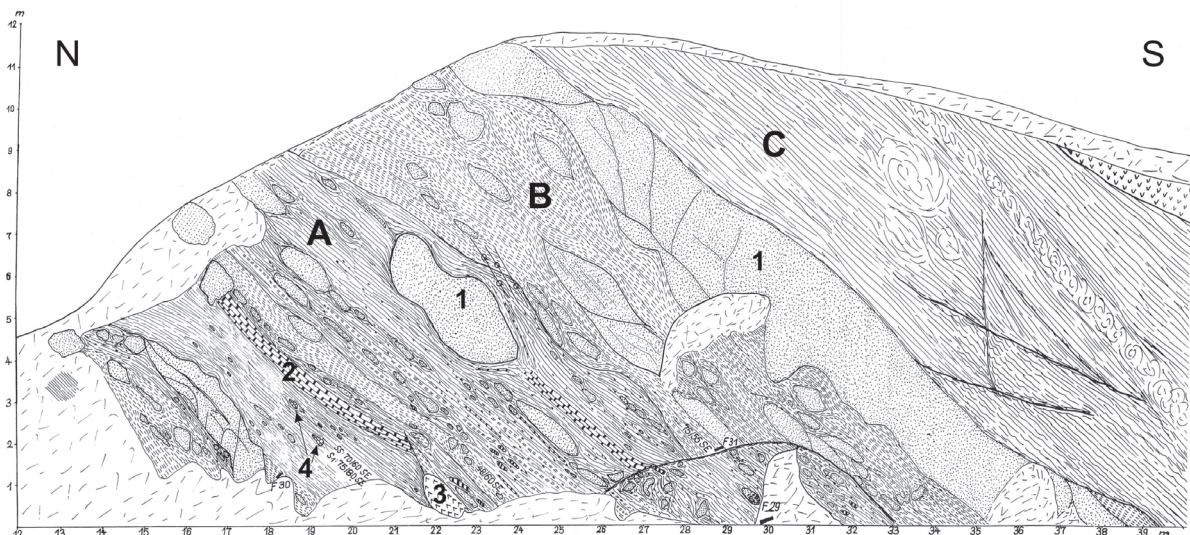
A: Tonschiefer mit kleinen Kieselschiefergeröllen, B: Buntschiefer mit oberdevonischen Conodonten, C: dunkle Tonschiefer (im Hangenden mit Diabas);
Blöcke: Quarzite (1), Kieselschiefer (2), Keratophyr (3), Kalkstein (4).

Figure 9.2: Geological sketch of the outcrop at the Papenbach showing the variable lithological composition of the blocks (Lutzens 1972, Fig. 36). Three areas can be distinguished: A: Slates with chert clasts, B: variegated slates (Buntschiefer, Upper Devonian), C: Wissenbach slates (Eifelian). Blocks: 1) quartzite, 2) chert, 3) keratophyre, 4) limestone. The outcrop is now heavily overgrown, so that details are no longer recognisable.
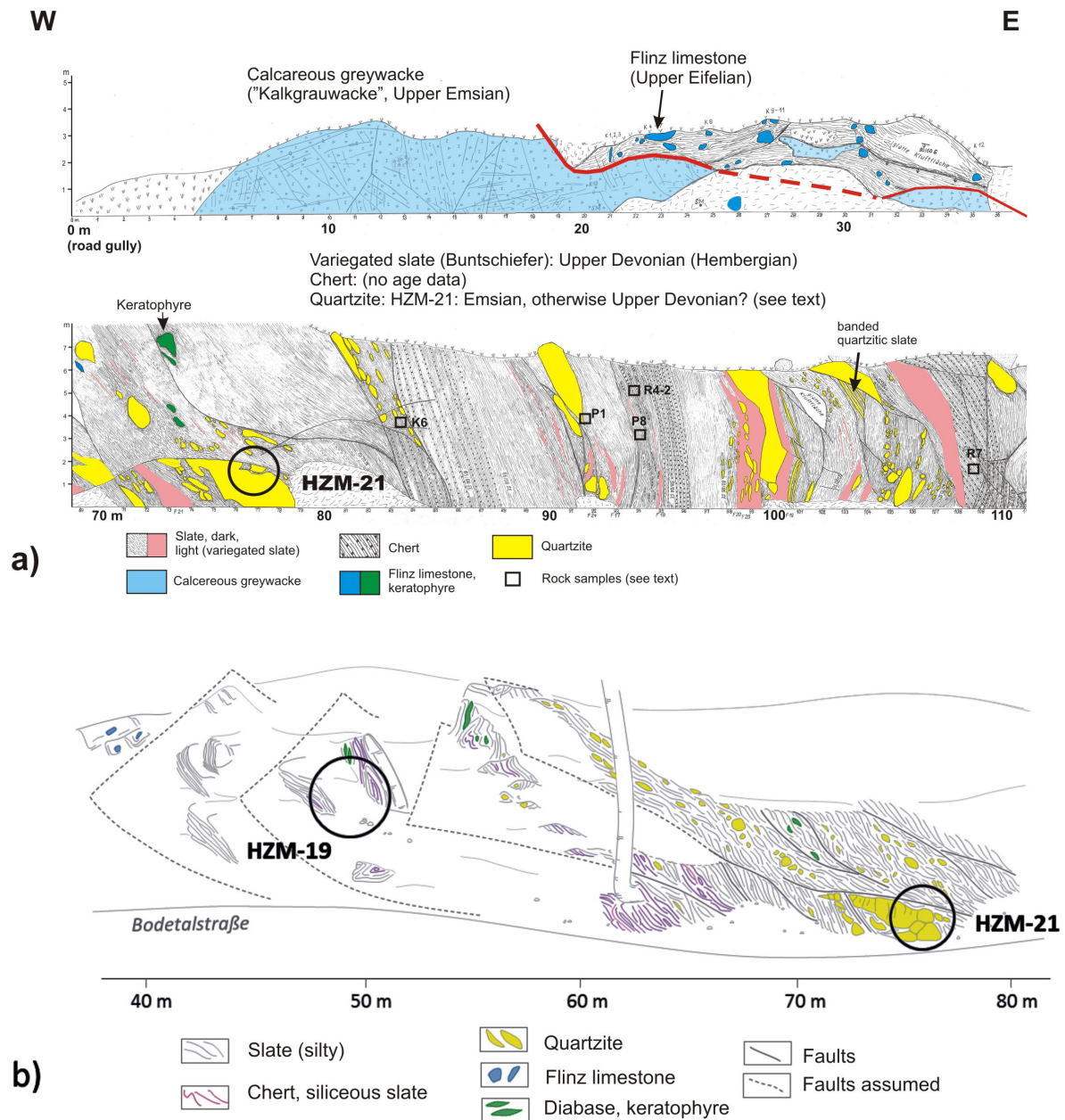
Figure 9.3: a) Geological cross-sections according to the detailed mapping of the road profile of H. Lutzens, 1966 (from Lutzens 1969, appendix 20a, b, sections 0-36 m and 69-110 m, slightly modified). b) Profile section between 40 and 80 m taken from Zweig et al. (2016). Stratigraphic data (without HZM samples) after Blumenstengel (1973, 1991, 1992, see text). Squares: Rock samples mentioned in the text. Circles/HZM: Samples of the U-Pb dating of detrital zircon grains (Zweig et al. 2016).

and fossil-rich micritic-arenitic limestone (allodapic Flinz limestone) as well as keratophyre and quartzite occur as blocks. At about 60 m, two to 50 cm-thick, strongly-boudinaged quartzite layers are present, which persist for several metres (Miosga 2014). The variety of the lithology of the blocks indicates this western part as a mélange zone. From 75 m eastwards, volcanic rocks and limestone are no longer present as blocks. Between 75 m to 110 m a rock sequence is exposed that consists of alternating slates, cherts and quartzites. In this area, lenticular quartzite bodies of up to 1 m thickness occur preferentially in 1-2 m thick bedding parallel zones. In between, there are more or less coherent, partly well-laminated units of chert and clayey to silty slates. The individual
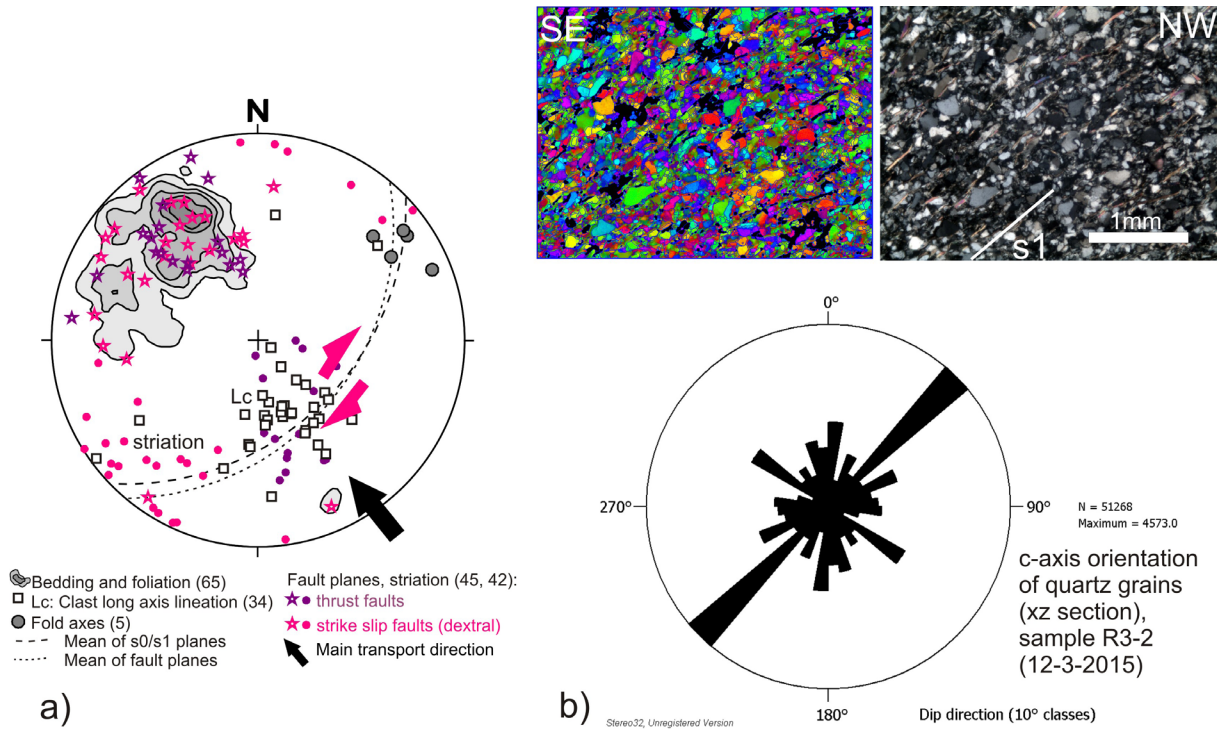
Figure 9.4: a) Equal-area, lower hemispheric, stereographic projection of the main tectonic features (s0, s1: bedding, 1st cleavage). Some of the SE dipping thrust faults are overprinted by dextral strike-slip faulting. Note the preferred NW orientation of the clast long axis. b) The cleavage in quartzite is penetrative and characterised by the alignment of detrital micas and a grain shape and crystallographic preferred orientation of the quartz grains (Rose diagram calculated with a software developed by Fueten & Goodchild 2001).
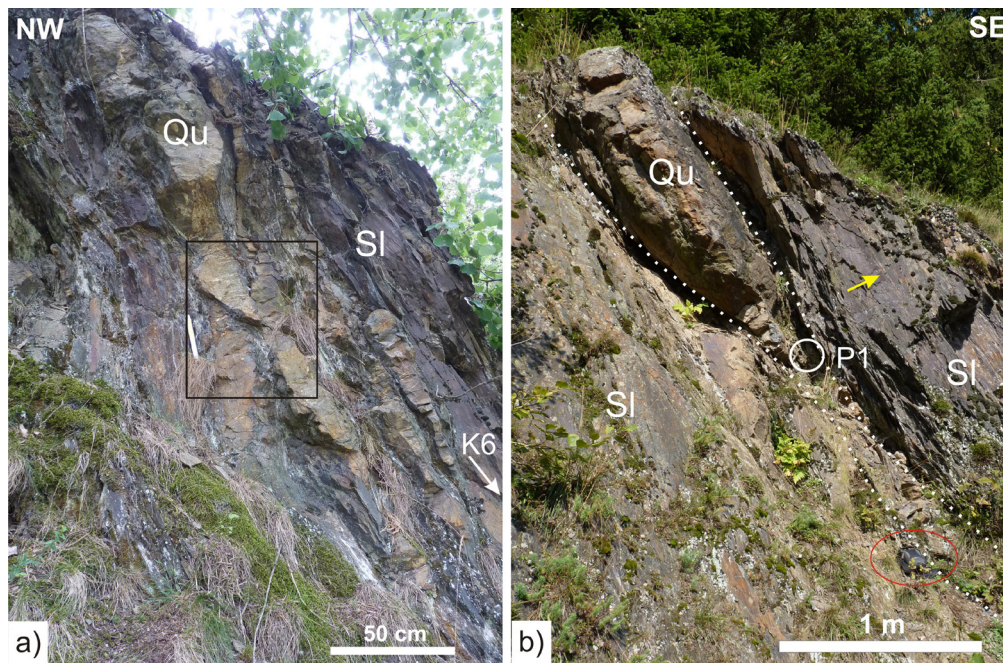
Figure 9.5: Boudinaged and sheared quartzite layers (Qu) in silty slates (Sl) at 82 m (a) and at 92 m (b) (cf. Fig. 9.3a); from Friedel & Leiss (2015). The framed area in a) is shown in Fig 9.7c. Fine-grained quarzitic layers (sample K6, Fig. 9.6b) and laminated radiolarite cherts (yellow arrow in b, cf. Fig. 9.6d) occur in silty slates in the hanging wall of the strongly-boudinaged quartzite layers. The location of sample P1 (white circle, Fig. 9.6a) and a camera bag (red circle) can be seen in b.

quartzite bodies are boudinaged and partly fragmented (block-in-matrix fabric), but they are often still recognisable as initially interconnected strata (Figs. 9.3a, 9.5). This section of the profile can be considered as broken formation, while at the eastern end there is again a mélange zone (Fig. 9.2).

Quartzites are the most frequent intercalations and occur as layers and blocks, both in light and dark clayey and silty slates. Locally, they also occur together with blocks of chert (Fig. 9.2, Fig. 9.3a at 105 m). Quartzite blocks arranged in bedding-parallel layers show a comparable lithological pattern (grain size, clay content). In some quartzite layers, a gradation (fining upward) can be observed (Fig. 9.6a). The adjacent silty slates also contain fine quartzitic layers (Fig. 9.6b) or they form cm-thick alternating layers of quartzite and slate (banded quartzitic slates, Fig. 9.3a), which can also contain radiolarites (see below).

The quartzite commonly exhibits a penetrative cleavage. The cleavage is characterised by the alignment of micas, and a grain shape and crystallographic preferred orientation of the quartz grains (Fig. 9.4b). The rocks are also intensively penetrated by mineralised veins (Miosga 2014, Riegel 2014). Quartz mineralisation is ubiquitous. Boudinaged layers and especially the ends (extremities) of lens-shaped blocks are downright saturated by blocky to fibrous quartz veins (Fig. 9.7a), whose fibres are often oriented subparallel to the cleavage. The quartz grains themselves are then more elongated parallel to the cleavage. During or after cleavage formation, shear planes were active, and intersect and dissect quartzitic layers, and thereby bend the cleavage planes (Fig. 9.7b, c).

The cherts often show a plate-like laminated appearance. Samples taken from typical chert areas prove to be rich in radiolarites. These radiolarian cherts (lydites) are finely bedded and graded (Fig. 9.6c, d). The high clay content of the samples is remarkable, and even stronger clayey layers may
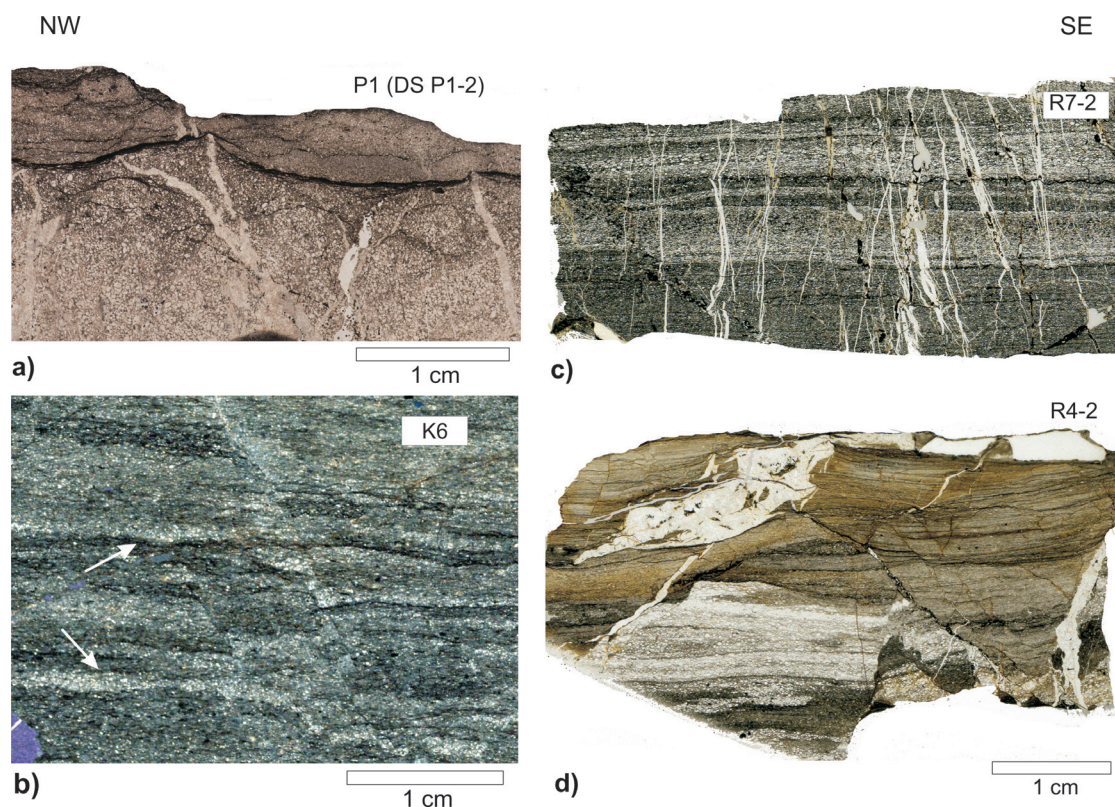
Figure 9.6: Thin sections of quartzite (a, b) and radiolarian chert (c, d), (from Friedel & Leiss 2015). a) Rim of a lensoid quartzite body (sample P1). Note the transition from medium-grained quartzite below to more clayed and fine-grained quartzite up to a clay-rich siltstone. b) Sandy lenses in siltstones in slates of the hanging wall of a quartzite layer (sample K6). c), d) Radiolarian chert (lydite) with high clay content (dark grey to greenish grey) and depositional gradation. Both chert samples are intensively mineralized with quartz, and the sample R4-2 is also strongly sheared. For sample location, see Fig. 9.3a.

NW   SE

a)

b)   c)
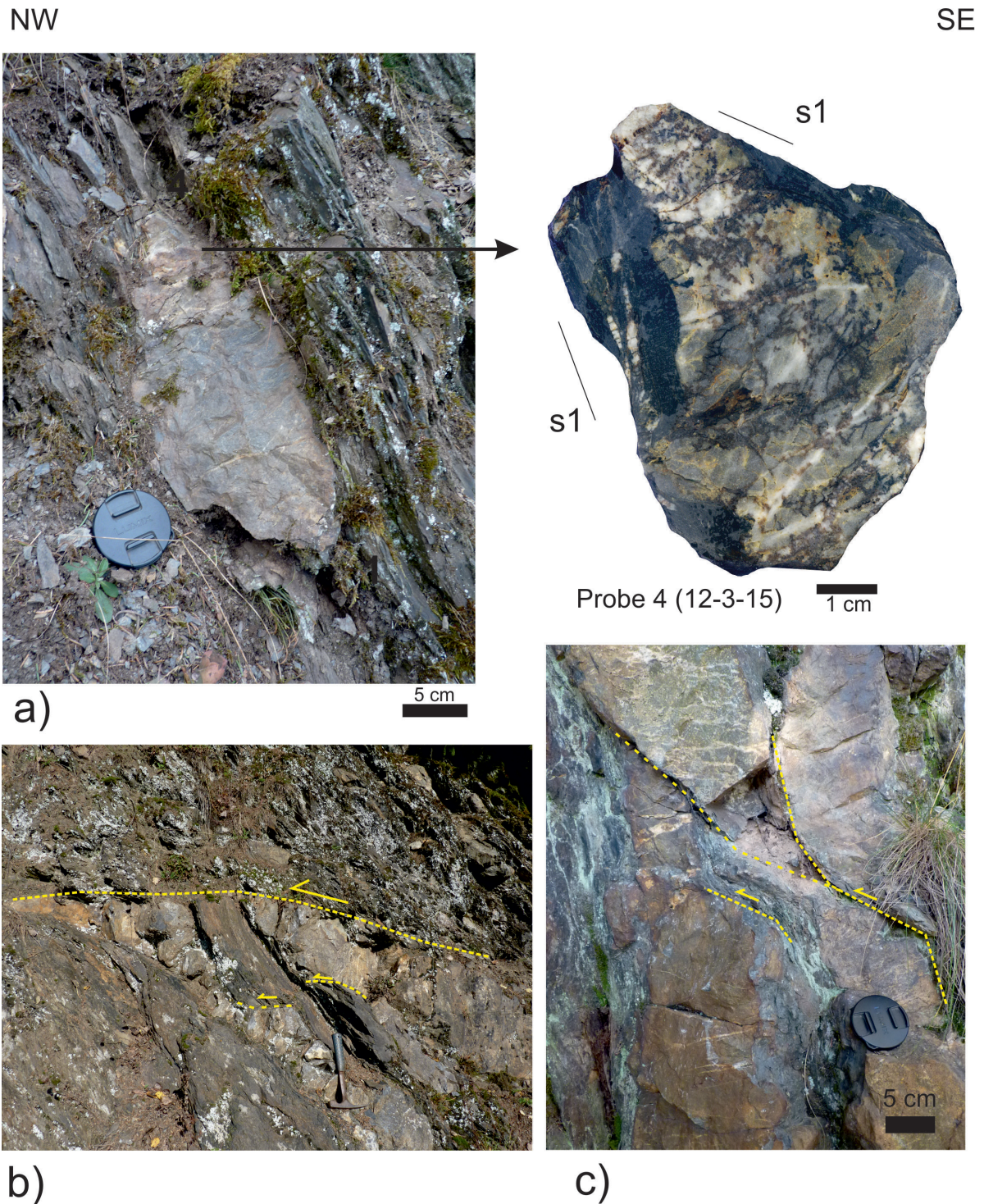
Figure 9.7: a) Strongly-mineralized tapered end of a quartzite lens at about 85 m (sample 4). b) and c) Shear planes (yellow) lines) dissect and offset quartzite layers and blocks (photos taken at about 70 m (b) and 82 m (c), cf. Fig. 9.3a). Note the associated bending of the cleavage planes and the widespread mineralisation, both of which points to a tectonic origin of the boudinage and fragmentation of former coherent quartzite layers (see text and Friedel & Leiss 2015).

still contain some radiolarites. They are therefore hardly distinguishable from common slates. The spatial restriction of cherts to single horizons (Fig. 9.3a at 84-87 m, 94-96 m, 108-110 m and at 117 m) is therefore only partially valid. Radiolarian cherts are much more common in the silty slates and are even present in the so-called banded quartzitic slates (at 103 and 113 m in Fig. 9.3a)

Shales/Slates: According Lutzens (1969), the fine-grained matrix consists of dark slates and lighter, greenish grey to yellowish variegated slates, whereby only the lighter variegated slates (Buntschiefer) has been biostratigraphically dated (see Age data). Both slates often occur closely adjacent as interlayers or clasts (Figs. 9.3a, 9.8a). It should be emphasised that quartzites occur as lensoid layers and blocks in both light and dark slates. Also the cherts are not only bound to the dark slates, and even the clay-rich parts in chert samples appear partly to belong to light variegated slates (Fig. 9.6d). In addition, the slates are strongly tectonically overprinted by cleavage-parallel shear planes and boudinage (Fig. 9.8). Whether the light and dark slates are two slate types of different ages remains open because no age data are available for the dark slates for the area east of 75 m (see below, Age data).
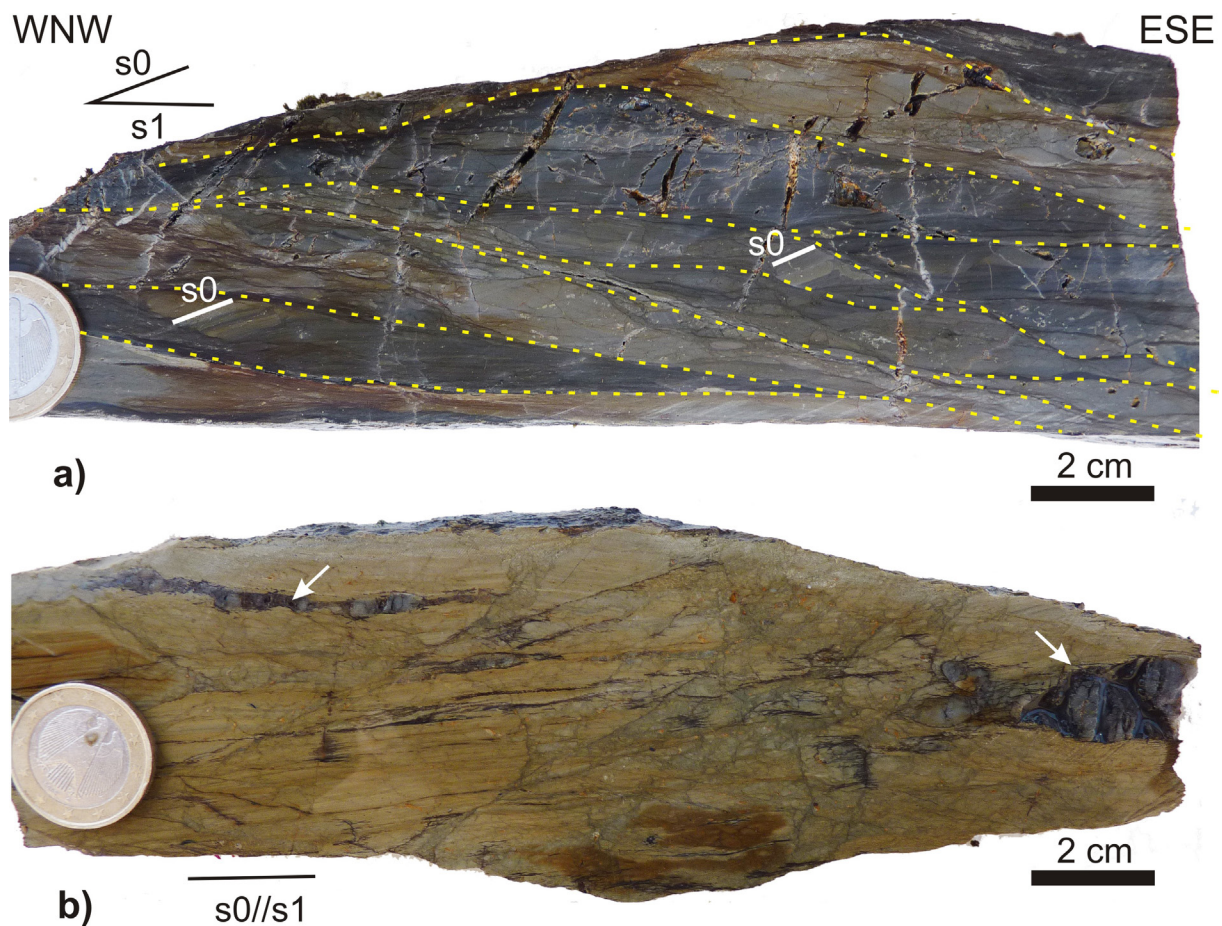
Figure 9.8: a) Along cleavage-parallel shear planes (dashed) intensively imbricated, dark and lighter sandy slates (Sample P8, Fig. 9.3a). The oblique position of the bedding (s0) in the lighter layers proves the s1-parallel alignment of the shear planes and thus a tectonic origin of these structure (see text).

b) Chert (arrows), partly boudinaged, in pale-greenish slightly brecciated slate (sample taken at about 175 m east of the starting point); from Friedel & Leiss (2015).

Age data

According to its ostracod fauna, the mica-rich, calcareous greywacke can be assigned to the Upper Emsian to Lower Eifelian (Blumenstengel 1992). The K/Ar cooling ages of detrital mica of this rock also prove a Lower Devonian sedimentation age (Huckriede et al 2004, sample Hg 216). The Flinz limestones belong to the Upper Eifelian (Blumenstengel 1973). The conodont dating of the clayey-slaty matrix yielded an Upper Devonian age only for the lighter slates (Buntschiefer, Hembergian to Dasbergian, Blumenstengel 1973; Fig. 9.3a). The dark slates were not dated and were considered to be either equivalents of the Eifelian Wissenbach slate or Kulm cherts (Lutzens 1969, 1973). Analogous to the Lower Carboniferous chert and Acker-Bruchberg quartzite, the cherts and quartzites found here were also considered to be Lower Carboniferous rock components (Lutzens 1972, p. 62). In contrast, Reichstein (1961) dated a lithologically-comparable alternating sequence of quartzites and slates about 2 km further east as Upper Devonian (Nehdenian to Hembergian, possibly also Dasbergian, outcrops P1 and P2 in Fig. 9.1).

Zweig et al. (2016) used U-Pb (LA-ICP-MS) age dating on detrital zircons to better constrain the age of the blocks and the clayey matrix. These data support a Lower Carboniferous age for the mainly dark slates (with quartzite and sandy to siliceous slate as components) from the profile area at c. 50 m (Viséan, sample HZM-19 in Fig. 9.3b). Whereas the dating of the large quartzite block and its surrounding silty slates at about 75 m revealed a Lower Devonian sedimentation age (Emsian, sample HZM-21, Fig. 9.3b). Here, block and matrix are of the same age and the age spectrum of the zircons points to the same delivery area for both rock components (Baltica-Avalonia, Zweig et al. 2016). The abrupt change from Lower Carboniferous to Lower Devonian age of the clayey matrix and quartzite block at 75 m (sample HZM-21) is attributed to thrusting.

Discussion and interpretation

To substantiate a sedimentary origin of this chaotic rock sequence as a mass flow deposit of Lower Carboniferous age, Lutzens (1969) referred to the lithological diversity of the clasts, the different slates (light Upper Devonian Buntschiefer and dark slates of unknown age) and to the possible Lower Carboniferous age of the chert. Although he also emphasised the strong fault-tectonic overprint, he considered the blocks as olistoliths and the whole sequence to be essentially of sedimentary origin (deformed olistostrome, Lutzens & Schwab 1972, Lutzens 1972).

The observed lithological and structural features and the new age data argue against a sedimentary origin of the exposed rocks sequence:

- The quartzites, cherts and slates form alternating layers with sedimentary transitions. Although the quartzite layers are partially dispersed, they are often still recognisable as distinct bedding-parallel horizons (Figs. 9.3a, 9.5). The quartzites show lithological transitions to the ambient clayey matrix and occur with slates of the same age (HZM-21, Fig. 9.3b, see also Reichstein 1961, p. 304). The bedded cherts also form transitions to the surrounding slates (Figs. 9.5b, 9.6c, d). The quartzitic lenses and blocks, and chert intercalations are therefore difficult to explain as olistoliths.

- Based on the results of the U-Pb-zircon dating, the assumption of a purely Devonian succession has not been confirmed (cf. Friedel & Leiss 2015). At least in the western part, late Lower Carboniferous slates are present. The chaotic, lithologically variably-composed areas in the western part and at the eastern end (Papenbach) form mélange zones. The western mélange is strong tectonically overprinted, the eastern is probably tectonically overlain by Wissenbach slate (Abb. 9.2).

- The profile exposes a tectonically disturbed, but in parts relatively intact sequence. The section from 75 m to almost the eastern end of the profile is characterised by alternating quartzite, chert and slate and represents a broken formation. For this area, a depositional model was proposed by Friedel & Leiss (2015) in which the quartzites represent turbiditic inputs into a deeper basin. The basin facies is characterised by the clayey slates and the sporadic input of radiolarites. Although not verified so far, this sequence is not considered to be of Lower Carboniferous age, but with reference to the biostratigraphic result of Reichstein (1961), it probably represents

an Upper Devonian sequence.

- There is no evidence for the previous assumption that emplacement of coherent units occurred by submarine sliding during mass-flow processes, here, as well as in other chaotic rock units of the Harz Mountains (Friedel et al. 2019). The rock contacts here are consistently tectonic down to the microscale. The present deformation features (e.g. intensive mineralisation, crystallographic preferred-orientation of quartz grains, stronger elongation of quartz grains in neck regions of blocks, shear planes acting syn- to post-tectonically to the s1 cleavage) point to a tectonic origin of the boudinage and fragmentation of formerly intact units, which obviously affected in particular alternating quartzite-slate sequences with their high competence contrast (Figs. 9.3a, 9.7).

- With the proposed purely-tectonic origin of the broken formation and mélange zones, especially the mixing of different rigid rock components causes difficulties. In subrecent thrust-and-fault-belt settings, mixing has resulted primary from sedimentary rather than tectonic processes (see review in Festa et al. 2022). The simpler explanation of mixing is the advantage of the olistostrome model. However, as stated above, we found no real evidence for any sedimentary mixing here. In the case of a tectonic origin of the mélange zones, mixing indicates the activity of out-of-sequence thrusts. The diversity of blocks will increase when different lithostratigraphic units occur adjacent to each other, which is obviously the case especially at the eastern end of the profile (Papenbach area, Fig. 9.2).

References

Blumenstengel, H. (1973): Exkursion B, Aufschluss B3. In: Schwab, M.: Exkursionsführer zur Vortrags- und Exkursionstagung „Lithologie , Paläogeographie und Tektonik des Paläozoikums im Rhenoherzynikum des Harzes und der Flechtinger Scholle. Gesellsch. f. Geol. Wiss., 30-34, Berlin.

Blumenstengel, H. (1991): Zur Bedeutung mikropaläontologischer Untersuchungsmethoden in Olisthostrom-Serien des Harzes, dargestellt am Beispiel der Hüttenröder Schichten bei Königshütte. In: Schwab, M., Jacob, G., Tschapek, B., Lutzens, H. Scheffler, H. & Weller, H.: Stratigraphische Probleme im Ostharz. Exkursionsführer Subkommission Karbonstratigraphie, S. 71, Halle/S.

Blumenstengel, H. (1992): Eine neue Ostrakodenfauna aus einem Vorkommen von Erbslochgrauwacke im Hüttenröder Olisthostrom der südlichen Blankenburger Zone. Z. geol. Wiss., 20, 277-280.

Festa, A., Barbero, E., Remitti, F., Ogata, K. & Pini, G.A. (2022): Mélanges and chaotic rock units: Implications for exhumed subduction complexes and orogenic belts. Geosystems and Geoenvironment, 1 (2022). doi.org/10.1016/j.geogeo.2022.10 0 030

Friedel, C-H. & Leiss, B. (2015) Variszische Tektonik im Harz (östliches Rhenoherzynikum). In: Röhling, H.-G. (Ed.): GeoBerlin 2015. DYNAMISCHE ERDE – von Alfred Wegener bis heute und in die Zukunft. Exkursionsführer. Exkursionsführer und Veröffentlichungen der Deutschen Gesellschaft für Geowissenschaften, 255, 44-86.

Friedel, C-H., Huckriede, H., Leiss, B. & Zweig, M. (2019) Large-scale Variscan shearing at the south-eastern margin of the eastern Rhenohercynian belt: a reinterpretation of chaotic rock fabrics in the Harz Mountains, Germany. International Journal of Earth Sciences, 108, 2295-2323.

Fueten, F. & Goodchild, J. S. (2001). Quartz c-axes orientation determination using the rotating stage polarizer microscope. Journal of Structural Geology, 23(6-7), 895-902.

Huckriede H., Wemmer K. & Ahrendt H. (2004) Palaeogeography and tectonic structure of allochthonous units in the German part of the Rheno-Hercynian Belt (Central European Variscides). International Journal of Earth Sciences, 93, 414-431.

Lutzens, H. (1969): Stratigraphie, Faziesbildung und Baustil im Paläozoikum des Unter- und Mittelharzes. Dissertation, 174 S., Martin-Luther-Universität Halle, Halle/S.

Lutzens, H. (1972): Stratigraphie, Faziesbildung und Baustil im Paläozoikum des Unter- und Mittelharzes. Geologie, Beih., 74, 1-105, Berlin.

Lutzens (1973): Exkursion B - Stratigraphische und lithologische Probleme im Paläozoikum des

Harzes. Aufschluß B3. In: Schwab, M.: Exkursionsführer zur Vortrags- und Exkursionstagung „Litho logie, Paläogeographie und Tektonik des Paläozoikums im Rhenoherzynikum des Harzes und der Flechtinger Scholle. Gesellsch. f. Geol. Wiss., 30-34, Berlin.

Lutzens, H. (1978): Zur tektogenetischen Entwicklung und geotektonischen Gliederung des Harz-varistikums unter besonderer Berücksichtigung der 0listhostrom- und Gleitdeckenbildung. Hall. Jb. f. Geowiss., 3, 81- 94, Gotha/Leipzig (H. Haack).

Lutzens, H. (1991): Flysch, Olisthostrome und Gleitdecken im Unter- und Mittelharz. Z. geol. Wiss., 19, 617-623, Berlin.

Miosga, N. (2014): Struktur und Petrographie devonischer „Block-in-Matrix-Gesteine" im Stra-ßenprofil (Abschnitt A) bei Königshütte im Harz – ein Beitrag zur Genese der Harzer Mélanges. Bachelorarbeit, 63 S., Geowiss. Zentrum Göttingen, Georg-August-Universität; Göttingen.

Reichstein, M. (1961): Parallelisierung eines Teiles des bisherigen Hauptquarzits vom Unterharz mit der Schichtfolge des Acker-Bruchberg-Systems. Geologie, 10 (1961), 302-314, Berlin.

Riegel, J. (2014): Struktur und Petrographie devonischer „Block-in-Matrix-Gesteine" im Straßenprofil (Abschnitt B) bei Königshütte im Harz – ein Beitrag zur Genese der Harzer Mélanges. Bachelorarbeit, 60 S., Geowiss. Zentrum Göttingen, Georg-August-Universität; Göttingen.

Schwab, M. (1976): Beiträge zur Tektonik der Rhenoherzynischen Zone im Unterharz. Jb. Geol., 5/6 (1969/70), 9-117, Berlin.

Schwab, M. & Ehling, B.C. (2008): 4.7 Karbon. In: Bachmann, G. H., Ehling, B.-C., Eichner, R. & Schwab, M. (eds): Geologie von Sachsen-Anhalt, 110-140, Stuttgart (E. Schweizerbart).

Zimmermann, G. (1968): Das Alter der Hüttenräder Schichten nördlich des Elbingeröder Komplexes (Harz). Geologie, 17, 466-467.

Zweig, M., Hofmann, M. & Linnemann, U. (2016): Radiometrische Datierung detritischer Zirkone aus dem "Hüttenröder Olisthostrom" bei Königshütte (Blankenburger Zone, Mittelharz). In: Friedel, C.-H. & Leiss, B. (eds.): Harzgeologie 2016. 5. Workshop Harzgeologie – Kurzfassungen und Exkursions-führer. Göttingen Contributions to Geosciences, 78, 53–61.

Stop 10: Blocks of imbricate stacks of Devonian limestones as indicator for a tectonic origin of chaotic rock units in the Harz Mountains - the Herzynkalk block of Güntersberge as an example.

Carl-Heinz Friedel [1], Julia Kreitz [2], Bernd Leiss [3]

1) Karl-Marx-Str. 56, 04158 Leipzig, chfriedel@gmx.de

2) Smart Asphalt Solutions GmbH, Goethestraße 2, 37120 Bovenden, j.kreitz@smart-asphalt- solutions.de

3) Geowissenschaftliches Zentrum der Universität Göttingen, Strukturgeologie und Geodynamik, Goldschmidtstr. 3, 37077 Göttingen, bleiss1@gwdg.de

Locality: Small abandoned limestone quarry and cliffs south of the dam of the water storage lake ("Bergsee") in the Selke valley at Güntersberge. The outcrops are located along the Selketal railway and above on a nature trail. Geological map 1:25,000, Sheet No. 4331, Hasselfelde.

UTM co-ordinates: East 636791.262, North 5722898.351 (Zone 32N, WGS84)

Geographic co-ordinates: N 51° 38' 25.56" E 10° 58' 36.71"

Exposed is an approx. 50 m wide, lens-shaped block of imbricated Devonian limestones of varying age (Fig. 10.1). The block is embedded in a pervasively-foliated, clayey-silty matrix of uncertain age (Lower Carboniferous is suspected, as greywackes often occur as layers and lenses in the surrounding slate, Reichstein 1962, Schwab 1976). The rather thick-bedded carbonate rocks are pelagic, more or less strongly condensed limestones, commonly termed "Herzynkalke" (Herzyn limestones), in reference to the open-marine facies called "herzynisch" in German (e.g. Hüneke 1998). Such imbricate limestone blocks embedded in a pervasively-foliated clayey matrix are widely exposed in the central and eastern part of the Harz Mountains, especially in the Harzgeröder Zone. These limestone blocks are usually regarded as olistoliths and are thus considered as important evidence for the existence of widespread olistostromes in the Harz Mountains (e.g. Harzgerode olistostrome, see also the Geopark information board in the outcrop).

Reichstein (1962) was the first to provide a detailed bio- and lithostratigraphic subdivision of this outcrop based on conodonts. The limestone beds range stratigraphically from the late Lower Devonian (Emsian) to the late Upper Devonian (Hembergian). The stratigraphic subdivision also revealed that the limestone sequence is stratigraphically inversely stacked (Fig. 10.1). Schwab (1976, Fig. 10.5) extended the profile to the west and towards the footwall and collected first tectonic data. According to this, the bedding in the outcrop consistently dips about 45° to the SE (see also Franzke & Schwab 2011). New structural investigations in combination with petrographic studies by Riegel (2017) yield the following results.

The outcrop consists in its lower part of an overturned limb of a foliated fold structure. It is overlain by a zone of SE-dipping imbricated limestones of different ages, followed by a limestone breccia on top (Fig. 10.1).

The steeply S-dipping overturned fold limb consists of Middle Devonian Stylioline limestone which extends from the center to the western edge of the outcrop. The bedding dips steeply S/SSW and is often thick-bedded (cm to 1 dm), thicker than the spacing of the pressure solution cleavage planes (s1). Thus, the cleavage planes used to be mistaken for the bedding. Accordingly, a greater thickness must be assumed for the Middle Devonian Stylioline limestone (over 20 m!). The steep bedding planes themselves are partly subsequently sheared by dextral strike-slip faulting.

With a tectonic contact, an approx. 50 cm thick, flat-lying slate layer overlies the overturned limb and marks a prominent shear plane (Fig. 10.2). Above this, in the eastern part a strongly-sheared sequence of SE-dipping limestones of Middle and Upper Devonian age occur. According to the
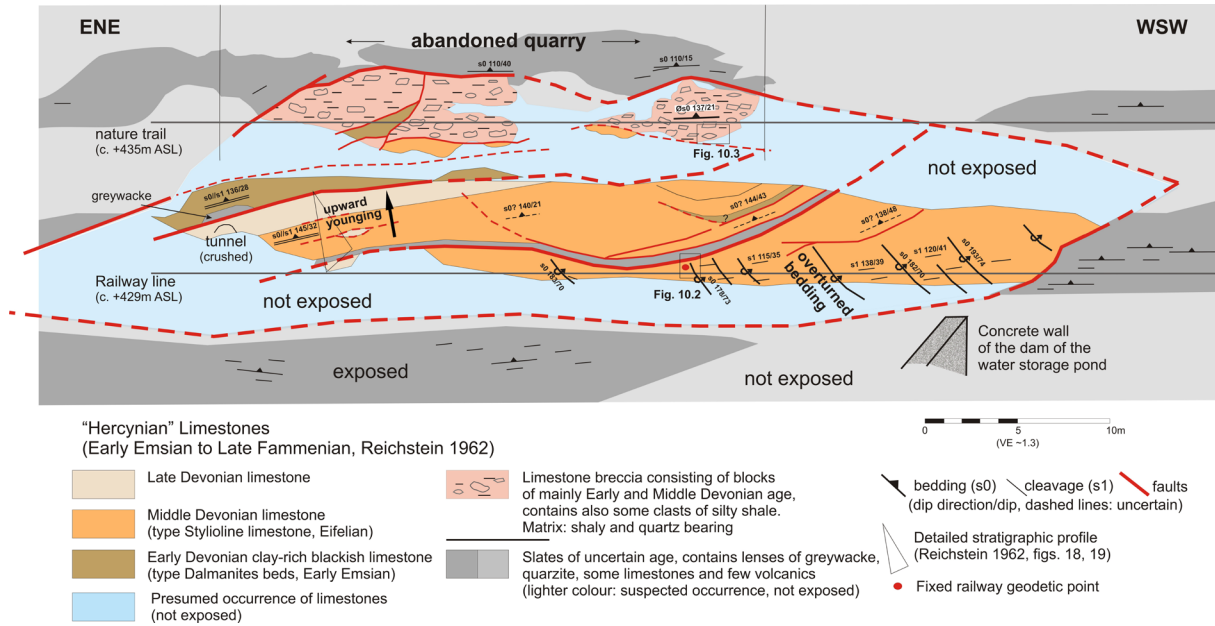
Figure 10.1: Geological sketch of the lens-shaped Herzynkalk block at the dam of the water storage lake at Güntersberge. Figure based on Reichstein (1962, fig. 10.17), modified and supplemented. The view is parallel to the mainly SE-dipping layering of the block.

Figure 10.2: Tectonic contact (S) between the overturned limb of steeply-dipping Stylioline limestone and a flat-laying slate layer on top (camera cap for scale; for photo position see Fig. 10.1).

stratigraphic data, this sequence forms the normal limb of the fold structure, which is however also internally imbricated. This is shown by lenses of Upper Devonian limestone within the Middle Devonian limestone (left side of Fig. 10.1, Reichstein 1962). In the eastern part, at the tunnel, the more clayey and boudinaged Lower Devonian limestone is thrust onto the younger strata along a shear plane containing a greywacke block. The bedding and cleavage presumably follows approximately the main layering (cleavage-parallel bedding). In the western part, the position of the bedding above the prominent slate layer is still uncertain due to the strong deformation.

In the upper part of the outcrop, Middle and Lower Devonian limestone again occur, here overlain by a limestone breccia. This occurrence formerly interpreted as conglomerate is composed of densely packed clasts in a silty-clayey matrix (Figs. 10.3, 10.4N). Only towards the outer edge of the breccia the proportion of quartz in the matrix increases significantly. The limestone clasts are mainly of Lower and Middle Devonian age, the amount of Upper Devonian clasts is low (< 10°%, Reichstein 1962, p. 36). We also found some fragments of black siltstone and greywacke. The limestone clasts are mostly lens-shaped, otherwise slightly rounded or even angular and preferably oriented parallel to the cleavage (Figs. 10.4N). In some larger clasts (up to several dm) the bedding is well preserved. The pressure-solution cleavage planes (s1) within them dip steeper than the bedding.

Fragmentation of the clasts by shearing is well visible and results in an angular shape of the clasts whereby the shear fractures are usually filled with clayey matrix, which is typical for cataclastic deformation (Fig 10.3c, Fig 10.4Nd). Some faulted clasts are even rotated (Figs. 10.3b, c). This rotation
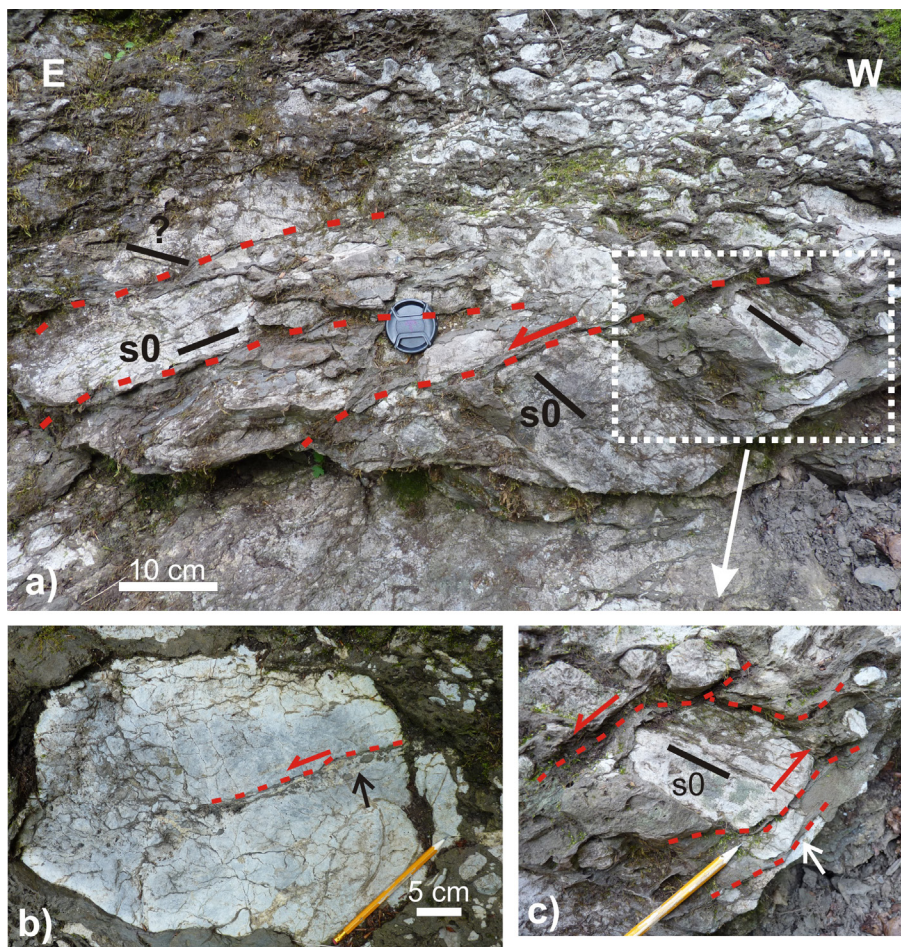
Figure 10.3: Detailed views of the limestone breccia. a) Limestone blocks/clasts with different orientation of their bedding planes (s0). b) A shear plane within a larger clast contains some fine greywacke debris (black arrow). c) Some cleavage-parallel shear planes are filled with clayey matrix (white arrow, see text). Camera cap and pencil for scale. For photo position see fig 10.1.
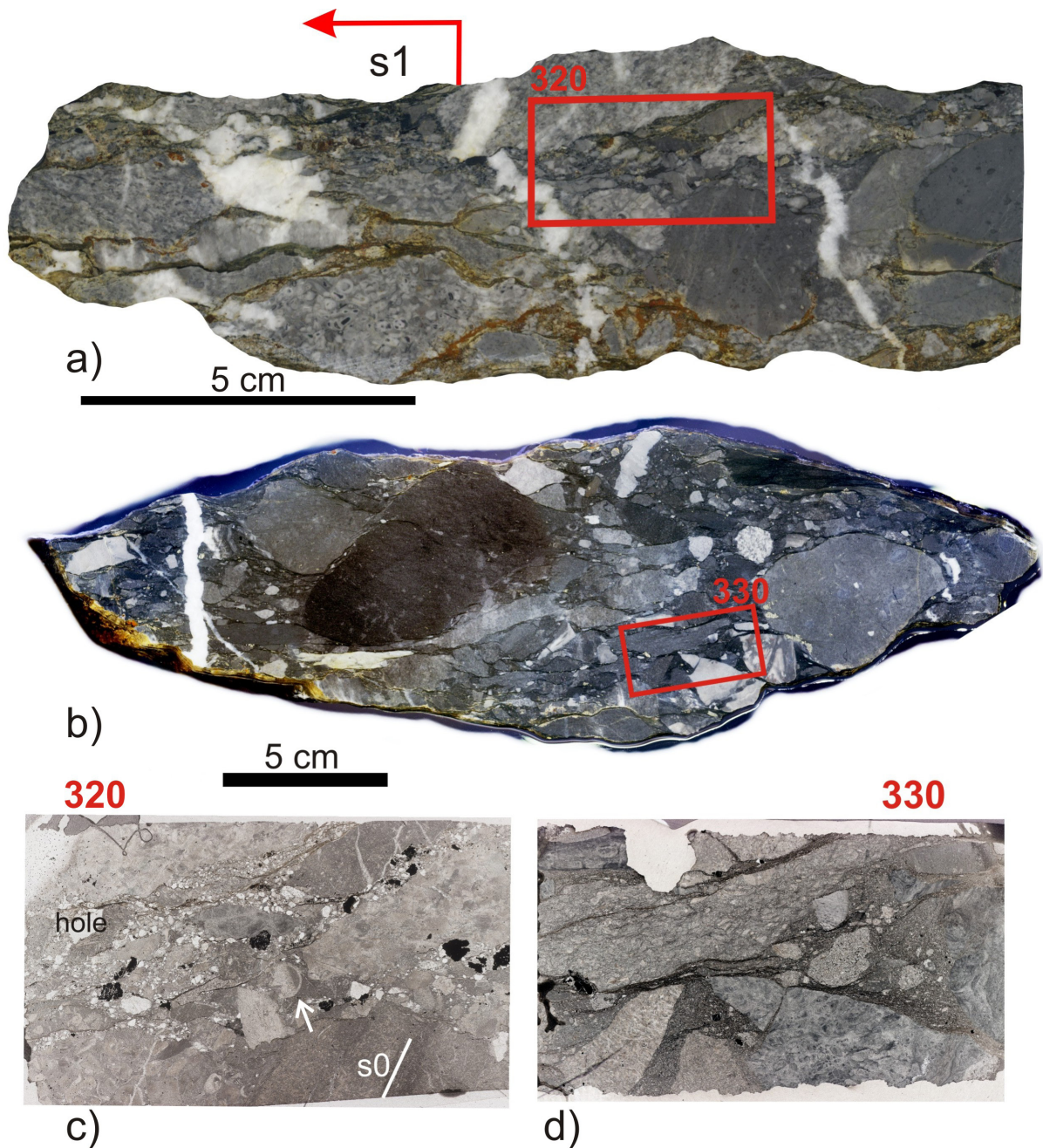
Figure 10.4: a), b) Polished hand specimens and related thin section of the limestone breccia showing clasts preferably oriented parallel to the cleavage (s1). c) White rather angular quartz grains occur along clasts but also along shear planes penetrating carbonate cements. Dark spots are newly-formed iron ore. Sometimes bedding traces (s0) are visible in clasts, in the centre also a geopetal fabric occur (white arrow). d) Angular fragmentation of clast and infill of the gaps with clay material.

and has also affected the orientation of s1 planes of the clasts (Fig 10.5a). Such SSE plunging axes are considered late compared to the more common NE-SW striking axis of F1/F2 folds (Schwab 1976). Shearing is also documented in the clayey-silty matrix. In samples from the edge of the breccia, the quartz grains are up to 1mm in size and usually have a slightly rounded to angular shape. Quartz-rich stripes outline the limestone clasts, but they can also penetrate cemented clasts along small, branched shear planes (Fig. 10.4c). Angular fragmentation occurs up to the microscopic scale (Fig. 10.4d).

a) Limestone breccia   **b) Limestone beds (early to late Devonian)**   **c) Ambient slates**
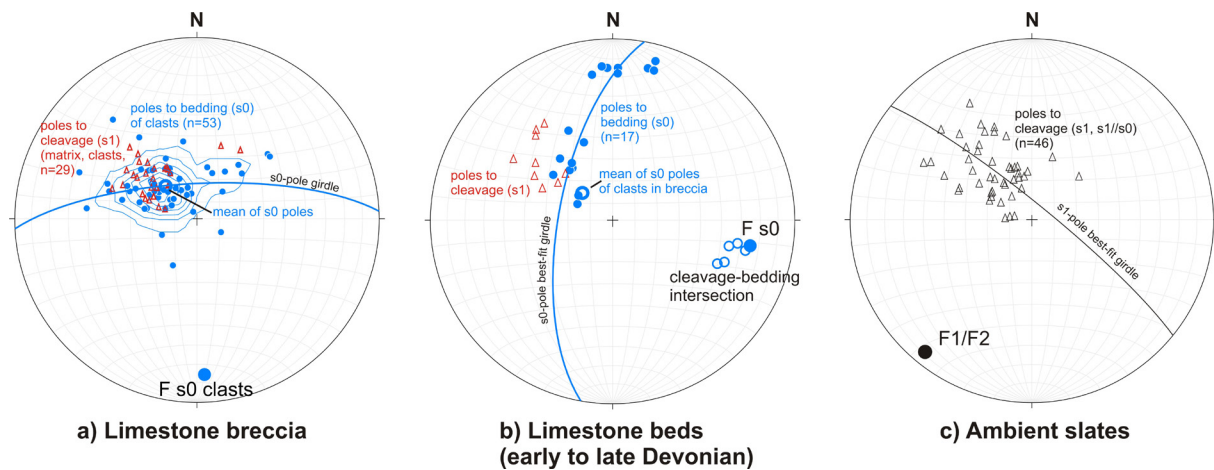
Figure 10.5: Equal-area, lower hemispheric, stereographic projections of fabric data from different areas of the outcrop. a) Bedding poles of clasts, cleavage poles of clasts, and the shaley matrix in the breccia. The bedding poles of clasts form a south-plunging fold axis (π pole) probably as result of internal shearing (see text and comp. Fig. 10.3). b) The best-fit great circle of bedding poles of limestone layers forms a π pole which coincide with the cleavage-bedding intersection lineation (open circles), indicating a close genetic relationship between folding and cleavage. c) The poles of the cleavage planes and cleavage-parallel bedding planes (s0/s1) in the ambient shales are arranged around a SW-NE trending axis, which is the common orientation of regional F1/F2 fold structures (Schwab 1976).

The shape of the clasts and the deformation pattern suggest rather a breccia formation than a conglomeratic origin of this rock unit. The regular arrangement of the bedding planes of the clasts indicates a coaxial deformation which seems to be the result of tangential shearing preferably along the cleavage planes (compare the similar observations in Stop 5). The infill of the shear fractures by the clayey matrix points to a high pore fluid pressure during this cleavage-related deformation. A sedimentary transition from this breccia unit to the surrounding slates could not be proven. Also in the central part of the outcrop (cf. Reichstein1962), where the breccia is more clayey and contains in the silty slates some strongly boudinaged limestone layers, the strong deformation prevents a clear conclusion. Elsewhere the breccia is abruptly bounded by faults.

The earlier interpretation of this unit as conglomeratic limestone (Reichstein 1962) is considered inappropriate, it is rather a breccia. However, it remains unclear whether there was a sedimentary phase of brecciation to mix the clasts. This mixing would have to be post-Upper Devonian, possibly even in the Lower Viséan (greywacke lenses of the Tanner greywacke type?). Due to the rapid lithification of these limestones (e.g. Hüneke 1998) such a reworking seems unlikely. Because of the tectonic development of the limestone block as a whole (see below), this unit could be a tectonically formed breccia evolved during the Late Carboniferous.

Discussion and conclusion

The fact that whole lens-shaped Herzynkalk block of Güntersberge is tectonically imbricated and stacked as well foliated, was early recognised (Reichstein 1962) and this occurrence was therefore addressed as deformed olistolith (Schwab 1976, Franzke & Schwab 2011). However, such an interpretation of the imbricate limestone block as olistolith is only correct if imbrication and fragmentation already occurred syn- to post-sedimentary, at the latest in the course of the assumed Early Carboniferous submarine mass-flow processes. If, however, imbrication and stacking of the limestone block occurred during the Variscan tectonic deformation in the Upper Carboniferous, which is generally accepted, then a problem in space and time arises.

In order to be able to tectonically stack the early to late Devonian limestone sequence in its present form, the limestone sequence must still have existed as a more or less intact, coherent unit, until the Upper Carboniferous. Otherwise, a syn- to post-sedimentary "olistostromal" imbricated sequence would have been destroyed by the intense subsequent fault tectonics. That this folding

and imbrication is of tectonic origin is demonstrated here by the foliated overturned fold structure, where the SE-dipping s1 cleavage corresponds to the general, regional orientation of the cleavage in the outcrop and its surroundings, even in the steeply dipping fold limb (Fig. 10.5b, c). This shows that sheared parts of a tectonic fold are exposed here. Due to late fault tectonics, the fold axis of the limestones was probably slightly rotated with respect to the fold axis in the surrounding slate (Fig. 10.5b, c). From the above observations, it appears that the limestone block was tectonically folded and foliated, and syn- to late kinematically imbricated and stacked along faults. However, its fragmentation and isolation as a lens-shaped block must have occurred even somewhat later in a final stage of deformation (Fig. 10.6).
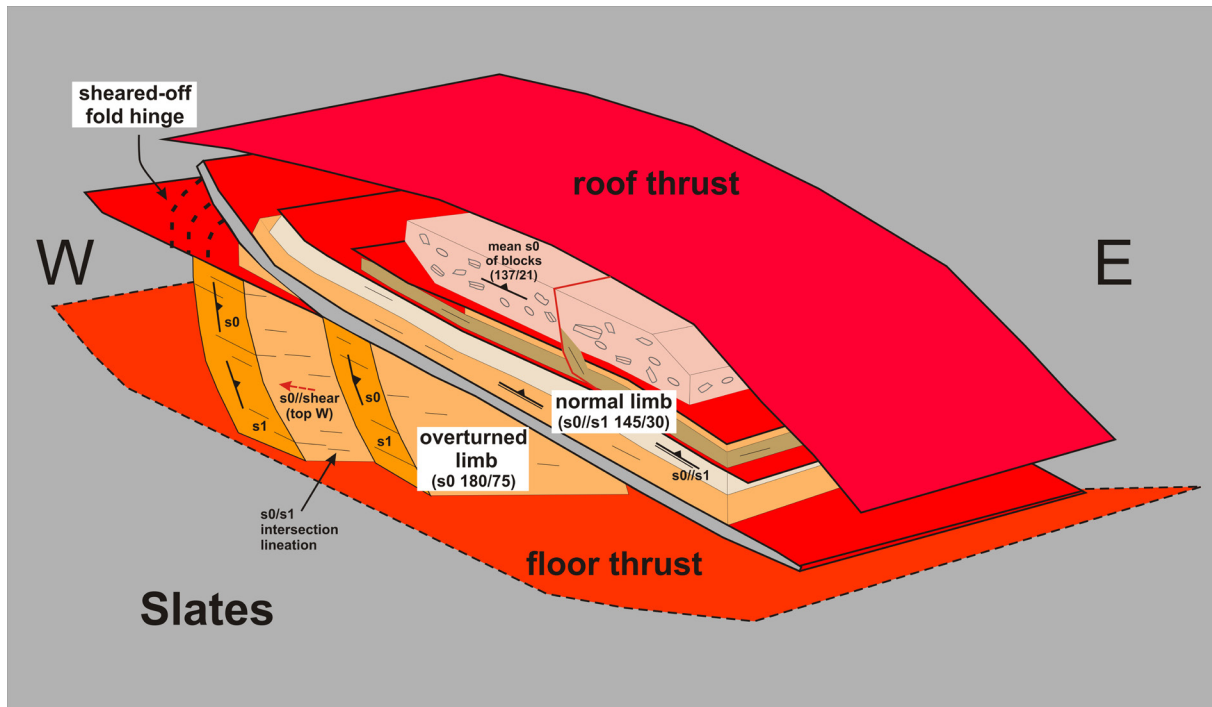
Figure 10.6: Simplified 3D view of the structure shown in Fig. 10.1. The only partly-preserved, NW-vergent, overturned fold structure is interrupted by several fault planes along which the hinge region was sheared off.

The studied outcrop was previously considered a classic example of a mass-flow deposit. However, this lens-shaped limestone block should not be further considered as deformed olistolith. Instead it is a fault-bounded block of tectonically folded and imbricated stacked Devonian limestone, i.e. a tectonic shear body whose fragmentation (isolation) took place after tectonic folding. The difficulties of interpreting such imbricate stacks as part of mass-flow deposits were pointed out early on by some researchers (Walliser & Alberti 1983, Koll 1984), but this was largely ignored when the olistostrome model was established.

As long as the tectonic nature of the folding and imbrication is proven, such blocks of imbricate stacks of limestone or other rocks can also be used, similar to "rootless folds", as a characteristic of a tectonic origin of chaotic rock fabrics. Similar limestone blocks are widely distributed especially in the Harzgerode zone, thus this feature, together with other criteria, indicate a dominant tectonic origin of the fabric of the chaotic rock units in the Harz Mts. (Friedel et al. 2019).

References

Franzke, H. J. & Schwab, M. (2011): Harz, östlicher Teil mit Kyffhäuser Kristallin. Sammlung geologischer Führer, 104, 1-327, Gebr. Bornträger (Stuttgart).

Friedel, C.-H., Huckriede, H., Leiss, B. & Zweig, M. (2019): Large-scale Variscan shearing at the south-eastern margin of the eastern Rhenohercynian belt: a reinterpretation of chaotic rock fabrics in the Harz Mountains, Germany. International Journal of Earth Sciences, 108, 2295-2323.

Hüneke, H. (1998): Die Herzynkalk-Entwicklung im Randgebiet der Selke-Einheit (S-Harz)-Abbild der Subsidenz im östlichen Rhenischen Trog während des Devons. Z. dtsch. geol. Ges., 149, 381-430.

Koll, J. (1984): Strukturanalyse allochthoner Serien des Südharz-Paläozoikums. Braunschw. geol. paläont. Diss., 1, 1-124.

Walliser, O.H. & Alberti, H. (1983): Flysch, olistostromes and nappes in the Harz Mountains. In: Martin, H. & Eder, F.W. (eds.) Intracontinental Fold Belt, 145-169, Springer, Berlin.

Reichstein, M. (1962): Die Stratigraphie der Hercynkalke bei Güntersberge im Unterharz und das Problem der Hercynkalkentstehung. Geol. Beih., 34, 1-73.

Riegel, J. (2017): Strukturelle Untersuchungen an pelagischen Kalksteinen (Herzynkalken) des Harzes. Master thesis, 122 S., Georg-August Universität Göttingen.

Schwab, M. (1976): Beiträge zur Tektonik der Rhenoherzynischen Zone im Unterharz. Jb. Geol., 5/6 (1969/70), 9-117.

Stop 11: Tectonic features of the epizonal Wippra Zone – the Klippmühle Quartzite Formation in the Wipper valley

Friedel, C.-H. [1], Stipp, M. [2]

1) Karl-Marx-Str. 56, 04158 Leipzig, chfriedel@gmx.de

2) Martin-Luther-Universität Halle-Wittenberg, Institut für Geowissenschaften und Geographie, Von-Seckendorff-Platz 3, 06120 Halle, michael.stipp@geo.uni-halle.de

Locality: Wipper valley, West of Biesenrode, at the stop "Gräfenstuhl-Klippmühle" of the Wippertal railway, Geological Map 1:25.000, Sheet No. 4334, Leimbach.

UTM Co-ordinates (train stop): East: 666500.135 North 5719553.691 (Zone 32N, WGS84)

Geographic co-ordinates: N 51° 36' 8.56", E 11° 24' 15.29"

The Wippra Zone is the southeasternmost unit of the Harz Mountains. In contrast to the mainly anchimetamorphic Rhenohercynian units of the Harz mountains, it is characterised by epizonal regional metamorphism up to lower greenschist grade. The Wippra Zone is part of the Northern Phyllite Zone S to SE of the Rhenohercynian Zone. Together with the Hunsrück and Taunus in the Rheinisches Schiefergebirge, the Wippra Zone forms prominent outcrops of the Northern Phyllite Zone, which has otherwise mainly been established by drilling (e.g. Schwab & Jacob 1996, Franke 2000).

The subdivision of the Wippra Zone into seven subunits (series 1-7, Fischer 1929, Reichstein 1964) is lithologically justified (Figs. 11.1, 11.2). In all subunits, phyllitic clay schists predominate, in which quartzites (series 3 and 5), metabasalts and their tuffs (series 6) and metagreywackes (series 7) are intercalated as characteristic rocks. Series 2 consists mainly of clayey slates (Silurian). The red slates of series 4 and the slates of series 3 are rich in Al-(Fe)-Mn. Therefore, carpholite and ottrelite could form during metamorphism. Series 3 and 4 are, like the quartzite series 5, of Ordovician age (Tremadoc-Arenig/Lanvirn, see overview in Schwab & Ehling 2008). Series 6 and 7 probably represent epizonal equivalents of the Upper Devonian Giessen-Harz-Nappe (e.g., Franke 2000). Series 1
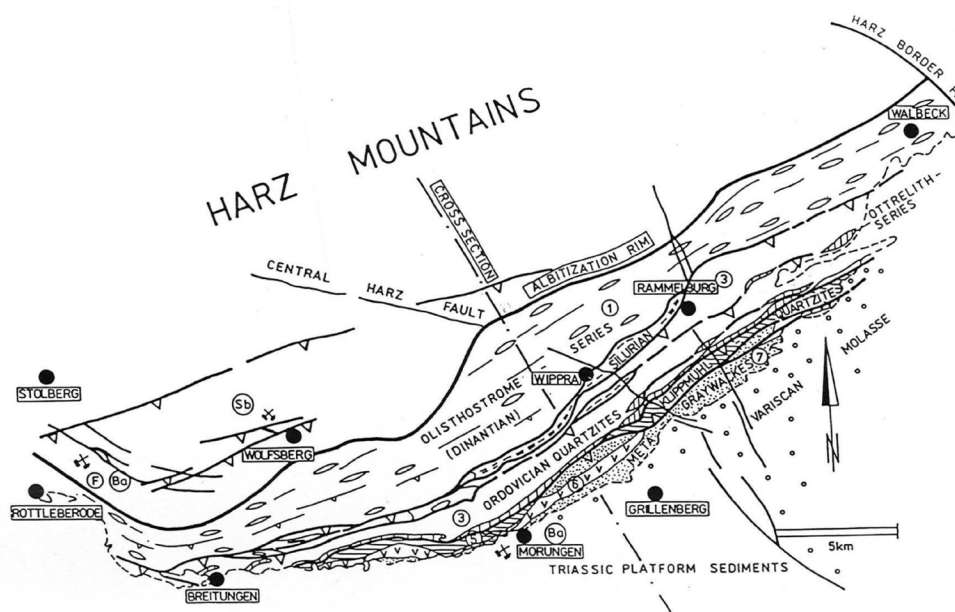
Figure 11.1: Geotectonic Overview of the Wippra Zone (Jakob & Franzke 1992; reprinted with permission from www.schweizerbart.de/series/zgp1).
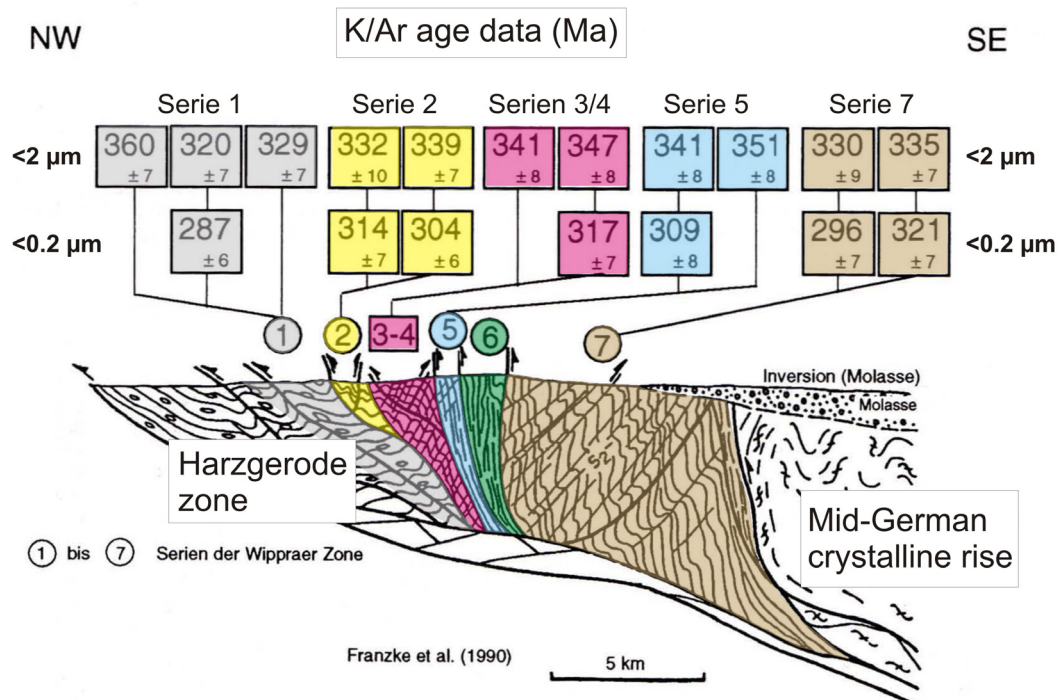
Figure 11.2: K-Ar-ages of regional metamorphism in the area of the Wippra Zone for the <2 μm and <0.2 μm fractions of clay (Ahrendt et al. 1996; reprinted with permission from www.schweizerbart.de/journals/zdgg). Most data point to an Viséan age of metamorphism, probably followed by a later thermal event (data from the <0.2 μm fraction). The diverging structure of the Wippra Zone is indicated by a NW-vergence of the folds and thrust/reverse faults in the NW and a SE-vergence in the SE. For the position of the cross section, see Fig. 11.1.
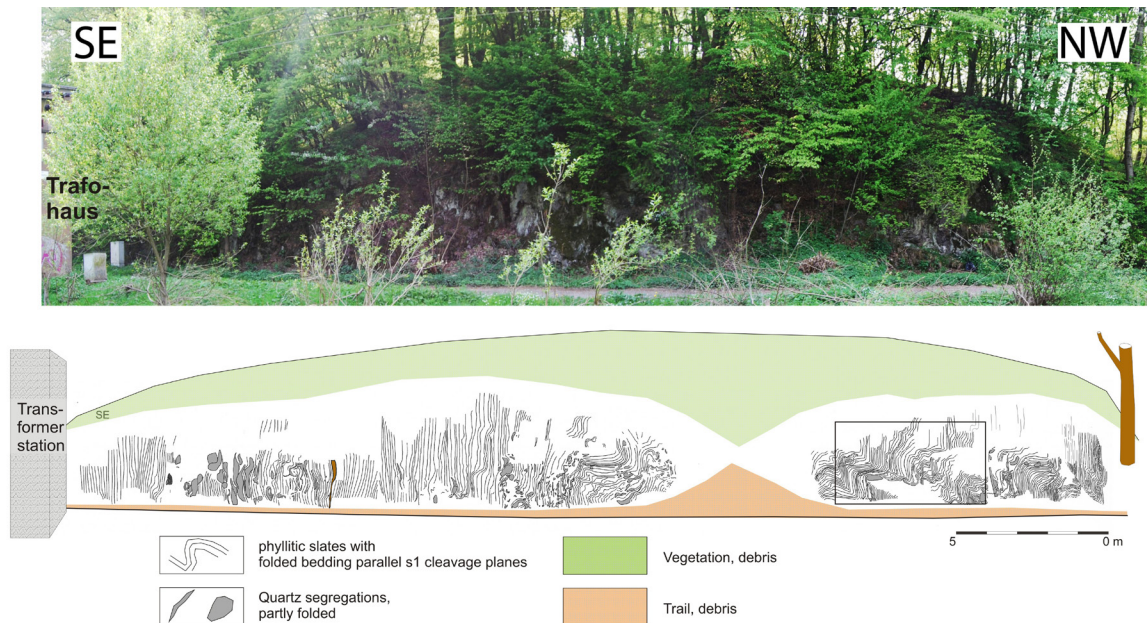
Figure 11.3: Photograph and drawing of the folded Klippmühle formation along the road to the train stop of the Wippertal railway (drawing from Fischer 2011). Rectangular frame marks position of Fig. 11.4a.

forms the transition to the anchizonal metamorphic conditions further to the northwest and belongs to the Harzgerode Zone (contains amongst others Hercynian limestones). The epizonal, i.e., very low-grade metamorphism is of Carboniferous age (Fig. 11.2) and mainly characterised by differences in the pressure conditions due to tectonic burial. The lowest pressures were determined for series 6 (1-2 kbar), the highest pressures for series 7 (6-8 kbar). The contacts between the sub-units are tectonic contacts (Siedel & Theye 1993, Theye 1995).

Folding and the first cleavage (F1, S1) were formed in the Wippra Zone under prograde conditions up to the onset of dynamic recrystallization of quartz at approximately 270-300°C (Jakob & Franzke 1992; Jakob 1995). Subsequently, the F2 folding and associated second cleavage (S2, see below) developed under retrograde metamorphic conditions. Further deformation proceeded by brittle
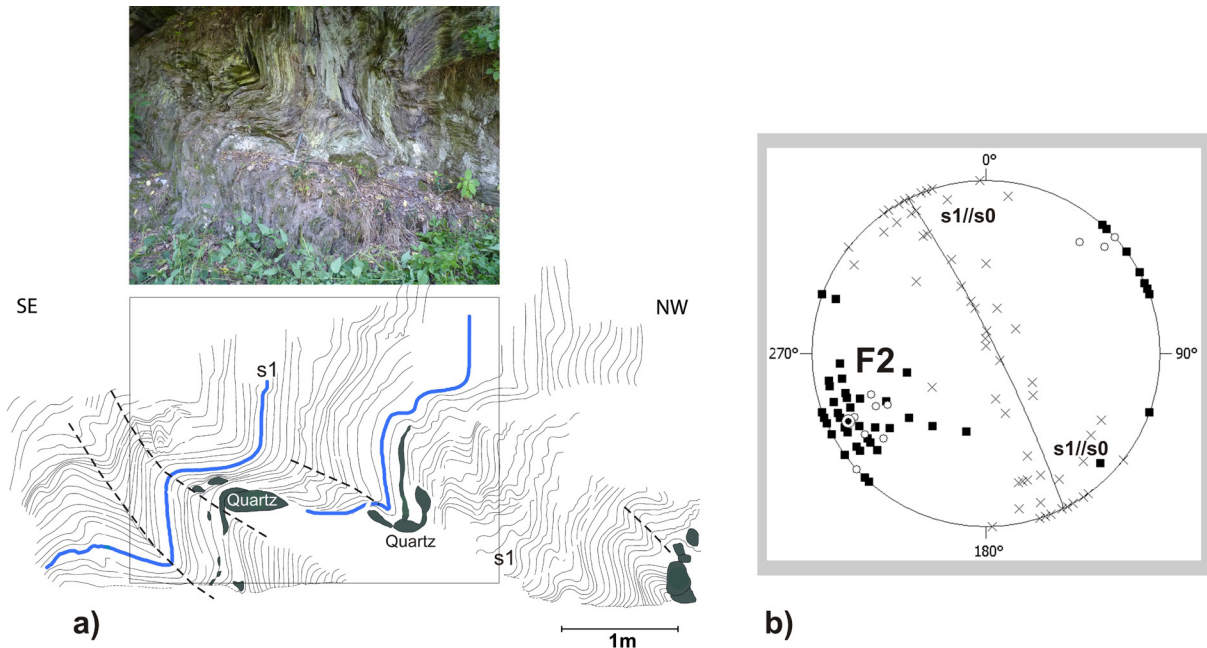
Figure 11.4: a) Sketch and photograph of the NW part of the road profile from Fig. 11.3. Note the intense folding of the bedding plane-parallel first cleavage (S1//S0) by F2 folding with SE-vergent fold axial planes (dashed lines). b) Equal-area, lower-hemisphere stereographic projection of main fabric data from the outcrop area (S1//S0: 1st cleavage parallel to bedding; F2: fold axes of folded S1). Sketch and stereoplot from Fischer (2011).

faulting and cataclasis. There are two tectonic transport lineations: a 45-70° striking main direction corresponding to the main NE-SW orientation of the Wippra Zone and a presumably older one directed approximately NW-SE (100-130°) (Jakob 1995).

The rock sequence in the outcrop belongs to series 5, which is exposed as the "quartzite zone of the Klippmühle" in the Wipper valley. The outcrop is located at the road to the train stop of the Wippertal railway. The Klippmühle formation essentially consists of an alternating sequence of fine-grained, grey, poorly-sorted quartzite schists and quartzites as well as dark phyllitic silty-sandy clayey schists of Tremadoc to Arenig age (Burmann et al. 2001, Schwab & Ehling 2008). Along the road, a clayey-rich, intensively folded sequence is exposed (Fig. 11.3, 11.4).

The first folding F1 produced the layer-parallel first cleavage (S1/S0). The later F2 folds visible in the outcrop are clearly SE-vergent (Fig. 11.4). An associated second cleavage (crenulation cleavage, S2) is poorly developed here (visible as intersection lineation and crenulation). Quartz is the most conspicuous newly-formed metamorphic mineral occurring frequently in veins, which are either layer-parallel and folded or which intersect the folded layers (Fischer 2011).

The SE-vergence of the F2 fold contrasts with the NW-vergence of both the F1 and F2 folds and their

associated S1 and S2-fabrics, which otherwise predominate further NW (Fig. 11.2). This "vergence fan" of the Wippra Zone is interpreted as an effect of continuous NW-directed shortening with progressive rotation of the F1 folds and S1 cleavage (Jakob & Franzke 1992).

References

Ahrendt, H., Franzke, H. J., Marheine, D., Schwab, M. & Wemmer, K. (1996): Zum Alter der Metamorphose in der Wippraer Zone/Harz – Ergebnisse von K-Ar-Datierungen an schwachmetamorphen Sedimenten. Z. dt. Geol. Ges., 147, 39-56, Stuttgart. Doi 10.1127/zdgg/147/1996/39

Burmann, G., Ehling, B.-C., Franzke, H. J., Hoth, K., Kopp, J. & Wunderlich J. (2001): Nördliche Phyllitzone (an der MKZ). In: Hoth, K. & Leonhardt, D. (eds.): Stratigraphische Kommission Deutschlands – Stratigraphie von Deutschland II, Ordovizium, Kambrium, Vendium, Riphäikum. Teil III, Courier Forsch.-Inst. Senckenberg, 235, 11-67, Frankfurt/M.

Fischer, G. (1929): Die Gesteine der Metamorphen Zone von Wippra mit besonderer Berücksichtigung der Grünschiefer. Abh. Preuß. geol. Landesanst., N.F., 121, 1-64, Berlin.

Fischer, S. (2011): Das Geotop am Bahnhof Gräfenstuhl-Klippmühle in der Wippraer Zone (Unterharz). Bachelor thesis, 36 S., Martin-Luther Universität Halle/Wittenberg.

Franke, W. (2000): The mid-European segment of the Variscides: tectonostratigraphic units, terrane boundaries and plate tectonic evolution. In: Franke, W., Haak, V., Oncken, O. & Tanner, D. (eds): Orogenic Processes: Quantification and Modelling in the Variscan Belt. Geological Society, London, Special Publications, 179, 35-61.

Jakob, G. (1995): Ergebnisse mikrogefügeanalytischer Untersuchungen an schwachmetamorphen Gesteinen der Zone von Wippra (Harz). Zbl. Geol. Paläont. Teil I, Heft 9/10 (1993), 1201-1211.

Jakob, G. & Franzke, H.J. (1992): Die tektonische Entwicklung der Wippraer Zone im Unterharz. Zbl. Geol. Paläont., Teil I Heft 1-2 (1992), 51-61.

Reichstein, M. (1964): Stratigraphische Konzeptionen zur Metamorphen Zone des Harzes. Geologie, 13, 5-25.

Siedel, H. & Theye, T. (1993): Very low-grade metamorphism of pelites in the Wippra Zone, Harz Mountains, Germany. N. Jb. Miner. Mh., 1993, 115-132; Stuttgart.

Schwab, M. & Jacob, G. (1996): Wippraer Zone-Taunus-Hunsrück. Ein struktureller Vergleich. Z. geol. Wiss., 24(3/4), 305-316.

Theye, T. (1995): Metamorphosesprünge in der Wippraer Zone (Unterharz). Zbl. Geol. Paläont. Teil I (1993), 9/10, 1187-1200.